Matrix Node Theory / Evans Node Dialect

Conservative Dynamics and Physical Consequences

A mathematical reconstruction of the
Evans Quantum Energy Field proposal

Jordan Ryan Evans

Independent research

Volume I: Foundations, derivations and implications

6 September 2026

This edition gives a fully specified finite conservative model, works out its exact and limiting consequences, and separates those results from conditional connections to quantum field theory, gravity and observations. Mathematical closure of the constructed model is established under explicit assumptions; unique microscopic selection and empirical closure of a theory of everything are not claimed. Numerical data and reproducibility details appear in Volume II and the accompanying source package.

The physical proposal and its interpretation are attributed to the author. The mathematical reconstruction, numerical verification and editorial work were developed with AI assistance. Established methods and experimental results are credited to their original authors in the external bibliography.

Abstract

Potential, coherent expression and localized actuation are formulated as distinguishable states of a conservative system rather than as creation or destruction of energy. A compact-phase network is coupled to explicit reserve oscillators through a positive Hamiltonian. The resulting initial-value problem has a unique global finite-graph solution, conserves total energy and a common-phase Noether charge, and allows energy to return from the reserve. Eliminating the reserve gives an exact nonlinear memory equation. Apparent drag, reactive response and, under a separately specified thermal preparation, fluctuations then follow from one spectral measure.

A reciprocal threshold readout is constructed without an unexplained energy-erasing reset. Proper-time evolution and reference-clock observation are distinguished; their transformations are derived rather than applied as arbitrary numerical multipliers. The full coupled normal-mode spectrum, its low-wave-number dispersion and a dimensionless nonlinear-period relation supply definite conditional predictions. The lowest acoustic branch contains both a cubic-lattice directional correction and an isotropic reserve correction. The difference between axial and body-diagonal quadratic phase-speed coefficients is $-1/36$ under the stated identical-edge, gapped-reserve assumptions.

Conventional quantum, gauge, particle, gravitational and cosmological descriptions are then developed as explicitly conditional effective completions. Particular attention is given to observable normalization, stable matter, quantum probabilities, chiral representations, covariant stress-energy and the difference between an analogue propagation metric and dynamical gravity. A reference atlas reconstructs atomic, thermal, nuclear, gravitational and cosmological identities without treating their measured inputs as independent predictions.

The accompanying execution record contains 946 successful software and mathematical assertions across six suites. It includes nonlinear conservative evolution, exact memory elimination, coupled spectra, threshold feedback, clock covariance, synthetic inference controls and selected published-data comparisons. The fixed supplied-background DESI result remains $\chi^2 = 28.5062$ for 13 measurements. No new parameter-free physical constant or distinctive experimental alignment is established. The work closes an explicit mathematical realization and identifies the remaining physical selection and matching requirements without replacing them by an accuracy percentage.

Guide to the argument

The main text moves from physical statements to a Hamiltonian, then from that Hamiltonian to energy exchange, memory, thresholds and spectra. These are the constructive results of the reconstruction. Later sections explain how the same interpretation can be expressed in standard quantum and relativistic language and which additional physical assumptions are needed.

The word *potential* denotes content that is available or stored relative to a declared resolved description. It does not mean an unmeasurable numerical residual that can be chosen to fit an answer. *Actuation* denotes the formation or registration of a resolved configuration. *EQEF* retains the author's field-like conversion-resistance interpretation; the reserve Hamiltonian is one explicit realization of that interpretation, not its uniquely deduced form.

A theorem applies to its stated model and assumptions. A conditional prediction is a consequence of that model before choosing a physical apparatus map. A published-data comparison uses external measurements with the inputs and uncertainties declared. These three roles are kept distinct throughout.

The appendices provide the primitive state-space formulation, a separate statistical first-passage construction, corrected differentiation rules, a reference-physics atlas and exact inverse-problem details. Volume II contains the numerical parameters, intermediate outputs, controls and executable scripts. The source package preserves a separate provenance ledger so that the publication bibliography can remain restricted to external scientific sources.

Contents

Abstract i

Guide to the argument ii

I Physical premises and a closed conservative realization 1

1 Physical premises and the scope of a mathematical completion 1

2 An explicit conservative node–reserve Hamiltonian 3

3 Deriving resistance, memory and return from the reserve 8

4 One response function for storage, drag and fluctuations 11

5 Actuation as a conservative threshold process 14

6 Relational clocks and the limits of a universal timing correction 17

II Clocks, conversion and inference 19

7 Proper time, event rates and energy measurements 19

8 Conservative dynamics and their exact solutions 22

9 What observations can determine 25

III Coherence, propagation and geometry 28

10 Continuum propagation and definite spectral predictions 29

11 The spectrum with the reserve retained 32

12 Coherence and capacity: the theorem chain 35

13 Phase boundaries, comparison and geometry 39

14 Discrete dynamics, conservation and the continuum 42

IV Quantum descriptions, matter and constants 45

15 Quantum mechanics and field-theory recovery 45

16 From a phase factor to actual coherent conversion 48

17 Gauge fields, matter and the Standard Model bridge 52

18 Particles as stable structures: spectrum, charge and decay 56

19 Constants without numerical retrofitting **60**

20 Atomic structure and the meaning of a constant calculation **63**

V Gravity, cosmology and thermodynamics 66

21 From conversion resistance to a field model **66**

22 A covariant phase–gravity completion **69**

23 What it takes for a network to reproduce gravitational dynamics **74**

24 Cosmology and the age of the universe **77**

25 Statistical mechanics, radiation and a conservative reserve **81**

VI Predictions, computations and physical implications 84

26 From a common physical model to experimental observables **84**

27 Predictions fixed by the reconstruction **88**

28 Executed calculations and comparison with measurements **91**

29 Physical implications and the completed reconstruction **94**

Technical appendices 98

A A precise primitive framework **98**

B An auxiliary threshold model and a persistent statistical clock **101**

C Dimensional normalization and complete differentiation **104**

D Reference identities and observable definitions **108**

E A detailed two-reservoir solution and inverse problem **115**

F An explicit correlated-error calculation **117**

G Notation and dimensional conventions **117**

External references **119**

Part I

Physical premises and a closed conservative realization

1. Physical premises and the scope of a mathematical completion

1.1 The physical idea in ordinary language

The hypothesis investigated in this monograph is that observable particles and fields are maintained patterns of a more basic system. Some of the system's content is expressed in such patterns; some remains available in other degrees of freedom. Conversion can be incomplete, and a previously expressed pattern can transfer content back to the reserve. The proposed Evans Quantum Energy Field, abbreviated EQEF, names the physical influence associated with this resistance and exchange. In this interpretation, a reduction in observed expression does not mean that the conserved total has disappeared.

Only three specialized terms are needed. *Potential* means an available reserve, once the relevant physical quantity has been specified. *Actuation* means expression in a resolved physical pattern or recorded event. *EQEF* refers to the proposed influence on conversion and return. Energy, momentum, probability, phase, temperature, time and curvature keep their conventional meanings. In particular, a wave and a particle are not separate substances whose energies should automatically be added: they can be two descriptions of the same excitation.

The problem is to turn these meanings into equations without using measured target values to select the answer. It is not enough to attach a quantity called "reality" to a familiar constant. A useful physical model must define a state, its evolution, its conserved quantities, the initial and boundary conditions, and the map from that state to an observation. This paper constructs a finite dynamical realization with those ingredients, then develops its approximations and its relation to conventional effective physics.

1.2 Three different meanings of closure

Dynamical closure means that a state and a parameter set determine its future without another unspecified function being supplied at each step. The finite Hamiltonian model in Section 2 has this property. Its phase variables and reserve coordinates evolve by explicit ordinary differential equations. It is not necessary to guess a new correction after an observable has been calculated.

Interpretive closure means that the model's variables have operationally specified meanings. A resolved oscillator energy is well defined in the constructed model. Calling it an electron mass, a detector count, or dark energy requires an additional map. The paper provides explicit maps for some mathematical examples and identifies the physical maps that are not obtained from the finite model.

Empirical closure means that the same physically selected construction predicts measured quantities across the proposed domains, with its parameter provenance and uncertainties

controlled. No count of successful algebraic identities establishes that condition. The present reconstruction does not claim a first-principles value of the fine-structure constant, a complete Standard Model spectrum, or a newly confirmed cross-domain physical signal. It instead makes the mathematical construction and the remaining physical matching problem precise.

These distinctions are useful because they localize the work. A complete set of equations for a model can be delivered and tested even when the identification of that model with all of nature is not established. Conversely, a table of nearly equal numbers is not a closed microscopic theory when the quantities on the right side were supplied as experimental inputs.

1.3 Conservation before conversion efficiency

For a stationary closed system, after an energy partition has been defined,

$$E_{\text{total}} = E_{\text{resolved}} + E_{\text{reserve}} + E_{\text{interaction}}. \tag{1.1}$$

A forward current and a reverse current redistribute this total. Negated conversion is different: it is the part of an attempted forward process that never leaves the reserve. It should not be subtracted from both sides. When the interaction energy is included in the reserve convention, the elementary balance is

$$\dot{E}_A = J_+ - J_-, \qquad \dot{E}_P = -J_+ + J_-. \tag{1.2}$$

Dots in this opening discussion denote local proper-time derivatives in the regime where a local clock interpretation exists. The later Hamiltonian construction first uses a local model time. Its calibration to proper time is stated separately rather than assumed to emerge from the word node.

The balance does not determine either current. For example, a constant-rate current, a delayed response, a coherent oscillatory exchange and a threshold-gated current can all preserve the same total. The construction below therefore specifies the additional modes that receive the transferred content. Resistance then appears after those modes are eliminated, not as an unexplained energy sink.

1.4 A field is not the same as a measured shortfall

For a specified forward interval with no reverse flow and common units, the dimensionless residual

$$\epsilon = \frac{E_{\text{available}} - E_{\text{actuated}}}{E_{\text{available}}} \tag{1.3}$$

is well defined when $E_{\text{available}} > 0$. It lies between zero and one only if both quantities refer to the same available budget and $0 \le E_{\text{actuated}} \le E_{\text{available}}$. If external work is supplied, energy returns during the interval, or an interaction contribution is omitted, those conditions need not hold.

A physical field, in contrast, has degrees of freedom, an energy or action, and evolution. The field cannot be reconstructed uniquely from one residual without an independently specified response law. In this monograph the explicit reserve coordinates provide one such realization. Their effect is a causal memory kernel and a force determined by their initial state. A residual is then a consequence of that dynamics and of the observation protocol.

1.5 Universal law, different circumstances

The strongest version of the proposal uses the same local law and the same fundamental parameters for every link of the constructed system. Different outcomes are generated by different initial states, geometry, accumulated proper time and accessible modes. A different result in a different environment is not a violation of universality. A different required fundamental coefficient in otherwise matched conditions would be.

This does not authorize arbitrary response functions for individual particles. If a response is invoked, it must be calculated from the selected dynamics before comparison. A proposed relation $O_i = f_i(g_*, \mathcal{I}_i)$ is informative only when the f_i and the allowed independent inputs $\mathcal{I}_i$ are fixed. Replacing each f_i after seeing its discrepancy would remove the test.

The old label n_c is therefore not assigned a new numerical meaning by decree. A coupling energy, a fractional conversion per interval, a rate, and a clock factor have different dimensions and different transformation rules. The constructed Hamiltonian uses explicit dimensional symbols. A future identification of one of them with a node constant would have to state the map.

1.6 What is chosen, what is derived

The conservative realization makes a specific choice: compact phases on a finite graph, a positive phase stiffness, positive inertias, and harmonic reserve modes coupled to phase differences through a periodic function. The lowest nontrivial periodic coupling is chosen as a convenient definite representative. These choices are new model assumptions, not uniquely forced by the qualitative premises.

From those assumptions the paper derives existence of trajectories, a lower energy bound, exact conservation, global phase symmetry, a reserve memory equation, equilibrium fluctuation–dissipation relations under an additional ensemble assumption, and explicit long-wavelength dispersion. A nonlinear readout example shows how a threshold can arise from an energy landscape. A quantum version and a covariant effective version are developed as additional, separately identified structures.

No physical target value was optimized to select the new finite-model demonstration. Reference calculations using measured constants are retained as reference calculations. The two classes of work are not added together into an empirical accuracy percentage. The methodology follows the same distinction used in dimensional metrology: exact numerical unit definitions, measured constants, and derived relations play different roles [38, 13, 39].

2. An explicit conservative node–reserve Hamiltonian

2.1 The state and the graph

Take a finite connected graph with n vertices and m oriented edges. The orientation is a bookkeeping choice. Its incidence matrix $B \in \mathbb{R}^{n\times m}$ has a $+1$ at the starting vertex and a -1 at the ending vertex of each edge. Each vertex carries a compact phase $\theta_i \in \mathbb{R}/(2\pi\mathbb{Z})$ and a

conjugate momentum p_i. The edge phase differences are

$$\delta = B^{\mathsf{T}}\theta. \tag{2.1}$$

For each edge e, introduce reserve coordinates $x_{e\lambda}$ and conjugate momenta $P_{e\lambda}$, with $\lambda = 1, \dots, s$. The phase variables represent the resolved node pattern. The additional coordinates represent degrees of freedom in which energy can be stored and from which it can return. They are not automatically a thermal bath, a dark-matter particle population, or a quantum vacuum.

Let $I > 0$ be the phase inertia, $K > 0$ the phase stiffness, $m_\lambda > 0$ reserve inertias and $\Omega_\lambda > 0$ reserve frequencies. A coupling c_λ has the units required by $c_\lambda x$ being an energy because the function f used below is dimensionless. The same parameter list is used on every edge. The graph, its size and the initial state are not fundamental coupling constants.

2.2 The master dynamical equation

The definite realization studied here is

$$\begin{aligned} H_* = {} & \sum_i \frac{p_i^2}{2I} + K \sum_e (1 - \cos\delta_e) \\ & + \sum_{e,\lambda} \left[\frac{P_{e\lambda}^2}{2m_\lambda} + \frac{m_\lambda \Omega_\lambda^2}{2} \left(x_{e\lambda} - \frac{c_\lambda f(\delta_e)}{m_\lambda \Omega_\lambda^2} \right)^2 \right], \qquad f(\delta) = \sin\delta. \end{aligned} \tag{2.2}$$

With $z = (\theta, x, p, P)$ and the canonical antisymmetric matrix $\mathbb{J}$, the evolution is

$$\boxed{\frac{\mathrm{d}z}{\mathrm{d}\tau} = \mathbb{J}\nabla H_*(z).} \tag{2.3}$$

This is the master equation of the constructed finite model. The state space, Hamiltonian and parameter class are explicit. The observable map is specified for each calculation. It is not presented as a uniquely established equation of all fundamental physics.

The form of the shifted square is important. Expanding it gives an interaction $-c_\lambda x_{e\lambda} f(\delta_e)$ and a positive counterterm $c_\lambda^2 f(\delta_e)^2/(2m_\lambda\Omega_\lambda^2)$. Omitting the counterterm changes the potential and the spectrum. Keeping the square also makes the lower energy bound transparent. Conservative reservoir constructions and their reduced dissipative equations have a substantial history [41, 44, 45]; the interpretation in terms of latent conversion is the hypothesis examined here, not a claim that the mathematical method is new.

2.3 Equations of motion

Define

$$y_{e\lambda} = x_{e\lambda} - \frac{c_\lambda f(\delta_e)}{m_\lambda \Omega_\lambda^2}, \qquad R_e = \sum_\lambda c_\lambda y_{e\lambda}. \tag{2.4}$$

Direct differentiation gives

$$\dot{\theta}_i = p_i/I, \tag{2.5}$$
$$\dot{p} = -B\big[K\sin\delta - f'(\delta)R\big], \tag{2.6}$$
$$\dot{x}_{e\lambda} = P_{e\lambda}/m_\lambda, \tag{2.7}$$
$$\dot{P}_{e\lambda} = -m_\lambda\Omega_\lambda^2 y_{e\lambda}. \tag{2.8}$$

Products of edge vectors in this section are componentwise. Since $f' = \cos\delta$, every term is smooth and periodic in the phases. Choosing a different periodic function would define a different model; it is not used as an adjustable correction to a residual.

The associated Lagrangian is obtained by eliminating the momenta:

$$L_* = \frac{I}{2}\sum_i \dot{\theta}_i^2 + \sum_{e\lambda}\frac{m_\lambda}{2}\dot{x}_{e\lambda}^2 - K\sum_e(1-\cos\delta_e) - \sum_{e\lambda}\frac{m_\lambda\Omega_\lambda^2}{2}\left(x_{e\lambda} - \frac{c_\lambda\sin\delta_e}{m_\lambda\Omega_\lambda^2}\right)^2. \tag{2.9}$$

The Euler–Lagrange equations reproduce (2.5). The kinetic and potential terms carry energy units. The action $\int L_*\mathrm{d}\tau$ carries energy times time. Nothing with energy-density units is added directly to a frequency or to a wavefunction.

2.4 Conservation and positivity

Theorem 2.1 (Conservative finite realization)**.** *For positive $I, K, m_\lambda, \Omega_\lambda$ and finite initial energy,* (2.3) *has a unique global trajectory on the finite graph. Its Hamiltonian is nonnegative and constant, and the total phase momentum $\sum_i p_i$ is conserved.*

Proof. All terms in (2.2) are nonnegative. The Hamiltonian vector field is locally smooth. Along a local solution,

$$\dot{H}_* = (\nabla H_*)^{\mathsf{T}}\mathbb{J}\nabla H_* = 0 \tag{2.10}$$

because $\mathbb{J}^{\mathsf{T}} = -\mathbb{J}$. Hence each momentum and each shifted reserve coordinate is bounded by the finite initial energy. Since $|\sin\delta| \le 1$, the unshifted reserve coordinates are bounded too. The phases lie on a compact torus; on an unwrapped representation their velocities remain bounded on any finite interval. Thus the solution cannot escape to infinity in finite time and the local solution extends globally. Finally $\mathbf{1}^{\mathsf{T}}B = 0$, so (2.5) implies $\mathrm{d}(\sum_i p_i)/\mathrm{d}\tau = 0$. □

The last conservation law is the Noether charge of a common phase shift $\theta_i \mapsto \theta_i + \theta_0$. It is an internal phase momentum. It should not be called physical electric charge until the electromagnetic representation and normalization have been established. The relation between a continuous symmetry and its conserved current is used in its conventional sense [40].

2.5 An explicit energy ledger

Partition the Hamiltonian as

$$H_A = \sum_i p_i^2/(2I) + K \sum_e (1 - \cos \delta_e), \tag{2.11}$$

$$H_R = H_* - H_A. \tag{2.12}$$

The reserve convention includes the interaction and counterterm. It is positive, but it is not a sum of independent free-reserve energies; changing δ changes the center of a reserve oscillator. This detail matters when interpreting an apparent shortfall.

Taking a time derivative gives

$$\dot{H}_A = \sum_e \dot{\delta}_e f'(\delta_e) R_e, \qquad \dot{H}_R = -\sum_e \dot{\delta}_e f'(\delta_e) R_e. \tag{2.13}$$

The current changes sign with the joint state. The reserve can absorb energy or return it. The quantity $\max(-\dot{H}_A, 0)$ measures instantaneous transfer out of the resolved sector in this partition, not destruction. Likewise $\max(\dot{H}_A, 0)$ measures transfer into it. There is no assumption that either is a universal constant.

An alternative partition separates a free oscillator energy and a signed interaction term. It produces the same total balance but different individual sector energies. Physical conclusions must therefore be phrased in terms of the total and explicitly chosen observables. A purported experimental energy deficit cannot be identified with H_R merely because both are unobserved.

2.6 How a frame is represented

A frame index can sample the exact flow:

$$z_{n+1} = \Phi_{\Delta\tau_n}(z_n), \tag{2.14}$$

where Φ_s is the Hamiltonian evolution for elapsed local time s. The group property is

$$\Phi_{s_2} \circ \Phi_{s_1} = \Phi_{s_1+s_2}. \tag{2.15}$$

Consequently a computational subdivision of the same interval does not alter the physical prediction. This is the appropriate standard for distinguishing a frame-dependent fraction from a universal rate or coupling.

Sampling a continuous flow does not establish that nature has a discrete elementary time step. A fundamental discrete update would be an additional selection. An explicit nearest-neighbor numerical stencil can possess an exact finite-step dependence cone but generally preserves a modified, rather than identical, Hamiltonian. An implicit exactly energy-preserving step need not have the same local dependence structure. These possibilities should not be conflated.

2.7 Time reversal and the meaning of return

The Hamiltonian is even in p and P. Reversing both momenta and evolving for an equal duration reverses the trajectory. Thus the finite model contains return without an independent

source term. It also means that irreversible conversion is not fundamental in this realization. Approximate irreversibility can result when reserve modes dephase, when their state is unobserved, or when a thermodynamic limit is taken.

That conclusion is constructive: it explains how conservative microscopic evolution can give a damped resolved pattern without deleting energy. It also identifies what is required before an exponential loss law is appropriate. A finite reserve with recurrent phases will generally remember its history, so a permanent one-way decay law cannot be assumed at every time scale.

2.8 Numerical realization and its meaning

The executed example uses six vertices in a ring, three reserve modes per edge, $I = K = 1$, $m_\lambda = 1$, frequencies $(0.65, 1.15, 2.4)$ and couplings $(0.22, 0.13, 0.07)$ in model units. These numbers were chosen to exercise nonlinear exchange and distinct reserve time scales. They were not chosen from a particle mass, a fine-structure measurement, a clock residual or a cosmological fit. Their full initial state is included in the machine-readable results.

For this example, the maximum relative Hamiltonian drift over sixty model-time units is 3.04×10^{-13}. Reversing the final momenta and integrating back gives a maximum state discrepancy of 1.67×10^{-13}. A nonuniform positive clock reparameterization agrees with the proper-time trajectory to 6.64×10^{-13}. These are checks of the stated equations and their implementation, not statements of nature's accuracy.

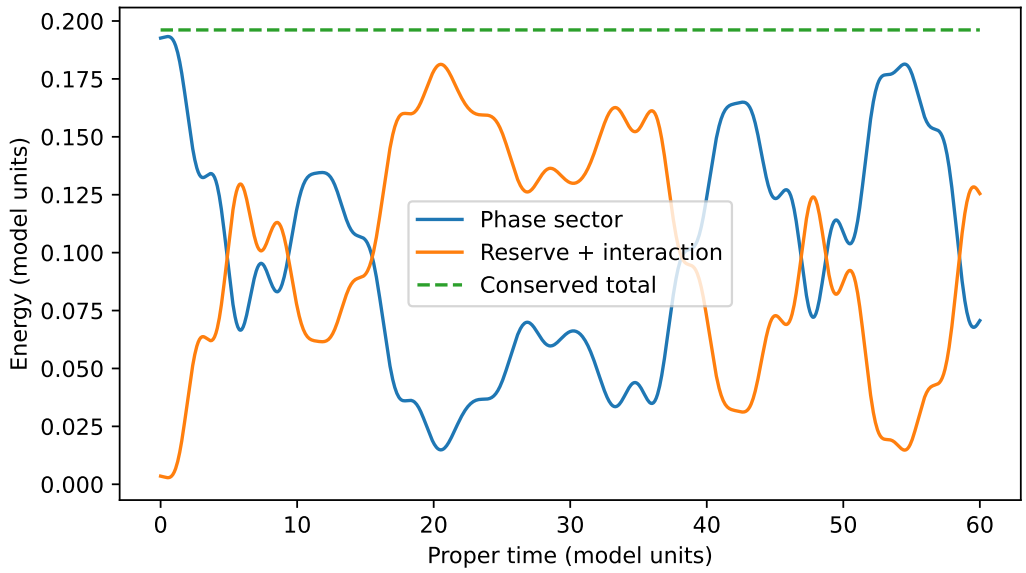

Figure 1: Executed conservative exchange in the six-node example. The reserve includes the interaction convention used in the Hamiltonian. The total remains constant while the resolved and reserve energies vary. All axes use declared model units; no physical measurement is plotted.

3. Deriving resistance, memory and return from the reserve

3.1 Eliminate a mode without losing its energy

The reserve equation is a driven oscillator,

$$\ddot{x}_{e\lambda} + \Omega_\lambda^2 x_{e\lambda} = \frac{c_\lambda}{m_\lambda} f(\delta_e). \tag{3.1}$$

Its exact solution is

$$x_{e\lambda}(\tau) = x_{e\lambda}(0)\cos\Omega_\lambda\tau + \frac{P_{e\lambda}(0)}{m_\lambda\Omega_\lambda}\sin\Omega_\lambda\tau + \frac{c_\lambda}{m_\lambda\Omega_\lambda}\int_0^\tau \sin[\Omega_\lambda(\tau-s)]f(\delta_e(s))\mathrm{d}s. \tag{3.2}$$

The integration is causal: only earlier values of the phase difference occur. This is an exact rewriting of the closed equations, not an additional random-force hypothesis.

Integrating the last term by parts and subtracting the moving equilibrium gives

$$y_{e\lambda}(\tau) = y_{e\lambda}(0)\cos\Omega_\lambda\tau + \frac{P_{e\lambda}(0)}{m_\lambda\Omega_\lambda}\sin\Omega_\lambda\tau - \frac{c_\lambda}{m_\lambda\Omega_\lambda^2}\int_0^\tau \cos[\Omega_\lambda(\tau-s)]\frac{\mathrm{d}f(\delta_e(s))}{\mathrm{d}s}\mathrm{d}s. \tag{3.3}$$

Define a memory function and an initial-state force,

$$M(\tau) = \sum_\lambda \frac{c_\lambda^2}{m_\lambda\Omega_\lambda^2}\cos\Omega_\lambda\tau, \tag{3.4}$$

$$\zeta_e(\tau) = \sum_\lambda c_\lambda\left[y_{e\lambda}(0)\cos\Omega_\lambda\tau + \frac{P_{e\lambda}(0)}{m_\lambda\Omega_\lambda}\sin\Omega_\lambda\tau\right]. \tag{3.5}$$

Then

$$R_e(\tau) = \zeta_e(\tau) - \int_0^\tau M(\tau-s)f'(\delta_e(s))\dot{\delta}_e(s)\mathrm{d}s. \tag{3.6}$$

Every coefficient in the memory function comes from the same Hamiltonian as the conservative force.

3.2 The exact reduced equation

Substitution into the node equation yields

$$I\ddot{\theta} + BK\sin\delta + B\left[f'(\delta)\int_0^\tau M(\tau-s)f'(\delta(s))\dot{\delta}(s)\mathrm{d}s\right] = B[f'(\delta)\zeta(\tau)]. \tag{3.7}$$

The notation inside the integral is componentwise on edges. The apparent resistance multiplies phase velocity, depends on history, and can depend on the current phase through f'. It is not a fixed percentage removed at each arbitrary frame. The reserve coordinates can always be reconstructed from the oscillator solution, restoring the exact energy ledger.

This is a nonlinear generalized Langevin equation of a specified conservative realization. The name does not mean that fundamental stochasticity has been introduced. For a specified initial state ζ_e is a deterministic function. A statistical force appears only when an ensemble of unknown reserve states is supplied. The distinction follows the separation between exact reservoir elimination and statistical coarse-graining [41, 42, 43].

3.3 Why the initial-state term cannot be discarded silently

Setting $\zeta = 0$ corresponds to a particular preparation, such as each reserve oscillator starting at its phase-dependent equilibrium with zero momentum. It is not the generic state of a reservoir. Starting instead from an equilibrium distribution generates both damping and fluctuations. Keeping the friction while discarding the accompanying preparation dependence can create false predictions for equilibrium, energy flow or conversion probability.

The microscopic current (2.13) becomes

$$\dot{H}_A = \sum_e \dot{f}(\delta_e(\tau))\zeta_e(\tau) - \sum_e \dot{f}(\delta_e(\tau)) \int_0^\tau M(\tau - s)\dot{f}(\delta_e(s))\mathrm{d}s. \tag{3.8}$$

The second term need not be negative at every instant for a finite memory kernel. A reservoir can return stored energy. Passivity constrains appropriate integrated work for a specified preparation; it does not require monotonic decrease of every resolved observable at every instant.

3.4 A memoryless approximation and its limits

Suppose a dense reserve spectrum produces a short correlation time τ_R, and suppose the resolved phase pattern changes slowly on that scale. If the causal convolution can be approximated by

$$\int_0^\tau M(\tau - s)\dot{f}(s)\mathrm{d}s \simeq \zeta_0 \dot{f}(\tau), \qquad \zeta_0 \geq 0, \tag{3.9}$$

then the reduced force is approximately viscous. The coefficient is the appropriate low-frequency integral of the causal kernel, not a new independently fitted correction. Conventions for a delta function on the causal endpoint can change a factor of two; defining the approximation through the integral avoids that ambiguity.

For small phase differences, $f' \simeq 1$, $\sin\delta \simeq \delta$, and $L = BB^{\mathsf{T}}$, giving

$$I\ddot{\theta} + KL\theta + \zeta_0 L\dot{\theta} = B\zeta_{\mathrm{noise}}. \tag{3.10}$$

In the deterministic zero-force approximation,

$$\frac{\mathrm{d}}{\mathrm{d}\tau}\left(\frac{I}{2}\|\dot{\theta}\|^2 + \frac{K}{2}\theta^{\mathsf{T}}L\theta\right) = -\zeta_0\|B^{\mathsf{T}}\dot{\theta}\|^2 \leq 0. \tag{3.11}$$

The lost resolved energy is assigned to the eliminated reserve. The homogeneous phase mode has $L\mathbf{1} = 0$ and is not damped by this difference coupling. That is a definite consequence of the symmetry, not an adjustable property.

A finite set of three reserve frequencies is not assumed to produce the memoryless limit. The numerical finite-ring experiment tests the exact memory relation. The viscous calculation is separately labeled as a limiting model and has its own declared parameter ζ_0.

3.5 A conditional fluctuation–dissipation theorem

Assume, additionally, that the initial shifted reserve coordinates are independent canonical variables at temperature T_R with the node phases held fixed. Then

$$\langle y_{e\lambda}(0) y_{e'\lambda'}(0)\rangle = \delta_{ee'}\delta_{\lambda\lambda'}\frac{k_B T_R}{m_\lambda \Omega_\lambda^2}, \tag{3.12}$$

$$\langle P_{e\lambda}(0) P_{e'\lambda'}(0)\rangle = \delta_{ee'}\delta_{\lambda\lambda'} m_\lambda k_B T_R, \tag{3.13}$$

and the mixed covariance vanishes. Substitution into (3.4) gives

$$\boxed{\langle \zeta_e(\tau)\zeta_{e'}(s)\rangle = \delta_{ee'} k_B T_R M(\tau - s).} \tag{3.14}$$

The proof uses $\cos a \cos b + \sin a \sin b = \cos(a - b)$. It exposes a valuable linked prediction: the same reserve coupling that determines the response also determines fluctuations, once the state and temperature are known. A damping fit and a noise fit cannot then be chosen independently.

Equation (3.14) is classical. In the harmonic quantum equilibrium version, the symmetrized force spectrum contains $\hbar\Omega \coth(\hbar\Omega/(2k_B T_R))$ in place of its classical thermal limit. That statement relies on quantization and thermal preparation, not solely on deterministic node dynamics [44, 45]. No temperature is inferred from an unrelated cosmological discrepancy.

3.6 Spectral density and positivity

For a continuum reserve, define

$$J(\Omega) = \frac{\pi}{2}\sum_\lambda \frac{c_\lambda^2}{m_\lambda \Omega_\lambda}\delta(\Omega - \Omega_\lambda), \qquad M(t) = \frac{2}{\pi}\int_0^\infty \frac{J(\Omega)}{\Omega}\cos \Omega t \mathrm{d}\Omega. \tag{3.15}$$

The spectral measure is nonnegative because the microscopic inertias are positive and the coefficients are squared. It is the allowed reserve spectrum, rather than a freely chosen function added independently in each domain, that controls the reduced response. An Ohmic low-frequency form may yield viscous behavior after a finite cutoff and suitable time-scale separation are specified.

The real and imaginary parts of a causal linear response are connected under the usual analyticity and falloff conditions. Therefore a proposal to change attenuation while leaving every reactive frequency correction untouched requires checking the entire response, including any subtraction or instantaneous term. The positive microscopic construction provides a direct way of doing this without guessing unrelated corrections.

3.7 An exact numerical check of elimination

The reserve oscillator equations were integrated directly. Independently, the force on each edge was calculated from (3.6) using quadrature of the recorded phase trajectory. Seven proper times and all six edges were used. The largest discrepancy between the direct and eliminated expressions is 3.15×10^{-14} in model-force units. The state-dependent $\cos\delta$ factors and the preparation term were retained.

This check is more informative than verifying only a total-energy sum: it tests the proposed mechanism that turns conservative storage into apparent resistance. It establishes that the reduced equation is an accurate rewriting of the constructed model. It does not identify the reserve with a measured cosmological field or select its physical frequencies.

3.8 The result for the EQEF interpretation

The reserve realization supplies a mathematically concrete meaning for resistance and return. It replaces an unspecified scalar shortfall with a state, energy and response. It also shows why the two common simplified pictures differ. Coherent exchange can oscillate; a memoryless ensemble can relax exponentially. Both may approximate different regimes of one conservative system, but neither should be called universal without the preparation and scale assumptions that justify it.

The outstanding physical task is now narrower: determine which reserve degrees of freedom, spectral measure and observable map are physically selected. The mathematical result does not depend on hiding that selection problem. Once it is supplied, dispersion, damping, fluctuations and conversion statistics must be calculated from the same parameters.

4. One response function for storage, drag and fluctuations

4.1 The observable consequence of eliminating the reserve

The microscopic construction does more than conserve a sum. It links effects that would otherwise be independently adjustable. The same reserve spectrum enters the delayed force, the frequency response, and, after a thermal preparation is specified, the fluctuations. This linkage is the most direct experimental content of the reconstructed conversion picture. It is a familiar physical mechanism, developed in the generalized Langevin and linear-response literature [41, 42, 43], rather than a new interpretation of every unexplained experimental residual.

Linearize about aligned phases and write $L = BB^T$. For an eigenvector of L with positive eigenvalue λ, denote the mode coordinate by Q. Its equation with an external generalized force F is

$$I\ddot{Q} + K\lambda Q + \lambda \int_0^\tau M(\tau - s)\dot{Q}(s)\,\mathrm{d}s = F(\tau) + \xi(\tau). \tag{4.1}$$

Dots in this section mean the local evolution parameter τ. A common preparation at a finite initial time introduces the initial terms already derived in Section 3. A stationary response is a later idealization in which the perturbation was applied sufficiently far in the past. The distinction matters for an experiment that prepares the reserve and immediately measures conversion.

The graph zero mode, $\lambda = 0$, is special. Link forces cannot damp a uniform rotation because they depend on phase differences. It obeys $I\ddot{Q}_0 = F_0$. An asserted universal loss that also damps this zero mode would change the symmetry and would not be the present Hamiltonian model. Thus the same construction predicts both where drag acts and where it does not.

4.2 Derivation of the susceptibility

Use the convention $Q(\tau) \propto e^{-\mathrm{i}\omega\tau}$ and define the retarded transform

$$\widetilde{M}(\omega) = \lim_{\varepsilon\downarrow 0} \int_0^\infty M(s) e^{(\mathrm{i}\omega-\varepsilon)s}\,\mathrm{d}s. \tag{4.2}$$

For a response to a force of the same frequency, substitution in (4.1) gives

$$\chi_\lambda(\omega) = \frac{Q(\omega)}{F(\omega)} = \frac{1}{K\lambda - I\omega^2 - \mathrm{i}\omega\lambda\widetilde{M}(\omega)}. \tag{4.3}$$

The infinitesimal convergence factor specifies the causal prescription. For a finite oscillator reserve the transform contains sharply located poles and distributional spectral weights; it should not be interpreted as a smooth constant friction function.

Writing $\widetilde{M} = M_R + \mathrm{i}M_I$ shows separately the reactive and dissipative terms:

$$\chi_\lambda^{-1} = K\lambda - I\omega^2 + \omega\lambda M_I - \mathrm{i}\omega\lambda M_R. \tag{4.4}$$

The real part shifts the response frequency. The imaginary part broadens or damps it. It is not consistent to choose a desired frequency correction from one reserve spectrum and a damping correction from an unrelated spectrum while calling the two a single prediction. Their common origin is the selected Hamiltonian and preparation.

For a harmonic drive $F(\tau) = \mathrm{Re}(F_0 e^{-\mathrm{i}\omega\tau})$, the averaged input power is

$$\overline{F\dot{Q}} = \frac{\omega|F_0|^2}{2}\,\mathrm{Im}\,\chi_\lambda(\omega). \tag{4.5}$$

Positive absorption therefore requires $\mathrm{Im}\,\chi_\lambda \geq 0$ at positive ω. In this passive construction that follows from $M_R \geq 0$ on its spectral support. Negative absorption can occur in an actively prepared or driven reserve, but then the delivered work comes from its changing state. It is not energy from nothing.

4.3 A finite-memory example that can be solved without a fit

An analytically useful limiting reserve has

$$M(s) = \frac{\zeta}{t_b} e^{-s/t_b}, \qquad s \geq 0, \quad \zeta, t_b > 0. \tag{4.6}$$

The one-sided transform is

$$\widetilde{M}(\omega) = \frac{\zeta}{1 - \mathrm{i}\omega t_b}, \quad M_R = \frac{\zeta}{1+\omega^2 t_b^2}, \quad M_I = \frac{\zeta\omega t_b}{1+\omega^2 t_b^2}. \tag{4.7}$$

The friction is approximately memoryless only when $|\omega t_b| \ll 1$. At larger frequency it rolls off, and the reactive contribution changes at the same time. The single number ζ is not a per-frame conversion fraction. The pair (ζ, t_b) characterizes this deliberately specified effective spectrum.

Define an auxiliary variable

$$Z(\tau) = \int_0^\tau M(\tau - s)\dot{Q}(s)\,\mathrm{d}s. \tag{4.8}$$

Differentiation gives $t_b\dot{Z} = -Z + \zeta\dot{Q}$. The deterministic homogeneous system becomes

$$\frac{\mathrm{d}}{\mathrm{d}\tau}\begin{pmatrix} Q \\ V \\ Z \end{pmatrix} = \begin{pmatrix} 0 & 1 & 0 \\ -K\lambda/I & 0 & -\lambda/I \\ 0 & \zeta/t_b & -1/t_b \end{pmatrix}\begin{pmatrix} Q \\ V \\ Z \end{pmatrix}. \tag{4.9}$$

Its characteristic polynomial, after multiplication by It_b, is

$$It_b s^3 + Is^2 + (K\lambda t_b + \lambda\zeta)s + K\lambda = 0. \tag{4.10}$$

For positive $I, K, \lambda, \zeta, t_b$, all coefficients are positive, and the cubic stability inequality is

$$I(K\lambda t_b + \lambda\zeta) > It_b K\lambda, \tag{4.11}$$

which reduces to $I\lambda\zeta > 0$. Thus all poles lie in the left half-plane. This proves stability for this effective memory law; it is not a proof that every phenomenological drag function is stable.

The accompanying calculation evaluates 25 combinations of mode eigenvalue and frequency, verifies the response identity and passivity, and checks five pole spectra. The numerical choices $I = K = 1$, $\zeta = 0.12$, $t_b = 0.7$ are declared model units. They are not inferred from the six-node finite reserve or from astronomical measurements. Keeping the two examples distinct avoids presenting a change of reserve as an unannounced improvement of one model.

4.4 Fluctuations and an independent cross-check

With a classical canonical preparation of the reserve at temperature T, the mode-force covariance is

$$\langle\xi(\tau)\xi(s)\rangle = \lambda k_B T M(|\tau - s|). \tag{4.12}$$

Let $S_\xi(\omega)$ denote its two-sided stationary spectrum. Fourier transformation gives

$$S_\xi(\omega) = 2\lambda k_B T M_R(\omega). \tag{4.13}$$

The phase spectrum is $S_Q = |\chi_\lambda|^2 S_\xi$. Because

$$\operatorname{Im}\chi_\lambda = \omega\lambda M_R|\chi_\lambda|^2, \tag{4.14}$$

we obtain the classical fluctuation–dissipation relation

$$\boxed{S_Q(\omega) = \frac{2k_B T}{\omega}\operatorname{Im}\chi_\lambda(\omega).} \tag{4.15}$$

This is a second measurement channel, not a second free coefficient. A measured susceptibility and a measured fluctuation spectrum must agree through the same T and the same preparation assumptions. The formula is classical. In a quantum equilibrium calculation the symmetrized spectrum contains the corresponding $\hbar\coth(\hbar\omega/2k_B T)$ factor; a quantum preparation and operator correlations must be supplied before using that expression [43].

The finite thermal reserve need not make the deterministic equations stochastic. Randomness enters this calculation only through the ensemble of initial bath coordinates. A single fully specified initial state has a definite trajectory. Thermal probabilities are therefore a coarse-grained description in this construction. This explains how an effectively noisy reduced equation can coexist with deterministic full dynamics without claiming to derive the quantum Born rule.

4.5 A practical three-observable test

An implementation of the reconstruction can measure a free ringdown, a driven susceptibility and an undriven fluctuation spectrum. The microscopic parameters, reserve preparation and mode normalization are recorded once. Ringdown determines pole locations. Driven response checks both amplitude and phase over frequency. Equilibrium fluctuations test (4.15). The test fails for the selected model if one spectrum cannot account for all three after stated measurement uncertainties.

A damping fit alone is weak because many kernels reproduce an approximately exponential envelope over a short interval. The cross-observable requirement is stronger: it predicts the dispersive shift and noise from the same kernel. A successful laboratory analogue would validate the specified conservative transfer mechanism on that platform. Connecting it to elementary particles, clocks or spacetime would still require identifying the same degrees of freedom and normalization in those systems.

4.6 What the memory time means for frames

An observation interval much shorter than t_b resolves reversible storage. An interval much longer than t_b, but shorter than a finite-reserve recurrence time, may support an effective one-way description. A frame fraction therefore depends on temporal resolution even when microscopic couplings are unchanged. This is the precise version of the idea that the observed conversion changes with elapsed time.

Changing temporal resolution is not the same operation as changing physical clock rate. The first changes which features of a fixed trajectory are resolved; the second changes the parameter used to describe the same trajectory. Both must be recorded when comparing apparent losses. Neither authorizes adjusting the underlying reserve spectrum separately for every particle.

5. Actuation as a conservative threshold process

5.1 A threshold must belong to dynamics

A threshold can be a useful definition of an event, but a label alone does not explain how a system changes state. In particular, replacing a wavefunction by a localized state and deleting the remainder need not conserve energy, probability or information. The conservative formulation instead includes a physical readout coordinate. Its energy landscape can have two stable regions separated by a barrier. A sufficiently strong interaction changes that landscape and produces a transition.

This is a model of a threshold event, not a derivation of the quantum measurement postulate. It is introduced to implement the intended meaning of actuation without a nonconservative reset. Nonlinear instability, metastability and readout are familiar physical concepts, so they do not require a new vocabulary.

5.2 Coherence as an available control variable

For a finite cluster of N node phases define

$$S = \sum_{j=1}^{N} e^{i\theta_j}, \qquad C = \frac{|S|^2}{N^2}. \tag{5.1}$$

The triangle inequality gives $0 \le C \le 1$. Complete phase alignment gives $C = 1$. This dimensionless number measures coherence, not energy. To turn it into an energy bias, a coupling with energy units must be supplied. It is invariant under a common phase shift but not under independent local phase rotations unless comparison links are included.

Its derivative is

$$\frac{\partial C}{\partial \theta_i} = -\frac{2}{N^2} \sum_j \sin(\theta_i - \theta_j), \qquad \sum_i \frac{\partial C}{\partial \theta_i} = 0. \tag{5.2}$$

The second identity shows that coupling a readout to C preserves the global phase symmetry. For locality, the cluster must be restricted to a declared finite neighborhood. An unbounded sum over the whole lattice would be a different interaction.

5.3 An explicit readout potential

Introduce a dimensionless readout coordinate z with conjugate momentum p_z, inertia M_D and energy scale E_D. Choose

$$H_D = \frac{p_z^2}{2M_D} + E_D \left[\frac{1}{4}(z^2 - 1)^2 - uz \right], \qquad u = u_0 + \lambda C. \tag{5.3}$$

Here u_0 and λ are dimensionless. For a frozen control u, stationary readout states satisfy

$$z^3 - z - u = 0, \qquad U''(z) = E_D(3z^2 - 1). \tag{5.4}$$

A minimum loses stability when $U' = U'' = 0$. For the initially negative well this occurs at

$$z_c = -\frac{1}{\sqrt{3}}, \qquad u_c = \frac{2}{3\sqrt{3}} = 0.3849001794\ldots. \tag{5.5}$$

There is no microscopic numerical fit in this value: it follows from the chosen quartic normal form. The normal form itself is a model assumption.

For $|u| < u_c$ there are two local minima and a barrier. For $u > u_c$ the negative local minimum is absent. A system near that well is driven away. The subsequent motion can overshoot; a transition is not automatically an irreversible settled record. Coupling the readout to additional conservative reserve modes allows energy to spread and the readout to remain near the new well over a useful observation time.

5.4 Back-reaction and energy accounting

When $u = u_0 + \lambda C(\theta)$ is dynamical, the readout force acts back on the node phases. The interaction contribution is $-E_D \lambda z C$, giving

$$\dot{p}_i\big|_D = E_D \lambda z \frac{\partial C}{\partial \theta_i}, \qquad M_D \ddot{z} = -E_D [z^3 - z - u_0 - \lambda C]. \tag{5.6}$$

Using both equations with the total Hamiltonian preserves total energy. Treating C as an externally imposed function but omitting its work would not. The quartic z^4 term dominates the bounded-coherence linear coupling for large $|z|$, so the total potential remains bounded below.

The frozen-control threshold is an adiabatic diagnostic. In the full coupled system, the source can react, the bias can vary, and finite-rate passages can delay the transition. Therefore the value u_c is not a universal measured particle-formation energy. It is a precisely derived conditional threshold, suitable for checking a dynamical implementation.

5.5 Negation and return in this model

Negated conversion can mean that the source does not maintain a sufficient bias or supply sufficient energy to cross a barrier during the observation interval. The energy then remains in the source and reserve. Return can mean that a readout excitation or localized pattern transfers energy back through the same conservative couplings. Both processes can occur without deleting part of the state.

A detector event can be defined by a specified crossing and a persistence interval, for example $z > z_{\mathrm{read}}$ for a time $\Delta\tau_{\mathrm{read}}$. These are instrument definitions, not new universal constants. A fundamental actuation claim would require a source-independent reason for identifying this readout process with physical realization itself.

5.6 Why the threshold does not determine Born probabilities

Let λ_0 denote the complete initial microstate and let D_k be the set of initial microstates whose deterministic trajectories produce outcome k. For an initial ensemble measure μ, the event frequency is

$$P(k) = \mu(D_k). \tag{5.7}$$

Determinism specifies the basins D_k once the full dynamics is known. It does not by itself specify the ensemble measure. Changing μ can change $P(k)$ without changing the equations. Showing that $P(k) = |a_k|^2$ therefore requires a derivation of the relevant state space, preparation measure and measurement map, not merely a threshold.

The Hilbert-space construction later in this monograph supplies a conventional quantum completion and proves its own probability and no-signalling properties. Those results are conditional on that structure [4, 6, 7, 5]. The conservative readout model here neither replaces those theorems nor evades their assumptions by a change in terminology.

5.7 A useful separation of tasks

The threshold construction closes a specific mathematical task: it gives a conservative mechanism with a calculable instability and back-reaction. The particle spectrum, quantum statistics and physical detector coupling remain distinct tasks. This separation prevents a successful double-well simulation from being counted as an electron-mass prediction or a Bell experiment.

It also offers an economical experimental strategy. Once the source coupling and readout potential are independently calibrated, the threshold, finite-rate delay, energy redistribution and return behavior are linked outputs. A discrepancy cannot be repaired by assigning an unrelated threshold to every observed event. That is the same universality standard applied elsewhere in the paper.

6. Relational clocks and the limits of a universal timing correction

6.1 Order does not yet specify a clock

An autonomous differential equation orders states. It does not, by itself, tell an experimenter which internal process measures a second. A phase recurrence can serve as a clock when its period is reproducible under the conditions of use. The nonlinear period calculation in the previous section demonstrates that amplitude is one condition which matters. Exchange with a reserve can also change a clock's trajectory unless the clock is protected or its response is modeled.

A microscopic theory of clocks must distinguish the coordinate used to solve equations, the reading of a material clock, and relativistic proper time. The three can be related, but equating them by notation is not a derivation. This section makes a relational formulation explicit before the ordinary relativistic comparison equations are developed.

6.2 A parameter-independent action

Introduce an ideal clock coordinate T and conjugate momentum P_T. A parametrized action is

$$S = \int \mathrm{d}\lambda \left[\sum_a p_a q_a' + P_T T' - N(\lambda)(P_T + H_*(q,p)) \right]. \tag{6.1}$$

Here λ is an arbitrary trajectory label, primes are its derivatives, and $N > 0$ is a lapse. Variation gives

$$T' = N, \quad P_T' = 0, \quad P_T + H_* = 0, \quad q_a' = N\frac{\partial H_*}{\partial p_a}, \quad p_a' = -N\frac{\partial H_*}{\partial q_a}. \tag{6.2}$$

Dividing by T' recovers the Hamilton equations in the clock variable T. Replacing the arbitrary label λ leaves the relational trajectory $q(T)$ unchanged.

This construction is exact, but it introduces an ideal clock. It does not prove that the physical universe possesses a globally perfect internal clock or that the total physical energy of the universe is zero. The constraint expresses a parametrization convention for the enlarged system. Relational formulations have a well-developed literature [47, 48]; the present use is an explicit representation of the required distinction.

6.3 Material clocks and finite monotonic intervals

A real clock coordinate can oscillate or turn around. It can parameterize another trajectory only over a region where its reading is monotonic and distinguishable. To make a continuing clock one can count complete cycles in addition to phase, or use a stable train of events. A clock observable is therefore a function of state and a history convention, not merely the name of an update index.

In the finite conservative model, changing the initial energy or reserve state can change recurrence periods. A universal physical proper-time law would require all acceptable material clocks to compare consistently after their known environmental shifts are included. That stronger equivalence has not been derived from the six-node example.

The stochastic first-passage examples later in the book are used as diagnostic ensemble models for recurrence. Their input distributions describe preparation uncertainty or an effective process; they are not substituted for the deterministic Hamiltonian at the microscopic level. Their finite-mean statements are conditional mathematical results.

6.4 Proper time is local to timelike trajectories

With an effective metric of signature $(-, +, +, +)$,

$$\mathrm{d}\tau^2 = -g_{\mu\nu}\mathrm{d}x^\mu \mathrm{d}x^\nu / c^2. \tag{6.3}$$

This is a worldline interval. It is not a single global scalar time simultaneously assigned to all trajectories. For an inertial clock with speed v in a Minkowski coordinate system, $\mathrm{d}\tau/\mathrm{d}t = \sqrt{1 - v^2/c^2}$. A photon travels on a null trajectory and has no nonzero elapsed proper time along that trajectory. Photonic phases and observed rates must be compared through emitter and receiver clocks or a field propagation calculation, not through a photon rest clock.

Consequently replacing t by τ in every expression cannot be a universal correction procedure. A rest-frame particle lifetime, an observed photon frequency, a detector exposure and a cosmological age require distinct but consistent operational definitions. The next section works these out using conventional relativity [28, 29, 30].

6.5 A uniform rescaling can be unobservable

Suppose every local evolution law and every measuring clock receives the same positive scalar factor $q(t)$:

$$\frac{\mathrm{d}z}{\mathrm{d}t} = q(t)F(z), \qquad \frac{\mathrm{d}T}{\mathrm{d}t} = q(t). \tag{6.4}$$

Then $\mathrm{d}z/\mathrm{d}T = F(z)$. Without a separately predicted geometric effect or a differently responding reference, the factor is removed from the comparison. This is a mathematical degeneracy, not evidence that the factor vanishes physically.

It follows that a universal EQEF effect cannot be measured solely by comparing two processes which it rescales identically. An experiment needs independently known attempts, a response difference fixed by the theory, a measurable reserve flux, a spectral effect or a gravitational consequence. This is why an absolute conversion fraction cannot be extracted from an arbitrary set of accurately ticking clocks.

6.6 Why timing does not repair every constant formula

The rest mass defined from a Lorentz-invariant energy–momentum relation is not multiplied by a coordinate lapse. A dimensionless coupling inferred from dimensionless observables is not changed simply by calling a different interval one second. Actual field dependence of masses or couplings is possible, but it must be derived from an interaction in the action and tested against the corresponding observables.

A consistent response calculation can contain both a dynamical EQEF contribution and a proper-time comparison. It must not count the same effect twice. The retained-relativity branch computes the metric clock factor and then tests additional conversion effects. A replacement-relativity branch would have to derive the metric and clock comparisons from node dynamics. The two branches are not combined opportunistically when one result fits better.

Part II

Clocks, conversion and inference

7. Proper time, event rates and energy measurements

7.1 An invariant interval before a rate correction

In the retained-relativity branch, a timelike trajectory has proper time

$$\mathrm{d}\tau^2 = -\frac{1}{c^2} g_{\mu\nu} \mathrm{d}x^\mu \mathrm{d}x^\nu, \tag{7.1}$$

with signature $(-,+,+,+)$. In flat spacetime, $\mathrm{d}\tau/\mathrm{d}t = \sqrt{1 - v^2/c^2}$ for a trajectory of speed v relative to the inertial coordinate system. This relation concerns the interval on a worldline. It is not a blanket rule for replacing an invariant particle mass or a dimensionless coupling by a smaller number. Relativistic kinematics and the standard interpretation of invariant mass provide the reference convention used here [28, 8].

A photon has zero proper time along its null trajectory. Consequently, a photon emission or detection rate must be expressed using the source, detector or other specified observer's clock, not a photon rest clock. Likewise an ultrarelativistic neutrino oscillation calculation conventionally uses a laboratory baseline and propagation energy. The symbol τ in an effective generator must always identify whose clock it represents.

For weak gravitational fields and slow velocities, the retained metric gives

$$\frac{\mathrm{d}\tau}{\mathrm{d}t} = 1 + \frac{\Phi}{c^2} - \frac{v^2}{2c^2} + O(c^{-4}). \tag{7.2}$$

The gravitational potential and the velocity are inputs determined independently of the output used to test conversion. Estimating them from that same unexplained residual would create a circular correction.

7.2 The transformation of a count

An event count N is independent of how its history is parametrized. If $r_\tau = \mathrm{d}N/\mathrm{d}\tau$, then

$$r_t = \frac{\mathrm{d}N}{\mathrm{d}t} = q\, r_\tau. \tag{7.3}$$

Integrating, rather than merely comparing instantaneous symbols, gives

$$N(t_2) - N(t_1) = \int_{t_1}^{t_2} q(t) r_\tau(\tau(t))\, \mathrm{d}t = \int_{\tau_1}^{\tau_2} r_\tau(\tau)\, \mathrm{d}\tau. \tag{7.4}$$

This is an exact change of variable. A correct clock transformation changes quoted rates but not the number of observed events. If an analysis appears to create or remove events through a time-coordinate change, its intensity or its integration measure has been transformed inconsistently.

For a constant conversion fraction and a known time-dependent attempted rate, define the exposure

$$K = \int \epsilon_{\mathrm{det}}(t) q(t) r_0(t)\, \mathrm{d}t. \tag{7.5}$$

The expected count is $\mu = \eta K$. With background b, it is $\mu = b + \eta K$. When η varies, the ratio $(\mu - b)/K$ is a weighted average,

$$\overline{\eta}_w = \frac{\int \epsilon_{\mathrm{det}} q r_0 \eta\, \mathrm{d}t}{\int \epsilon_{\mathrm{det}} q r_0\, \mathrm{d}t}, \tag{7.6}$$

not the unweighted arithmetic mean of the efficiency. This is important when the source changes over an orbit, a pulse or a cosmological epoch.

7.3 Finite transition probabilities are not rates

A constant local return rate Γ produces survival

$$S(\tau) = \exp(-\Gamma\tau). \tag{7.7}$$

The probability of return during a step $\Delta\tau$ is

$$p(\Delta\tau) = 1 - \exp(-\Gamma\Delta\tau). \tag{7.8}$$

Subdividing an interval into m equal steps gives $[1 - p(\Delta\tau/m)]^m = \exp(-\Gamma\Delta\tau)$, exactly. Holding the same numerical per-step fraction while changing the number of steps defines a different physical process. The approximation $p \simeq \Gamma\Delta\tau$ is appropriate only at small step size.

Thus a frame-dependent apparent fraction is not necessarily a particle-dependent fundamental constant. A rate can be universal while its integrated probability changes with the elapsed proper time. Conversely, a physically fundamental discrete frame interval, if asserted, is additional structure and must be defined rather than treated as an arbitrary numerical integration step.

7.4 Three different treatments of relativity

Retained metric. The main numerical branch uses the metric clock factor already specified by relativity and asks whether an additional conversion effect is identifiable. Its event equation is $\lambda = \epsilon_{\mathrm{det}} q_{\mathrm{GR}} \eta r_0$. This is a clear conservative extension test. It does not derive the metric from EQEF.

Modified clock dynamics. A second branch could derive a clock response $q(\phi, x, u)$ from a common action. The same action must determine photon propagation, matter response and the relevant comparison standards. A freely selected function $q_i(t)$ for every dataset is not a universal modification. An additional conversion factor is permissible only for an effect not already encoded in q.

Replacement. A third branch could derive the entire observable clock progression from the conversion dynamics. Write $\mathrm{d}T = \chi(s, \phi)\mathrm{d}t$ and predict the detector intensities directly in T. Multiplying by q_{GR} again after identifying χ with the full clock effect would double count time dilation. Such a replacement must reproduce the measured relations between clocks, moving particles, light signals and gravitational trajectories. Optical-clock and stored-muon measurements supply independent empirical anchors [29, 30, 31, 32].

These are distinct hypotheses, not interchangeable choices made after a residual is known. This edition fully develops the retained-metric balance and its transformations. The other two are defined as alternative physical constructions requiring additional equations.

7.5 Energy transmission includes more than clock rate

For a photon with four-momentum p^μ, an observer with normalized four-velocity u^μ measures energy proportional to $-p_\mu u^\mu$, with the chosen factors of c restored consistently. The ratio between receiver and emitter is an invariant contraction evaluated at the two endpoints. A received *power* includes both energy per photon and photons per receiver time. Therefore it cannot in general be corrected by the single factor used for a local event rate.

For a stationary gravitational comparison with no absorption, the same frequency redshift factor changes both photon energy and the arrival rate; received power can contain its square before geometric collection effects. For cosmological bolometric flux, luminosity distance already includes the energy and arrival-time redshifts. Adding another $(1 + z)^{-1}$ to a correctly defined luminosity-distance formula repeats a correction.

The operational rule is simple: identify the observable first. Is it a count, frequency, energy, probability, cross section, flux or invariant mass? Then derive its transformation. The count-intensity relation $\lambda = \epsilon_{\mathrm{det}} q \eta r_0$ applies directly to a local event count. Other observables need their own forward map.

7.6 Rate ratios and the common-factor cancellation

Suppose two co-located clock processes have baseline frequencies ν_1^0, ν_2^0 and share a factor $q\eta$. Then

$$\frac{\nu_1^{\mathrm{obs}}}{\nu_2^{\mathrm{obs}}} = \frac{q\eta\nu_1^0}{q\eta\nu_2^0} = \frac{\nu_1^0}{\nu_2^0}. \tag{7.9}$$

A shared clock factor is unobservable in that ratio. A nonzero relative effect requires different predicted sensitivities, separated physical conditions, or a reference process not subject to the same factor. The sensitivities must follow from the chosen microscopic or effective dynamics.

This cancellation explains why a universal time correction cannot be used as a universal repair for incorrect values of dimensionless constants. It may alter inferred event rates when clock intervals were mismatched. It cannot alter a properly formed same-clock ratio merely by changing time units. A dynamical change to the underlying spectrum or interaction is a separate hypothesis.

7.7 Uncertainty must follow the transformation

For the local estimate $\widehat{\eta} = R/(qr_0)$, omitting detector factors only for clarity, first-order propagation gives

$$\mathrm{d}\log\eta = \mathrm{d}\log R - \mathrm{d}\log q - \mathrm{d}\log r_0. \tag{7.10}$$

If Σ is the covariance matrix of these three logarithmic estimates, the variance of $\log\eta$ is $v^T\Sigma v$ with $v = (1, -1, -1)$. Correlations matter. If the same calibration enters R and r_0, treating it as two independent uncertainties is wrong. If q was fitted from R, treating it as an independent correction is also wrong.

Near a physical boundary such as $\eta = 1$, a noisy central estimate can exceed one. This should not be silently truncated and then described as evidence of complete conversion. The likelihood, boundary and interval construction must be stated. The computational volume retains signed residuals and distinguishes them from the allowed parameter space.

8. Conservative dynamics and their exact solutions

8.1 A minimal two-reservoir closure

The conservation equation becomes executable after currents are specified. A useful illustrative closure is

$$J_+ = aE_P, \qquad J_- = bE_A, \qquad a \geq 0, \quad b \geq 0, \tag{8.1}$$

where $a = \eta k$ may separate an attempted rate k from conversion efficiency. Both a and b have inverse-proper-time units. These are new effective choices, not quantities already fixed by the primitive node ontology. With constant total E,

$$\frac{\mathrm{d}E_A}{\mathrm{d}\tau} = a(E - E_A) - bE_A = aE - (a+b)E_A. \tag{8.2}$$

For $a + b > 0$, set $E_A^* = aE/(a+b)$. Subtracting the stationary equation and integrating yields

$$E_A(\tau) = E_A^* + [E_A(0) - E_A^*]e^{-(a+b)\tau}, \qquad E_P(\tau) = E - E_A(\tau). \tag{8.3}$$

This provides three distinct observables: the equilibrium fraction $a/(a+b)$, the relaxation time $(a+b)^{-1}$ and the initial condition. A single stationary fraction identifies the ratio a/b, not both rates separately. A time-resolved relaxation together with the equilibrium can identify both under this model.

Proposition 8.1 (Positivity and conservation)**.** *For $a, b \geq 0$ and initial $0 \leq E_A(0) \leq E$, the solution stays in $0 \leq E_A(\tau) \leq E$ for all $\tau \geq 0$, and $E_A + E_P = E$.*

Proof. Equation (8.3) is a convex combination of $E_A(0)$ and E_A^* because the exponential lies in $[0, 1]$. Both endpoints lie in $[0, E]$. The second expression gives conservation and positivity of the reserve. The case $a = b = 0$ is constant and satisfies the same conclusion. □

No energy has disappeared when E_A decreases. It is transferred into E_P. Likewise, positive attempted transfer is not itself proof of increased expression: reverse transfer can exceed forward transfer at a given state.

8.2 Nonuniform clocks

In a reference parameter t, the same solution is

$$E_A(t) = E_A^* + [E_A(0) - E_A^*] \exp\left[-(a+b) \int_0^t q(s)\, \mathrm{d}s\right]. \tag{8.4}$$

For the illustrative positive lapse $q(t) = 0.8 + 0.1 \cos t$,

$$\tau(t) = 0.8t + 0.1 \sin t. \tag{8.5}$$

The equilibrium fraction does not depend on this clock convention. The approach to equilibrium as a function of t does. This is a precise example of a common physical law producing different apparent reference-time rates without changing its intrinsic constants.

If q is bounded below by a positive number and reference time tends to infinity, proper time also tends to infinity and the solution reaches the same equilibrium. If the accumulated proper time remains finite, the limit is the finite-proper-time value instead. Thus conclusions about asymptotic convergence must identify which interval becomes infinite.

8.3 A finite-frame equation

For a finite step, let f_n transfer reserve into expression and r_n transfer expression back:

$$\begin{pmatrix} E_A^{n+1} \\ E_P^{n+1} \end{pmatrix} = \begin{pmatrix} 1 - r_n & f_n \\ r_n & 1 - f_n \end{pmatrix} \begin{pmatrix} E_A^n \\ E_P^n \end{pmatrix}, \qquad 0 \leq f_n, r_n \leq 1. \tag{8.6}$$

The columns sum to one, so the total is conserved and nonnegative inputs remain nonnegative. This matrix may represent a discrete physical rule, or an approximation to a continuous process. Those interpretations differ. For a continuous generator

$$M = \begin{pmatrix} -b & a \\ b & -a \end{pmatrix}, \tag{8.7}$$

the exact finite-step map is $K(\Delta\tau) = \exp(M\Delta\tau)$. Its nontrivial eigenvalue is $e^{-(a+b)\Delta\tau}$, and its transfer probabilities are

$$f = \frac{a}{a+b}(1 - e^{-(a+b)\Delta\tau}), \qquad r = \frac{b}{a+b}(1 - e^{-(a+b)\Delta\tau}). \tag{8.8}$$

These expressions account for arbitrarily many possible reversals within a finite interval. Independently assigning $1 - e^{-a\Delta\tau}$ and $1 - e^{-b\Delta\tau}$ to the two entries does not generally reproduce the exact two-way propagator.

8.4 Several expressed channels

Let $x = (E_P, E_1, \ldots, E_m)^T$ and write $\dot{x} = Mx$, where $M_{ij} \geq 0$ for $i \neq j$ and each column sums to zero. The diagonal element is minus the total outgoing rate from its column. Then $\mathbf{1}^T x$ is constant. Positivity follows from the exponential of a Metzler matrix: choose c so that $M + cI$ has nonnegative entries; the power series of $e^{(M+cI)t}$ is nonnegative and multiplication by e^{-ct} preserves that property.

This supplies a conservative kinetic framework for multiple channels. It does not determine their rates, charges or particle identities. A real decay chain must also account for momentum, conserved charges and phase space. When energies differ, the components should be energy inventories with the appropriate stoichiometric factors, or populations supplemented by an explicit energy balance. Summing unequal-energy particle counts is not energy conservation.

8.5 Entropy, irreversibility and return

For the normalized two-state process, the stationary distribution is

$$\pi_A = \frac{a}{a+b}, \qquad \pi_P = \frac{b}{a+b}, \qquad b\pi_A = a\pi_P. \tag{8.9}$$

The last equality is detailed balance. For $a, b > 0$, the relative entropy

$$D(p\|\pi) = \sum_i p_i \log \frac{p_i}{\pi_i} \tag{8.10}$$

contracts under the stochastic evolution. For two states, write $u = bp_A$ and $v = ap_P$. Differentiation gives

$$\frac{\mathrm{d}D}{\mathrm{d}\tau} = -(u - v)\log(u/v) \leq 0, \tag{8.11}$$

since log is increasing. This is a statement about probabilities approaching a stationary distribution. A thermodynamic entropy interpretation requires an energy function, temperature and physical reservoir model. The kinetic balance alone does not identify that temperature or prove that every return process is thermal.

A reduced irreversible equation may arise from a larger conservative system after degrees of freedom are ignored. This possibility is consistent with the author's conservation premise. It must not be confused with a derivation of irreversible rates from an arbitrary finite closed Hamiltonian, whose recurrences can matter.

8.6 Coherent exchange as an alternative realization

Consider two coupled canonical coordinates with Hamiltonian

$$H = \frac{p_A^2 + \omega_A^2 x_A^2}{2} + \frac{p_P^2 + \omega_P^2 x_P^2}{2} + g x_A x_P. \tag{8.12}$$

Hamilton's equations give

$$\ddot{x}_A + \omega_A^2 x_A + g x_P = 0, \tag{8.13}$$

$$\ddot{x}_P + \omega_P^2 x_P + g x_A = 0. \tag{8.14}$$

The squared normal-mode frequencies are

$$\omega_\pm^2 = \frac{\omega_A^2 + \omega_P^2}{2} \pm \frac{1}{2}\sqrt{(\omega_A^2 - \omega_P^2)^2 + 4g^2}. \tag{8.15}$$

For positive uncoupled frequencies, stability requires $g^2 < \omega_A^2 \omega_P^2$. Direct differentiation proves $\dot{H} = 0$. The individual uncoupled energies need not have a constant sum because the interaction term stores energy. This is a concrete demonstration of why a reserve picture needs a complete Hamiltonian when coherent exchange is important.

The two-reservoir kinetic model and the two-oscillator Hamiltonian are not two derivations of the same unique physics. They are different explicit closures of the conservation idea, with different transient behavior. The first relaxes; the second oscillates. A physical theory must select which behavior applies in a given regime and derive any coarse-grained relation between them.

8.7 Spatial transport and local conservation

For energy densities in a fixed local frame, a conservative continuum description reads

$$\partial_\tau e_A + \nabla \cdot \mathbf{j}_A = Q, \tag{8.16}$$

$$\partial_\tau e_P + \nabla \cdot \mathbf{j}_P = -Q. \tag{8.17}$$

Adding and integrating over a region V yields

$$\frac{\mathrm{d}}{\mathrm{d}\tau}\int_V (e_A + e_P)\mathrm{d}^3x = -\int_{\partial V} (\mathbf{j}_A + \mathbf{j}_P)\cdot \mathrm{d}\mathbf{S}. \tag{8.18}$$

A local observed deficit can therefore result from exchange, transport out of the measurement region, or detector inefficiency. Inferring EQEF requires separating these possibilities with independently specified transport and response. Setting all unobserved flux to EQEF would be a definition of the residual, not a discrimination between mechanisms.

9. What observations can determine

9.1 An inverse problem rather than a subtraction alone

The expression

$$\eta = \frac{\lambda}{\epsilon_{\mathrm{det}} q r_0} \tag{9.1}$$

is useful only after its denominator is specified independently. A potential reservoir E_P does not alone give r_0. A kinetic rule, spectrum, incident flux or attempted-transition mechanism is also needed. Without it, arbitrarily changing r_0 and compensating with η leaves the prediction unchanged.

This matters for the instruction to compare potential with observed expression. In an experimental design with individually counted attempts, the potential count may be measured directly. In a cosmological or field-theory setting, it must be calculated from an action and a state. In a collider, incident luminosity and parton distributions are not interchangeable with a latent field. In a detector, the unobserved part of an incoming flux is not automatically a returned contribution.

Proposition 9.1 (Rate-factor degeneracy)**.** *A single measured product $\lambda = qr_0\eta$ does not separately identify q, r_0, η when two or more of them are unrestricted positive quantities.*

Proof. For any positive a, b for which the allowed efficiency range is respected, replace q by aq, r_0 by br_0 and η by $\eta/(ab)$. The product is unchanged. Hence distinct parameter triples have identical predictions. □

The point is constructive: an independent clock comparison and an independent potential-rate calculation remove this degeneracy. Multiple known experimental conditions can also constrain a common constitutive law. Simply adding more unknown normalizations cannot.

9.2 Fisher information makes the same limitation explicit

For a Poisson count with mean $\mu = Kq\eta$, define parameters $u = \log q$ and $v = \log \eta$. The derivatives of $\log \mu$ with respect to u and v are both one. The Fisher information matrix is

$$I = \mu \begin{pmatrix} 1 & 1 \\ 1 & 1 \end{pmatrix}, \tag{9.2}$$

with eigenvalues 2μ and zero. More events improve the measured product, but do not remove the unmeasured direction. The zero eigenvalue is a structural issue rather than insufficient precision. An independent measurement of one factor supplies information in that direction.

Likewise, a constant detector efficiency and a constant conversion efficiency are exactly degenerate in a simple counting experiment. A physical conversion interpretation requires detector calibration, independent flux monitoring, or a distinct predicted change in shape, correlations or channel ratios.

9.3 One universal parameter and multiple conditions

Suppose the model predicts $\eta_i(\kappa) = e^{-\kappa I_i}$ with all I_i independently calculated. The expected counts are

$$\mu_i(\kappa) = b_i + K_i e^{-\kappa I_i}. \tag{9.3}$$

A common κ is testable because one number must account for all response-weighted changes. If each I_i is freely adjusted, only the products κI_i are identified and the universality claim

becomes empty. The inputs to I_i must therefore be part of the same frozen specification as the dynamics.

For the constant-efficiency special case $b_i = 0$ and $\eta_i = \eta$, independent Poisson counts have log likelihood, apart from constants,

$$\log L(\eta) = \sum_i [N_i \log(\eta K_i) - \eta K_i]. \tag{9.4}$$

Differentiating gives the unconstrained maximum $\widehat{\eta} = \sum_i N_i / \sum_i K_i$. A physical bound $0 \le \eta \le 1$ can be imposed in inference, but should not erase the signed unconstrained residual used to diagnose model or calibration errors.

The likelihood-ratio statistic against separate means is

$$D = 2 \sum_i \left[N_i \log \frac{N_i}{\widehat{\eta} K_i} - (N_i - \widehat{\eta} K_i) \right], \tag{9.5}$$

with $0 \log 0 = 0$. In a high-count interior regime its reference law is approximately χ^2_{m-1}. Sparse samples, physical boundaries and estimated backgrounds require a calibrated sampling distribution. The executable example checks this distribution with simulated counts rather than automatically assuming it.

9.4 A calibration is not counted again as a prediction

One measurement may be used to estimate a parameter, after which the parameter is frozen for other comparisons. Let channel 1 determine $\widehat{\eta}_1 = N_1 / K_1$. For held-out channels, the predictions are $\widehat{\eta}_1 K_i$. Because the calibration is common, their predictive uncertainties are correlated. At leading order,

$$V_{ij} = \delta_{ij} \widehat{\eta}_1 K_i + K_i K_j \operatorname{Var}(\widehat{\eta}_1), \qquad i, j > 1. \tag{9.6}$$

The off-diagonal term is not optional. Ignoring it falsely treats one uncertain calibration as several independent precise predictions.

This volume permits either a microscopic deduction or one-point calibration, provided their evidential roles remain distinct. A parameter selected by matching the measured fine-structure constant has not thereby predicted that constant. It may still yield new predictions if the model independently fixes how the same parameter enters other observables. The current EQEF interpretation has not yet supplied that complete cross-domain response map.

9.5 Why a coordinate correction does not manufacture agreement

For Gaussian data d with prediction m and covariance C, the residual statistic is

$$\chi^2 = (d - m)^T C^{-1} (d - m). \tag{9.7}$$

Under a known invertible linear representation change A,

$$d' = Ad, \quad m' = Am, \quad C' = ACA^T, \tag{9.8}$$

so

$$(d' - m')^T (C')^{-1} (d' - m') = (d - m)^T C^{-1} (d - m). \tag{9.9}$$

This exact identity is verified with the supplied DESI covariance. Changing only the prediction or only the uncertainty is not an innocent coordinate correction. It is a different analysis or a different physical model and must be justified as such.

For individual event times, an analogous result follows from the probability-density Jacobian. If $\tau(t)$ is fixed independently of the model parameters, then $f_t(t \mid \theta) = q(t) f_\tau(\tau(t) \mid \theta)$. The sum of $\log q(t_i)$ is independent of θ, so likelihood ratios between the same physical models are unchanged. Parameter-dependent clock laws are different: the Jacobian then contributes to the model likelihood and must be retained.

9.6 Common clock suppression and operational invisibility

If every local clock, process and measuring standard is multiplied by the same positive factor $\chi(x)$, define operational time by $\mathrm{d}T = \chi \mathrm{d}t$. A law $\mathrm{d}N/\mathrm{d}t = \chi r_0$ becomes $\mathrm{d}N/\mathrm{d}T = r_0$. Without another unaffected observable or predicted geometric consequence, χ is then a relabelling of local time rather than a separately measured conversion efficiency.

This does not preclude a physical EQEF field. A physical field can carry stress-energy, vary spatially, alter spectra or affect propagation in ways that cannot all be absorbed into one time coordinate. Those observable consequences must come from its dynamics. The universality of a coefficient is therefore useful only together with an operational experiment capable of seeing it.

9.7 How much data a small deficit requires

For a known baseline intensity and Poisson counting, a fractional uncertainty is approximately $N^{-1/2}$. Detecting a fractional deficit ϵ at a two-sided normal threshold z requires a scale $N \sim z^2/\epsilon^2$. At $\epsilon = 10^{-7}$ and $z = 1.95996$, the scale is about 3.84×10^{14} counts, before systematic errors. Comparing two equally noisy intensities doubles the required count in each sample at this approximation.

This is not the same problem as individually known conversion trials. With a known integer number of attempts and zero failures, a binomial one-sided 95% upper limit on the failure fraction is $1 - 0.05^{1/N}$, approximately $3/N$. Roughly thirty million perfectly identified trials can then test a 10^{-7} failure fraction, under the much stronger knowledge of the denominator and negligible false failures. The difference shows why an operational definition of potential attempts is as important as a small proposed number.

Part III

Coherence, propagation and geometry

10. Continuum propagation and definite spectral predictions

10.1 Linearization of the conservative phase sector

First set reserve coupling to zero and expand around a configuration with equal phase. The potential becomes

$$K(1-\cos\delta) = \frac{K}{2}\delta^2 - \frac{K}{24}\delta^4 + O(\delta^6). \tag{10.1}$$

The quadratic energy is positive. The exact cosine potential, rather than the negative quartic truncation used outside its range, should be retained for large excursions. A small-amplitude linearization gives

$$I\ddot{\theta} = -KL\theta, \qquad L = BB^{\mathsf{T}}. \tag{10.2}$$

Since L is positive semidefinite, its normal frequencies satisfy $\omega_j^2 = (K/I)\lambda_j(L) \geq 0$. The uniform phase is a zero mode. The absence of a negative quadratic mode proves linear stability at the aligned configuration; it does not prove the existence of a localized massive particle.

For a periodic chain of N nodes the eigenvalues are

$$\lambda_j = 4\sin^2(\pi j/N), \qquad j = 0, \ldots, N-1. \tag{10.3}$$

The numerical analysis checks these against direct diagonalization for three graph sizes. This supplies a spectrum from one operator, not one separately fitted energy per mode.

10.2 Correct continuum normalization

On a three-dimensional cubic lattice with spacing a, the site sum becomes $a^{-3}\int \mathrm{d}^3x$. The nearest-neighbor phase difference is $a\partial_\ell\theta + O(a^2)$. Consequently the continuum Lagrangian density is

$$\mathcal{L}_\theta = \frac{I}{2a^3}(\partial_\tau\theta)^2 - \frac{K}{2a}|\nabla\theta|^2 + O(a), \tag{10.4}$$

where the order statement concerns the unnormalized higher-gradient contributions; relative lattice corrections are organized in powers of ka. The leading equation is

$$\partial_\tau^2\theta - c_*^2\nabla^2\theta = 0, \qquad \boxed{c_*^2 = Ka^2/I.} \tag{10.5}$$

The factors a^{-3} and a^{-1} follow directly from volume counting. The spacing multiplies gradients but divides the number density of nodes. This prevents a common dimensional error in a naive continuum replacement.

The expression for c_* is a conditional relation among microscopic parameters. Identifying it with the measured speed of light calibrates a combination of K, I, a; it does not separately determine all three. Electromagnetic and tensor-gravity modes would also have to share the limiting speed through an actual symmetry or matching calculation.

10.3 Exact cubic-lattice dispersion

For a plane wave $\theta_{\mathbf{n}} \propto e^{\mathrm{i}(\mathbf{k}\cdot a\mathbf{n}-\omega\tau)}$,

$$\omega^2(\mathbf{k}) = \frac{4K}{I}\sum_{\ell=1}^{3}\sin^2(k_\ell a/2). \tag{10.6}$$

Expanding at fixed direction $\hat{\mathbf{k}}$ gives

$$\omega^2 = c_*^2k^2 - \frac{c_*^2a^2}{12}\sum_\ell k_\ell^4 + O(a^4k^6), \tag{10.7}$$

$$\frac{\omega}{c_*k} = 1 - \frac{a^2k^2}{24}\sum_\ell \hat{k}_\ell^4 + O(a^4k^4). \tag{10.8}$$

The coefficient of the leading phase-speed correction is $-1/24$ on an axis, $-1/48$ on a face diagonal and $-1/72$ on a body diagonal. Therefore the magnitude ratio between the axis and body-diagonal coefficients is exactly three for this selected stencil.

This is a dimensionless, untuned consequence of the specified nearest-neighbor model. It is not unique to MNT: conventional lattice oscillators have the same mathematics. Its value is that it is fixed once the microscopic stencil is fixed and can be falsified as part of this realization.

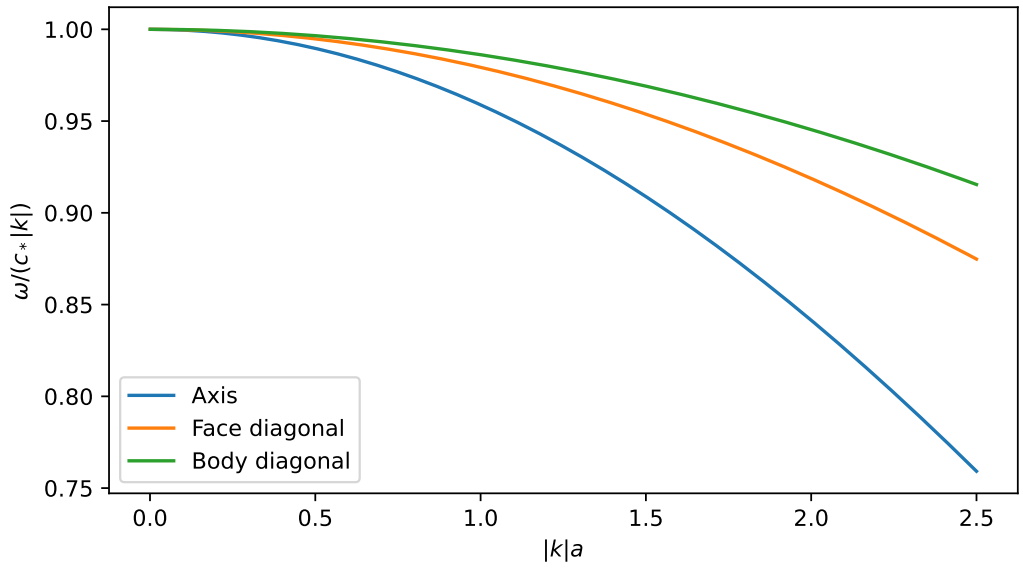

Figure 2: Conditional dispersion prediction of the cubic nearest-neighbor phase model. Directional departures from the continuum limit are fixed by the lattice stencil. No experimental spectrum is used to select these curves.

10.4 Phase speed, group speed and causality

Along a lattice axis in the first Brillouin zone,

$$\omega = 2\sqrt{K/I}\,\sin(ka/2), \qquad v_g = c_*\cos(ka/2), \tag{10.9}$$

so $v_g/c_* = 1 - (ka)^2/8 + O((ka)^4)$. The group coefficient differs from the phase coefficient by a factor of three. Quoting one as the other changes a time-of-flight prediction.

In three dimensions,

$$\frac{|\nabla_{\mathbf{k}}\omega|^2}{c_*^2} = \frac{\sum_\ell \sin^2(k_\ell a/2)\cos^2(k_\ell a/2)}{\sum_\ell \sin^2(k_\ell a/2)} \le 1. \tag{10.10}$$

A bounded group velocity does not mean that every continuous-time lattice Green function has compact support outside an exact cone. The matrix exponential or cosine propagator contains arbitrarily high powers of a nearest-neighbor matrix. A distant matrix element can be very small rather than exactly zero. Rigorous lattice locality bounds have a different logical role from exact relativistic microcausality [46].

A fixed spatial lattice also selects a microscopic frame and directions. A common phase symmetry does not remove those directions. The long-wavelength equation has an approximate Lorentz form after calibration, but exact Lorentz invariance of all sectors would require more than the leading scalar dispersion.

10.5 Reserve-induced attenuation linked to the spectrum

In the small-amplitude viscous approximation (3.10), a graph eigenmode with eigenvalue λ obeys

$$I\ddot{q} + \zeta_0\lambda\dot{q} + K\lambda q = 0. \tag{10.11}$$

For the convention $q \propto e^{-\mathrm{i}\omega\tau}$ the poles are

$$\omega_\pm = -\mathrm{i}\gamma_\lambda \pm \omega_{d,\lambda}, \qquad \gamma_\lambda = \frac{\zeta_0\lambda}{2I}, \qquad \omega_{d,\lambda}^2 = \frac{K\lambda}{I} - \gamma_\lambda^2. \tag{10.12}$$

The underdamped frequency is real only in the appropriate parameter range. For stronger damping the two poles lie on the negative imaginary axis and the motion is nonoscillatory. Stability is expressed by nonpositive real growth rates in $e^{s\tau}$, or equivalently nonpositive imaginary parts of poles under the stated frequency convention. A purely imaginary frequency is not automatically a stable oscillator.

The linked pole relation is

$$\boxed{\omega_{d,\lambda}^2 + \gamma_\lambda^2 = \omega_{0,\lambda}^2, \qquad \frac{2I\gamma_\lambda}{\lambda} = \zeta_0.} \tag{10.13}$$

Thus one damping coefficient determines all graph-mode attenuation rates in this approximation. At long wavelengths $\lambda \simeq a^2k^2$, so attenuation scales as k^2. A common coefficient that fails this mode relation cannot be protected by independently changing every mode's friction.

The memoryful model has a frequency-dependent response instead of (10.12). It must be compared with the full kernel when reserve correlation times are not short. The viscous limit is not substituted after a failed comparison merely to obtain a better fit.

10.6 A nonlinear recurrence prediction

For an isolated pair with fixed total phase momentum zero, let $\delta = \theta_1 - \theta_2$. Its relative kinetic energy is $I\dot{\delta}^2/4$, and

$$\ddot{\delta} + \frac{2K}{I}\sin\delta = 0. \tag{10.14}$$

For an oscillation of phase amplitude $A < \pi$, energy conservation yields

$$T(A) = 4\sqrt{\frac{I}{2K}}\,\mathsf{K}\left(\sin^2\frac{A}{2}\right), \tag{10.15}$$

where $\mathsf{K}(m) = \int_0^{\pi/2}(1 - m\sin^2 u)^{-1/2}\mathrm{d}u$ uses the parameter convention m, not the modulus convention. Dividing by $T_0 = 2\pi\sqrt{I/(2K)}$ removes the dimensional scale:

$$\frac{T(A)}{T_0} = \frac{2}{\pi}\mathsf{K}\left(\sin^2\frac{A}{2}\right), \qquad \frac{T(\pi/2)}{T_0} = 1.180340599016096\ldots. \tag{10.16}$$

The numerical integration reproduces the period for five amplitudes. This is an independently checked conditional prediction of a nonlinear recurrence, not a fit to a known particle constant. At $A \to \pi$ the period diverges at the separatrix. That divergence is a property of this mode; it is not a universal physical time-dilation law.

10.7 What can be tested without a microscopic SI scale

Dimensionless shape relations can be tested before the absolute lattice spacing is known: the directional dispersion coefficients, ratios of damping rates between identified modes, the recurrence period ratio, and the fluctuation–response relation under a known preparation. A laboratory analog can test the mathematics and parameter-sharing structure. Identifying an analogous effect in fundamental particles requires establishing that they realize the same modes.

Assigning the lattice spacing to the Planck length is a calibration hypothesis, not a deduction from these dispersion equations. Under that hypothesis low-energy lattice effects are extraordinarily small, but a small predicted correction is a bound-compatible forecast rather than a detected alignment. The paper keeps those roles separate.

11. The spectrum with the reserve retained

11.1 Why the reserve must appear in the same calculation

The bathless dispersion relation is a useful controlled limit, but it is not the entire spectrum of the Hamiltonian in Section 2. The same reserve that accepts energy also changes the frequency response. Consequently a dispersion test of the full constructed model must retain its reserve parameters rather than borrowing the bathless result and adding an unrelated attenuation coefficient.

Here the linearization is about the minimum $\theta_i = \theta_0$, $x_{e\lambda} = 0$, with zero momenta. Let $L = BB^{\mathsf{T}}$. For a normalized graph eigenvector v with $Lv = \ell v$, $\ell > 0$, define the corresponding normalized edge vector $w = B^{\mathsf{T}}v/\sqrt{\ell}$. Write the resolved displacement as Qv and the reserve displacement of species a as $X_a w$. Orthogonality of graph eigenvectors separates these blocks. Each positive graph mode has the quadratic Hamiltonian

$$H_\ell = \frac{P_Q^2}{2I} + \frac{K\ell Q^2}{2} + \sum_a \left[\frac{P_a^2}{2m_a} + \frac{m_a\Omega_a^2}{2}\left(X_a - \frac{c_a\sqrt{\ell}Q}{m_a\Omega_a^2}\right)^2\right]. \tag{11.1}$$

This is derived by expanding the fixed Hamiltonian, not by introducing a new potential for each spectral line.

11.2 Mass-weighted normal modes

Set $A_0 = \sum_a c_a^2/(m_a\Omega_a^2)$. The stiffness and inertia matrices for this block are

$$S_\ell = \begin{pmatrix} \ell(K + A_0) & -\sqrt{\ell}c_1 & \cdots & -\sqrt{\ell}c_s \\ -\sqrt{\ell}c_1 & m_1\Omega_1^2 & & 0 \\ \vdots & & \ddots & \\ -\sqrt{\ell}c_s & 0 & & m_s\Omega_s^2 \end{pmatrix}, \qquad M = \mathrm{diag}(I, m_1, \ldots, m_s). \tag{11.2}$$

The equation of motion is $M\ddot{q} + S_\ell q = 0$. Its squared frequencies are the eigenvalues of $M^{-1/2}S_\ell M^{-1/2}$. Positivity of the shifted-square Hamiltonian implies that they are positive for $\ell > 0$. A normal-mode transformation can be chosen with $U^\mathsf{T}MU = 1$ and $U^\mathsf{T}S_\ell U = \mathrm{diag}(\omega_j^2)$. This simultaneously identifies both the frequencies and how much resolved-node displacement each hybrid mode contains.

A graph with cycles also has edge vectors in $\ker B$. Reserve displacements in this subspace do not couple to a node gradient at linear order. They remain free modes at the bare frequencies Ω_a. The common node-phase mode has $\ell = 0$ and zero restoring force. It represents the global phase symmetry, not a particle with an automatically identified physical charge.

11.3 Eliminating reserve coordinates in frequency space

For a normal mode proportional to $e^{-i\omega\tau}$,

$$X_a = \frac{c_a\sqrt{\ell}}{m_a(\Omega_a^2 - \omega^2)}Q. \tag{11.3}$$

Substitution into the resolved equation yields

$$\boxed{K\ell - I\omega^2 - \ell\sum_a \frac{c_a^2}{m_a\Omega_a^2}\frac{\omega^2}{\Omega_a^2 - \omega^2} = 0.} \tag{11.4}$$

This rational equation is used away from its bare poles. At a pole the full matrix eigenproblem remains the appropriate definition. The equation is the Schur complement of the same stiffness matrix, so it must agree with direct diagonalization. It also agrees with the Fourier-domain form of the exact memory equation. These are three descriptions of one specified linear system.

A finite collection of undamped reserve oscillators creates hybridization and energy exchange, not a strictly irreversible linewidth for every normal mode. Smooth damping emerges only after an additional continuum or coarse-graining approximation. This explains why the finite-bath spectrum and the exponential-memory spectrum in the response section are distinguished in the numerical record.

11.4 The first low-frequency correction

Let

$$A_1 = \sum_a \frac{c_a^2}{m_a \Omega_a^4}, \qquad A_2 = \sum_a \frac{c_a^2}{m_a \Omega_a^6}. \tag{11.5}$$

A_1 has the same units as I. For $\omega \ll \min_a \Omega_a$, expansion of (11.4) gives

$$K\ell - (I + \ell A_1)\omega^2 - \ell A_2 \omega^4 + \cdots = 0. \tag{11.6}$$

The acoustic solution through second order in ℓ is

$$\omega^2 = \frac{K}{I}\ell - \frac{K A_1}{I^2}\ell^2 + O(\ell^3). \tag{11.7}$$

On a cubic lattice with spacing a, writing $k_j = k\widehat{k}_j$ and $q = ka$,

$$\ell = 4\sum_{j=1}^{3} \sin^2(q\widehat{k}_j/2) = q^2 - \frac{q^4}{12}\sum_j \widehat{k}_j^4 + O(q^6). \tag{11.8}$$

Therefore the full coupled acoustic branch obeys

$$\boxed{\frac{\omega}{c_* k} = 1 - \left(\frac{1}{24}\sum_j \widehat{k}_j^4 + \frac{A_1}{2I}\right)(ka)^2 + O((ka)^4), \qquad c_* = a\sqrt{K/I}.} \tag{11.9}$$

The reserve contributes an isotropic term to this order. The directional difference remains geometric. In particular, if $b(\widehat{k})$ denotes the coefficient multiplying $(ka)^2$, then

$$b_{\text{axis}} - b_{\text{body}} = -\frac{1}{36}, \qquad b_{\text{axis}} - b_{\text{face}} = -\frac{1}{48}. \tag{11.10}$$

These differences are independent of the reserve coefficient at this order, within the stated identical-edge, cubic and gapped-reserve assumptions. The bathless ratio of three between axial and body-diagonal corrections does not survive an arbitrary isotropic reserve contribution; the differences above are the correct corresponding test of the coupled model.

11.5 Executed numerical values

Using exactly the three reserve frequencies and couplings of the six-node example gives

$$A_0 = 0.1281857354395, \qquad A_1/I = 0.2809492855807. \tag{11.11}$$

The predicted quadratic phase-speed coefficients are

Direction	$b(\widehat{k})$
Lattice axis	−0.1821413094570
Face diagonal	−0.1613079761237
Body diagonal	−0.1543635316793

These are dimensionless, target-free outputs of the chosen demonstration. They are not identified with a measured electromagnetic or gravitational-wave coefficient. Numerical diagonalization at three successively smaller wave numbers agrees with the expansion. The full twenty-four-coordinate ring spectrum agrees with the decomposition into graph modes, free cycle-reserve modes and the common phase zero mode. The associated 67 checks, mode frequencies and resolved weights are provided in Volume II and the computational package.

11.6 What this adds to a cross-domain test

This result supplies a concrete restriction that a fit cannot evade by independently changing a damping law and a dispersion law. Once the reserve spectrum and coupling are specified, the reactive correction, hybrid mode frequencies and energy-exchange kernel are linked. In the thermal version the fluctuation spectrum is linked as well. The same construction can therefore be tested through energy exchange, response and propagation without introducing separate functions for each measurement.

The remaining physical step is the identification of actual particles and apparatus with these resolved and reserve coordinates. That map is not selected by the graph calculation. A numerical coefficient is a real prediction of the model while still being only a conditional prediction of nature. Keeping those two statements distinct prevents both dismissal of the mathematics and exaggeration of its empirical reach.

12. Coherence and capacity: the theorem chain

12.1 Random and aligned accumulation

Logical role: Derived from independent unit phasors.

Let $u_j = e^{\mathrm{i}\phi_j}$, with independent ϕ_j uniformly distributed on $[0, 2\pi)$, and define $Z_N = \sum_{j=1}^{N} u_j$. Independence is a physical modelling choice when these variables are used as a primitive ensemble. The following statements are exact mathematical consequences of that choice.

Theorem 12.1 (Second and fourth moments)**.** *For the isotropic unit-phasor ensemble,*

$$\mathbb{E}Z_N = 0, \qquad \mathbb{E}|Z_N|^2 = N, \qquad \mathbb{E}|Z_N|^4 = 2N^2 - N, \tag{12.1}$$

and $\mathrm{Var}(|Z_N|^2) = N^2 - N$.

Proof. The second moment is

$$\mathbb{E}|Z_N|^2 = \sum_{j,k} \mathbb{E}(u_j \overline{u}_k). \tag{12.2}$$

Terms with $j \neq k$ vanish because the variables are independent and have zero mean. Each of the N diagonal terms equals one. For the fourth moment, expand

$$\mathbb{E}|Z_N|^4 = \sum_{i,j,k,l} \mathbb{E}(u_i \overline{u}_j u_k \overline{u}_l). \tag{12.3}$$

A term survives only when each phasor has equal positive and negative powers. There are N^2 terms with $i = j$, $k = l$, and N^2 terms with $i = l$, $k = j$. The N terms with all indices equal were counted twice. The fourth moment is therefore $2N^2 - N$. Subtracting $(\mathbb{E}|Z_N|^2)^2$ gives the variance. □

The root-mean-square amplitude is $\sqrt{N}$. It is not the mean amplitude. Under the two-dimensional central-limit approximation, the latter is asymptotic to $\sqrt{\pi N}/2$. Perfect alignment, by contrast, gives $Z_N = Ne^{\mathrm{i}\phi}$ and amplitude N. Thus the coherent amplitude relative to the random root-mean-square amplitude grows as $\sqrt{N}$.

The theorem concerns a declared ensemble, not an assumption that every physical fluctuation is independent. It is precisely because the result is conditional and quantitative that departures caused by correlation can be calculated.

12.2 Partial coherence and weighted contributions

Proposition 12.2 (Nonzero mean resultant)**.** *For independent, identically distributed unit phasors with $m = \mathbb{E}u_j$,*

$$\mathbb{E}|Z_N|^2 = N + N(N-1)|m|^2. \tag{12.4}$$

Proof. Each diagonal contribution is one. Each off-diagonal contribution factors as $\mathbb{E}u_j\,\mathbb{E}\overline{u}_k = |m|^2$. There are $N(N-1)$ such terms. □

The change from predominantly random to predominantly coherent intensity occurs when $N|m|^2$ is of order one. This is an ensemble crossover, not a sharp universal phase transition. The strong law gives the sharper long-run statement

$$Z_N/N \longrightarrow m \quad \text{almost surely.} \tag{12.5}$$

If $m \neq 0$, the amplitude is eventually linear in N along almost every trajectory.

For deterministic nonnegative weights a_j and independent uniform phases,

$$\mathbb{E}\left|\sum_j a_j e^{\mathrm{i}\phi_j}\right|^2 = \sum_j a_j^2, \qquad \max_{\{\phi_j\}}\left|\sum_j a_j e^{\mathrm{i}\phi_j}\right| = \sum_j a_j. \tag{12.6}$$

The effective number of equal-amplitude contributors is

$$N_{\mathrm{eff}} = \frac{(\sum_j a_j)^2}{\sum_j a_j^2} \leq N. \tag{12.7}$$

The inequality is Cauchy–Schwarz, and equality holds for equal nonzero weights. The coherent-to-random gain is $\sqrt{N_{\mathrm{eff}}}$. A population dominated by one weight does not obtain the gain of N equal contributors.

12.3 Rigorous capacity selection

Use the amplitude capacity

$$B_N = \kappa N^p, \qquad \kappa > 0. \tag{12.8}$$

The symbol p is reserved for this exponent; α_{EM} denotes the electromagnetic coupling elsewhere in this volume.

Theorem 12.3 (Power-law capacity, including the boundary)**.** *For independent uniform unit phasors, the probability of random crossing tends to zero for every $p > 1/2$. For perfectly aligned phasors, crossing eventually occurs for every fixed $\kappa > 0$ when $p < 1$. Consequently $1/2 < p < 1$ is the range that achieves both properties for arbitrary positive κ. There is also a boundary family: $p = 1$ works when $0 < \kappa < 1$.*

Proof. Markov's inequality applied to $|Z_N|^2$ gives

$$\mathbb{P}(|Z_N| > \kappa N^p) \le \frac{\mathbb{E}|Z_N|^2}{\kappa^2 N^{2p}} = \kappa^{-2} N^{1-2p}, \tag{12.9}$$

which tends to zero for $p > 1/2$. For aligned phases the crossing condition is $N > \kappa N^p$, or $N^{1-p} > \kappa$. It is eventually satisfied when $p < 1$. At $p = 1$ it is satisfied exactly when $\kappa < 1$. For $p > 1$, the threshold ultimately exceeds even the maximum possible amplitude N. □

At $p = 1/2$, the central-limit theorem gives

$$\mathbb{P}(|Z_N| > \kappa\sqrt{N}) \longrightarrow e^{-\kappa^2}, \tag{12.10}$$

which is nonzero for fixed finite κ. For $p < 1/2$, the crossing probability tends to one. The strict inequality also matters at $p = 1$, $\kappa = 1$: no phasor configuration has amplitude greater than N.

The open-window result and its boundary case should be stated together. A claim that no capacity outside the open interval can ever separate the two ensembles would be stronger than the theorem and would miss the $p = 1$, $\kappa < 1$ branch.

12.4 A finite-size exponential bound

Each real or imaginary component of a unit phasor lies in $[-1, 1]$ and has mean zero. The bounded-variable concentration inequality of Hoeffding gives a simple finite-size bound [1]. If $|Z_N| > t$, at least one coordinate has magnitude greater than $t/\sqrt{2}$. Applying the two-sided bound to each coordinate and adding yields

$$\mathbb{P}(|Z_N| > t) \le \min\left\{1, 4\exp\left(-\frac{t^2}{4N}\right)\right\}. \tag{12.11}$$

The coordinates need not be independent of each other. Independence is required across the phasor increments used by the coordinate bound.

For a power-law capacity this becomes

$$\mathbb{P}(|Z_N| > \kappa N^p) \le \min\{1, 4e^{-\kappa^2 N^{2p-1}/4}\}. \tag{12.12}$$

For $p > 1/2$ its sum over N is finite. The probability of a crossing at some $N \geq M$ is bounded by the sum of the corresponding tail probabilities, and this sum tends to zero as $M \to \infty$. Hence only finitely many late random overflows occur almost surely.

This result does *not* say that an early first crossing is unlikely. A threshold may suppress large-N overflow while permitting a substantial early event probability. Section 8 calculates that distinction exactly. It also avoids replacing a finite-size bound by a Gaussian tail extrapolation at a threshold that itself moves with N. The ordinary central-limit theorem alone does not justify every such extrapolation.

12.5 An all-time capacity law

The preceding distinction suggests an alternative constructive law. Instead of selecting an exponent, choose a declared all-time false-event budget $0 < \eta < 1$ and set

$$B_N^{\mathrm{all}}(\eta) = 2\sqrt{N \log\left(\frac{4N(N+1)}{\eta}\right)}. \tag{12.13}$$

This law has no measured physical input. The parameter η is an operating specification, not a derived constant of nature.

Theorem 12.4 (All-time false-crossing control)**.** *For the independent zero-mean bounded unit-phasor ensemble,*

$$\mathbb{P}\left(\exists N \geq 1 : \ |Z_N| > B_N^{\mathrm{all}}(\eta)\right) \leq \eta. \tag{12.14}$$

Perfectly coherent phases eventually cross this same capacity. Independent unit phasors with a fixed nonzero mean resultant also cross almost surely.

Proof. Substitution of (12.13) into (12.11) bounds the crossing probability at N by $\eta/[N(N+1)]$. The union bound and the telescoping sum $\sum_{N=1}^{\infty} 1/[N(N+1)] = 1$ give the all-time result. Moreover $B_N^{\mathrm{all}}/N \to 0$. The coherent amplitude equals N, while in the nonzero-mean ensemble $|Z_N|/N \to |m| > 0$ almost surely. Both therefore eventually exceed this capacity. □

The theorem closes a useful mathematical design problem: a threshold can suppress random realization over an unlimited sequence while retaining eventual response to persistent coherence. It does not uniquely select the physical capacity law. Selecting between this law, the power-law family and another microscopic law is a separate model question.

For $\eta = 0.05$, aligned unit contributions first cross (12.13) at $N = 49$. In the recorded simulation, none of 50,000 independent random paths crosses it through $N = 1024$. The exact one-sided 95% binomial upper bound for the finite-horizon crossing probability after zero observed crossings is 5.9913×10^{-5}. The all-time theorem, not the finite simulation, provides the infinite-horizon guarantee.

12.6 How correlations modify the result

For a stationary, zero-mean complex sequence with $\mathbb{E}|u_j|^2 = 1$, define

$$\gamma(r) = \mathbb{E}(u_{j+r}\overline{u}_j). \tag{12.15}$$

Expanding the second moment by separations gives

$$\mathbb{E}|Z_N|^2 = N + 2\sum_{r=1}^{N-1}(N-r)\,\mathrm{Re}\,\gamma(r). \tag{12.16}$$

Absolute summability of γ keeps the second moment of order N, up to cancellations or a changed coefficient. Long-range positive correlations of the form $\gamma(r) \sim ar^{-\beta}$, $a > 0$ and $0 < \beta < 1$, instead produce an order-$N^{2-\beta}$ contribution. The root-mean-square growth exponent is then $H = 1 - \beta/2$.

More generally, if $\mathbb{E}|Z_N|^2 \le CN^{2H}$, the same Markov argument gives

$$\mathbb{P}(|Z_N| > \kappa N^p) \le C\kappa^{-2}N^{2H-2p}. \tag{12.17}$$

Thus $p > H$ suffices for suppression in this second-moment sense. Coherent linear growth still calls for $p < 1$, or the appropriate $p = 1$ boundary. A correlation law must therefore be part of the primitive specification whenever independent increments are not justified.

12.7 What the theorem chain accomplishes

The chain now distinguishes amplitude from intensity, root-mean-square from mean amplitude, instantaneous overflow from first passage, finite-horizon simulation from all-time control, and independent noise from correlated fluctuations. None of these refinements requires an observed particle mass or a measured coupling. They turn the reinforcement intuition into a set of exact, testable mathematical statements and make the next modelling choice much narrower.

13. Phase boundaries, comparison and geometry

13.1 The phase-convention question

Logical role: Derived phase relations; conditional quantum interpretation.

Suppose realized configurations are represented by normalized vectors $|\psi_n\rangle$ in a complex inner-product space. A tempting seam definition is

$$\delta_n^{\mathrm{raw}} = \mathrm{Arg}\langle\psi_n|\psi_{n+1}\rangle. \tag{13.1}$$

The expression is defined only when the overlap is nonzero. Its invariance depends on what counts as a descriptive redundancy. Under one common phase applied to every state, the overlap is unchanged. Under independent representative changes

$$|\psi_n\rangle \mapsto e^{\mathrm{i}\chi_n}|\psi_n\rangle, \tag{13.2}$$

it transforms as

$$\langle\psi_n|\psi_{n+1}\rangle \mapsto e^{\mathrm{i}(\chi_{n+1}-\chi_n)}\langle\psi_n|\psi_{n+1}\rangle. \tag{13.3}$$

Thus the raw overlap phase is not a well-defined function of two independently rephased quantum rays.

There are two coherent choices. One can make the individual phases physical components of the primitive state, allowing only a common overall redundancy. Alternatively, one can regard each state as a ray and supply a rule for parallel transport between representatives. This edition uses the latter when discussing quantum or gauge-covariant phase comparisons.

13.2 Covariant comparison across a seam

Let $P_{n\leftarrow n+1}$ map the representative space at $n+1$ to that at n. Define

$$w_n = \langle \psi_n | P_{n\leftarrow n+1} | \psi_{n+1} \rangle, \qquad \delta_n = \operatorname{Arg} w_n \quad (w_n \neq 0). \tag{13.4}$$

Require the transporter to transform as

$$P_{n\leftarrow n+1} \mapsto e^{\mathrm{i}\chi_n} P_{n\leftarrow n+1} e^{-\mathrm{i}\chi_{n+1}}. \tag{13.5}$$

Substitution makes all endpoint phases cancel, so w_n and its argument are invariant. In a vector gauge representation the same calculation uses matrices G_n and G_{n+1}, with $P \mapsto G_n P G_{n+1}^{-1}$.

The transporter is additional structure. It may be derived from a microscopic link rule or specified as part of an effective theory. Gauge covariance fixes how it transforms; it does not by itself fix its dynamics or its coupling strength. The lattice-gauge construction later in this volume provides an explicit effective implementation [2, 3].

13.3 Two comparisons that require no open-link phase

The fidelity and its associated ray distance are

$$F_n = |\langle \psi_n | \psi_{n+1} \rangle|^2, \qquad d_n = \arccos \sqrt{F_n}. \tag{13.6}$$

They remain invariant under independent endpoint phases. They measure distinguishability, not the same information as a transported phase.

A closed sequence also cancels the representative phases. For three states with nonzero overlaps,

$$\mathcal{B} = \langle \psi_1 | \psi_2 \rangle \langle \psi_2 | \psi_3 \rangle \langle \psi_3 | \psi_1 \rangle \tag{13.7}$$

has invariant argument. Every representative phase appears once with a positive and once with a negative sign. A longer cycle works in the same way. This construction shows why closed-loop phase information is fundamentally different from a bare open-link phase.

At an orthogonal overlap, an argument is undefined. A numerical program should record that fact, use another local chart or choose a separately specified transport prescription. Assigning the value zero to every orthogonal seam would add a discontinuous and unjustified physical rule.

13.4 Circular differences and the smooth limit

Phases are angles modulo 2π. A branch-safe difference of two seam phases is

$$\epsilon_n = \operatorname{Arg} \exp\{\mathrm{i}(\delta_n - \delta_{n-1})\}. \tag{13.8}$$

For example, the change from $\pi - 0.01$ to $-\pi + 0.01$ is 0.02 radians on the circle, not an approximately -2π acceleration. If a smooth unwrapping has been justified and $\delta_n = \theta_{n+1} - \theta_n$, then

$$\epsilon_n = \theta_{n+1} - 2\theta_n + \theta_{n-1}, \qquad \frac{\epsilon_n}{(\Delta t)^2} \longrightarrow \ddot{\theta}(t). \tag{13.9}$$

The second statement requires a differentiable interpolation and an identified physical step Δt. A raw update count alone supplies neither.

13.5 Topology supplies integers, not a coupling normalization

For a continuous nonvanishing complex field on a closed loop, write $\Phi = \rho e^{\mathrm{i}\theta}$. Single-valuedness gives

$$\oint \mathrm{d}\theta = 2\pi w, \qquad w \in \mathbb{Z}. \tag{13.10}$$

The integer is stable under continuous deformations that do not pass through a zero of the field. This is a legitimate route from a compact phase to discrete sectors. If an action-phase relation $S = \sigma\theta$ is added, it gives $\oint \mathrm{d}S = 2\pi\sigma w$. The action scale σ has not been determined by the winding argument; identifying it with $\hbar$ requires another relation.

Similarly, quantized charge ratios can follow after a compact gauge group and its representations are chosen. Their common interaction strength still depends on the normalization of the gauge kinetic term. Section 19 makes that remaining calculation explicit.

13.6 From links to an operational geometry

A graph supplies an adjacency relation and a graph distance: the minimum number of links in a path. A local update on that graph supplies a propagation bound in units of links per update. Together these can support an operational geometry, but the construction needs two further checks.

First, distance must have a stable coarse-grained interpretation. A lattice with $N(r) \propto r^d$ within graph radius r has a volume-growth dimension d. A diffusion kernel whose return probability behaves as $P(\sigma) \propto \sigma^{-d_s/2}$ supplies a spectral dimension d_s. These dimensions need not agree for a general irregular graph, and choosing a cubic graph with three spatial axes inserts rather than derives that dimensionality.

Second, the physical interval must have the appropriate causal and clock structure. A finite propagation cone does not on its own prove invariance under Lorentz transformations. That requires a continuum limit with the relevant symmetry, a common limiting speed for the sectors being compared, and controlled corrections. The next section derives an example of precisely those corrections instead of assuming that discreteness automatically becomes exact relativity.

13.7 Numerical phase check

The executable test independently rephases 24 normalized four-component states. The raw overlap phase changes by as much as 3.1168 radians. The transported overlap changes by at most 2.22×10^{-16} in absolute magnitude; fidelity and the closed-cycle product remain invariant to numerical precision. The orthogonal-overlap case is explicitly recorded as

undefined, and the branch-cut test gives 0.02 radians. These checks verify the corrected definitions, not a physical interpretation of a particular phase seam.

14. Discrete dynamics, conservation and the continuum

14.1 An action is an additional dynamical specification

Logical role: Conditional effective construction with explicit derivations.

A seam variable describes a comparison. An action specifies how an entire sequence is weighted or selected. To move from one to the other, introduce a discrete Lagrangian $L_d(q_n, q_{n+1})$ and the action

$$S_d[q] = \sum_{n=0}^{T-1} L_d(q_n, q_{n+1}). \tag{14.1}$$

With the endpoints fixed, varying an interior q_n gives

$$D_2 L_d(q_{n-1}, q_n) + D_1 L_d(q_n, q_{n+1}) = 0. \tag{14.2}$$

This is the discrete Euler–Lagrange equation. The momenta $p_n^- = -D_1 L_d(q_n, q_{n+1})$ and $p_n^+ = D_2 L_d(q_{n-1}, q_n)$ agree on a solution. An action of this form is a concrete bridge from seam costs to dynamics. It is not yet a derivation of which cost the primitive model selects.

For

$$L_d = \frac{M}{2\Delta t}(q_{n+1} - q_n)^2 - \Delta t\, V(q_n), \tag{14.3}$$

(14.2) gives

$$M\frac{q_{n+1} - 2q_n + q_{n-1}}{(\Delta t)^2} = -V'(q_n). \tag{14.4}$$

A smooth interpolation therefore approaches $M\ddot{q} = -V'(q)$ as $\Delta t \to 0$. The coefficient M and the time scale have been supplied by this effective construction. The result establishes the variational route, not their microscopic origin.

14.2 A local graph wave equation

Let $q_{n,i}$ be a real variable at vertex i of an undirected graph, and let L be its positive graph Laplacian. In dimensionless step units, choose

$$S_d = \frac{1}{2}\sum_n \left[\|q_{n+1} - q_n\|^2 - q_n^T A q_n\right], \qquad A = \nu^2 L + \mu_0^2 I. \tag{14.5}$$

Here ν is a dimensionless propagation parameter and μ_0 is a dimensionless restoring frequency. Equation (14.2) becomes

$$q_{n+1} - 2q_n + q_{n-1} = -Aq_n. \tag{14.6}$$

This construction is separate from R0. It is an explicit effective dynamics to which a more microscopic realization could be matched.

Proposition 14.1 (Finite graph support)**.** *If the update at a vertex uses only that vertex, its neighbours and the preceding local state, a perturbation initially supported on a vertex set S cannot influence vertices farther than n graph links from S after n updates.*

Proof. At the first update, only S and its immediate neighbours can differ. If the statement holds after n updates, the next update can extend the support by at most one neighbour relation. Induction gives the claim. □

The proposition requires local operations. A globally evaluated threshold or a dense matrix inverse can introduce nonlocal dependence, so such operations must not be silently included in the same causal proof.

14.3 Exact energy for the quadratic branch

Define the staggered energy

$$E_{n+1/2} = \frac{1}{2}\|q_{n+1} - q_n\|^2 + \frac{1}{2}q_{n+1}^T A q_n. \tag{14.7}$$

Since A is symmetric,

$$E_{n+1/2} - E_{n-1/2} = \frac{1}{2}(q_{n+1} - q_{n-1})^T \left(q_{n+1} - 2q_n + q_{n-1} + Aq_n\right) \tag{14.8}$$

$$= 0. \tag{14.9}$$

This is an exact conservation law for the specified quadratic action. It should not be generalized to arbitrary nonlinear discrete actions: a variational integrator does not automatically conserve the continuum energy exactly.

To see when (14.7) is nonnegative, put $v = q_{n+1} - q_n$ and $u = (q_{n+1} + q_n)/2$. Then

$$E_{n+1/2} = \frac{1}{2}v^T(I - A/4)v + \frac{1}{2}u^T A u. \tag{14.10}$$

Thus $0 \le A \le 4I$ suffices for nonnegativity. Strict interior eigenvalues avoid marginal repeated-root behaviour at the edge of the stability interval. A massless zero mode retains the usual freely evolving constant-displacement component.

14.4 A discrete phase charge

Replace q by a complex field z and retain the real Hermitian quadratic action. Global phase rotation $z \mapsto e^{i\chi}z$ is a symmetry. Its discrete charge can be written

$$Q_{n+1/2} = \mathrm{Im}(z_n^\dagger z_{n+1}). \tag{14.11}$$

Using (14.6),

$$Q_{n+1/2} - Q_{n-1/2} = \mathrm{Im}\left[z_n^\dagger(2I - A)z_n\right] = 0, \tag{14.12}$$

because a Hermitian quadratic form is real. This is a genuine phase-related conservation law within the declared dynamics. Naming the charge electric charge still requires a coupling and normalization map.

14.5 Dispersion and the long-wavelength equation

On a d-dimensional hypercubic spatial lattice, substitute

$$q_{n,\mathbf{j}} = q_0 e^{\mathrm{i}(\mathbf{k}\cdot\mathbf{j}a - \omega n\Delta t)}. \tag{14.13}$$

Writing $\nu = c\Delta t/a$ and $\mu_0 = \Omega_0\Delta t$, the dispersion relation is

$$\sin^2\left(\frac{\omega\Delta t}{2}\right) = \nu^2 \sum_{i=1}^{d} \sin^2\left(\frac{k_i a}{2}\right) + \frac{(\Omega_0\Delta t)^2}{4}. \tag{14.14}$$

Real frequencies for every lattice mode require

$$4d\nu^2 + (\Omega_0\Delta t)^2 \le 4. \tag{14.15}$$

In practice the strict inequality provides a margin from the highest-frequency boundary. In the smooth limit,

$$\omega^2 = c^2|\mathbf{k}|^2 + \Omega_0^2, \tag{14.16}$$

which is the Klein–Gordon dispersion if $\Omega_0 = mc^2/\hbar$. That identification is a physical matching condition, not a mass derivation from the graph.

For the massless branch, the leading correction is

$$\omega^2 = c^2k^2 + \frac{c^4(\Delta t)^2(k^2)^2 - c^2a^2\sum_i k_i^4}{12} + O(c^2k^6a^4 + c^4k^6a^2\Delta t^2 + c^6k^6\Delta t^4). \tag{14.17}$$

The two fourth-order terms display temporal discretization and spatial anisotropy explicitly. In one dimension,

$$\frac{\omega}{ck} = 1 + \frac{(\nu^2 - 1)(ka)^2}{24} + O((ka)^4). \tag{14.18}$$

The numerical test halves ka repeatedly and finds error-reduction ratios 4.0074, 4.0019 and 4.0005, as expected for a quadratic leading correction.

14.6 What the limiting speed means

The algorithmic support bound is one link per update, corresponding to $a/\Delta t$. The long-wavelength wave speed is $c = \nu a/\Delta t$. These are not the same statement. Small lattice precursors and the full dispersion relation must be treated before interpreting either as a universal physical causal speed.

A Lorentz-invariant low-energy sector additionally requires the same limiting cone for the fields being coupled, appropriate transformation properties, and control of symmetry-violating operators under interactions and coarse graining. A single scalar dispersion calculation verifies one part of that programme. It does not select the entire relativistic matter and gravity sector.

A massive-propagation correction and the quartic lattice correction are also different. A mass term gives $1 - v/c \propto f^{-2}$ at high frequency. Equation (14.17) instead gives frequency-growing corrections in its low-ka regime. The graviton-mass bound in Volume II is therefore not a numerical constraint on the lattice spacing without an additional matching derivation.

14.7 Numerical conservation and locality checks

The recorded massless one-dimensional run uses 257 periodic sites, 60 updates and $\nu = 0.5$. A localized perturbation has exactly zero computed amplitude outside its graph support cone. The staggered energy begins at 0.25 and drifts by at most 5.55×10^{-17}. A separate complex plane wave conserves the discrete phase charge to 1.42×10^{-14} in absolute value.

The control case $\nu = 1.1$ has a highest-frequency recurrence root with magnitude 2.4282, explicitly detecting the expected instability. This matters: the same implementation identifies both a stable branch and an unstable parameter choice, rather than reporting a success that is insensitive to the mechanism being tested.

Part IV

Quantum descriptions, matter and constants

15. Quantum mechanics and field-theory recovery

15.1 The additional structure needed for a quantum state

Logical role: Conditional recovery from stated quantum assumptions.

Complex interference is compatible with quantum mechanics, but also occurs in classical waves. A quantum completion adds a complex Hilbert space, a composition rule for separate systems, a rule assigning probabilities to measurement outcomes, and appropriate reversible or open-system dynamics. These assumptions cannot all be inferred from $\mathbb{E}|Z_N|^2 = N$.

An isolated state is represented by a normalized ray. A composite system uses a tensor product $\mathcal{H}_A \otimes \mathcal{H}_B$, allowing states that cannot be written as a product. A mixed state is represented by a positive operator ρ with $\operatorname{Tr}\rho = 1$. The distinction between the classical ensemble Π of Section 6 and the quantum density operator ρ remains essential: identifying them requires a specified map, not a change of notation.

15.2 Norm-preserving dynamics and the phase-energy relation

Suppose a differentiable isolated update is linear and norm preserving, with

$$U(\Delta t) = I - \mathrm{i}G\Delta t + O((\Delta t)^2). \tag{15.1}$$

Expanding $U^\dagger U = I$ gives $G^\dagger = G$. Defining an action scale σ and the energy generator $H = \sigma G$ gives

$$\mathrm{i}\sigma\partial_t|\psi\rangle = H|\psi\rangle. \tag{15.2}$$

When the scale is matched to $\hbar$, this is the Schrödinger equation. An energy eigenstate evolves as $e^{-\mathrm{i}Et/\hbar}$, so its phase-rate magnitude satisfies $E = \hbar\omega$. The relationship follows from the

generator and the scale identification; it does not independently determine the numerical action scale.

For a finite Hermitian matrix H, the Cayley update

$$U_C = \left(I + \frac{\mathrm{i}\Delta t H}{2\hbar}\right)^{-1} \left(I - \frac{\mathrm{i}\Delta t H}{2\hbar}\right) \tag{15.3}$$

is exactly unitary where the inverse exists. This follows because both factors are functions of the same Hermitian matrix. However, the inverse is generally dense even for a local H. Exact norm preservation therefore does not prove the strict graph support cone of Section 10. A finite-depth local quantum circuit provides another discrete architecture, with its locality established directly from the gates.

15.3 Recovering the Schrödinger equation from a specified short-time kernel

A different conditional route starts with the short-time kernel

$$K(\mathbf{x}, \mathbf{x} + \boldsymbol{\eta}; \Delta t) = \left(\frac{m}{2\pi \mathrm{i}\hbar\Delta t}\right)^{d/2} \exp\left[\frac{\mathrm{i}m\eta^2}{2\hbar\Delta t} - \frac{\mathrm{i}V(\mathbf{x})\Delta t}{\hbar}\right]. \tag{15.4}$$

Assume composition by integration and a wavefunction smooth enough for the short-time expansion. The normalized oscillatory Gaussian has vanishing first moment and second moment $\langle \eta_i \eta_j \rangle = \mathrm{i}\hbar\Delta t\, \delta_{ij}/m$. Expanding the wavefunction to second order therefore gives

$$\psi(t + \Delta t) = \psi + \frac{\mathrm{i}\hbar\Delta t}{2m}\nabla^2\psi - \frac{\mathrm{i}V\Delta t}{\hbar}\psi + O((\Delta t)^2), \tag{15.5}$$

and hence

$$\mathrm{i}\hbar\partial_t\psi = -\frac{\hbar^2}{2m}\nabla^2\psi + V\psi. \tag{15.6}$$

The kernel already contains the action scale, mass, measure and composition structure. This derivation explains how a phase-weighted action can recover quantum propagation once those ingredients are supplied; it does not obtain them from a threshold crossing alone.

15.4 The probability rule and its assumptions

Under the usual Hilbert-space setting, a normalized noncontextual probability assignment to projectors that is additive on mutually orthogonal subspaces has a strong mathematical restriction. Gleason's theorem, in Hilbert-space dimension at least three and under its measure assumptions, yields

$$p(P) = \mathrm{Tr}(\rho P) \tag{15.7}$$

for a positive trace-one operator ρ [4]. For a pure state and a one-dimensional projector this becomes the Born expression $p_i = |\langle i|\psi\rangle|^2$.

This is a useful conditional bridge: the probability law is constrained once the Hilbert-space and measurement assumptions hold. It is not a proof that the phasor model necessarily has that measurement structure. The elementary dimension-two case is not covered by the same projector-only theorem without additional assumptions or an embedding in a larger system. A proposed primitive realization must therefore supply or derive the appropriate event algebra and composition rule.

15.5 Measurements and realization as an instrument

An effective quantum realization can be represented by outcome operators M_r satisfying

$$\sum_r M_r^\dagger M_r = I. \tag{15.8}$$

The probability and conditional post-event state are

$$p_r = \mathrm{Tr}(M_r \rho M_r^\dagger), \qquad \rho_r = \frac{M_r \rho M_r^\dagger}{p_r} \quad (p_r > 0). \tag{15.9}$$

When the outcome is not conditioned upon, the map is

$$\mathcal{E}(\rho) = \sum_r M_r \rho M_r^\dagger. \tag{15.10}$$

It preserves positivity, normalization and positivity when the system is coupled to an arbitrary ancillary system. Such completely positive dynamics provide the standard framework for a physically consistent open-system limit; the continuous Markovian generator has the Lindblad form [5].

For a local operation on subsystem A,

$$\rho'_B = \mathrm{Tr}_A \sum_r (M_r \otimes I)\rho_{AB}(M_r^\dagger \otimes I) \tag{15.11}$$

$$= \mathrm{Tr}_A \left[\rho_{AB} \sum_r (M_r^\dagger M_r \otimes I) \right] = \rho_B. \tag{15.12}$$

Thus the nonselective operation does not change the distant reduced state. Conditioning on an outcome changes the conditional description, but the outcome label must be communicated to use that conditioning. A nonlinear threshold rule on normalized quantum states must be checked against this distinction rather than assumed to inherit it.

15.6 Entanglement and a Bell-type check

A local hidden-variable factorization with settings independent of the hidden variable gives a simple bound. For outcomes $A, A', B, B' \in \{-1, 1\}$,

$$A(B + B') + A'(B - B') = \pm 2. \tag{15.13}$$

Averaging yields the familiar absolute bound two on the corresponding four-correlation combination. Quantum singlet correlations, obtained with the quantum probability and tensor-product rules, instead have $E(\mathbf{a}, \mathbf{b}) = -\mathbf{a} \cdot \mathbf{b}$ and can give $2\sqrt{2}$ for suitably chosen axes. This is the kind of distinction any quantum completion must confront, following the Bell framework [6, 7].

The nonselective no-signalling calculation above and the failure of local hidden-variable factorization are different statements. A viable completion should recover the quantum correlations without turning a choice of measurement at one site into an operational signal at another.

15.7 Canonical variables, fields and statistics

An action can provide a symplectic structure and classical Poisson brackets. Canonical quantization then postulates or derives an operator representation with

$$[\hat{x}_i, \hat{p}_j] = \mathrm{i}\hbar\delta_{ij}. \tag{15.14}$$

For Hermitian observables A and B, positivity of $\|(A - \langle A\rangle + \mathrm{i}\lambda(B - \langle B\rangle))|\psi\rangle\|^2$ for all real λ gives

$$\Delta A\,\Delta B \geq \frac{1}{2}|\langle[A, B]\rangle|. \tag{15.15}$$

The uncertainty relation follows within the operator structure; the structure itself is not selected by a classical phasor sum.

For field modes, bosonic creation and annihilation operators satisfy commutation relations, whereas fermionic operators satisfy anticommutation relations. In particular $(a_i^\dagger)^2 = 0$ for a fermionic mode. Compact scalar winding does not by itself choose these statistics or a spinor representation. A relativistic field completion must supply the representation, locality and positivity assumptions on which spin and statistics are linked.

15.8 Open-system phase coherence as an engineering application

The effective density matrix may obey

$$\dot{\rho} = -\frac{\mathrm{i}}{\hbar}[H, \rho] + \sum_a \left(L_a \rho L_a^\dagger - \frac{1}{2}\{L_a^\dagger L_a, \rho\}\right). \tag{15.16}$$

For a simple dephasing channel, off-diagonal matrix elements decay at a calculable rate. A phase-aware controller can be evaluated by comparing fixed control and baseline protocols on interleaved hardware runs, including calibration drift and the distribution of outcomes.

This is a distinct empirical route from fundamental unification. An improvement in coherence control could establish the usefulness of an algorithm without demonstrating that all of physics emerges from the same ontology. No hardware improvement factor is treated as verified in this edition because the underlying shot records and matched controls were not available for a fresh calculation.

16. From a phase factor to actual coherent conversion

16.1 Why an additive energy in a phase is not enough

Let H be a Hermitian Hamiltonian and let $b(\tau)$ be a real number independent of the state. Replacing H by $H + b(\tau)I$ gives

$$U_b(\tau, 0) = e^{-\mathrm{i}\int_0^\tau b(s)\mathrm{d}s/\hbar} U(\tau, 0). \tag{16.1}$$

For every observable O,

$$U_b^\dagger O U_b = U^\dagger O U. \tag{16.2}$$

Thus a common scalar energy shift has no effect on populations, transition probabilities or expectation values. It changes an unobservable overall phase. A spatially varying potential or a channel-dependent operator is different: it can change relative phases and forces. The distinction identifies the additional mathematical structure required by a conversion interpretation.

A general time-dependent Hamiltonian also cannot be replaced by $e^{-\mathrm{i}H(\tau)\tau/\hbar}$ without checking commutation. The correct propagator is

$$U(\tau_2, \tau_1) = \mathcal{T} \exp\left[-\frac{\mathrm{i}}{\hbar}\int_{\tau_1}^{\tau_2} H(s)\,\mathrm{d}s\right]. \tag{16.3}$$

Time ordering is unnecessary when the Hamiltonians commute at distinct times. Even in that case the integral, not generally the terminal value times the duration, is required. This is a correction of dynamics, not a numerical factor chosen to improve a constant.

16.2 The minimum Hamiltonian that transfers a population

Use a two-dimensional Hilbert space with basis $|P\rangle, |A\rangle$. Here the labels mean potential and actuated sectors of a specified effective quantum model. They are not literal extra particle species until an experimental identification is made. Set

$$H_2 = E_0 I + \begin{pmatrix} \Delta/2 & g \\ g^* & -\Delta/2 \end{pmatrix}, \qquad \Omega = \sqrt{|g|^2 + \Delta^2/4}. \tag{16.4}$$

The traceless part squares to $\Omega^2 I$. Expanding the exponential into even and odd powers therefore yields

$$U_2(\tau) = e^{-\mathrm{i}E_0\tau/\hbar}\left[I\cos\frac{\Omega\tau}{\hbar} - \frac{\mathrm{i}(H_2 - E_0 I)}{\Omega}\sin\frac{\Omega\tau}{\hbar}\right]. \tag{16.5}$$

For initial state $|P\rangle$, the resulting actuated population is

$$\boxed{P_A(\tau) = \frac{|g|^2}{|g|^2 + \Delta^2/4}\sin^2\left(\frac{\sqrt{|g|^2 + \Delta^2/4}}{\hbar}\tau\right).} \tag{16.6}$$

The unconverted population is $1 - P_A$. Population returns without disappearing from the Hilbert space. Off-resonant detuning reduces the maximum transfer, and exact resonance permits complete transfer in this ideal two-mode model. These are consequences of the Hamiltonian, not assumptions about a universal decimal deficit.

The numerical implementation compares matrix exponentiation with (16.6) at three detunings and 21 times each. It independently verifies total population and invariance under a scalar energy shift. A plot illustrates the three complete trajectories, rather than selecting the moment closest to a desired conversion fraction.

16.3 Probability conservation and energy conservation are different

Unitary evolution ensures $\langle\psi|\psi\rangle = 1$. For an autonomous H_2, it also ensures $\langle H_2\rangle$ is constant. The diagonal energy assigned to each label can change, while the off-diagonal interaction

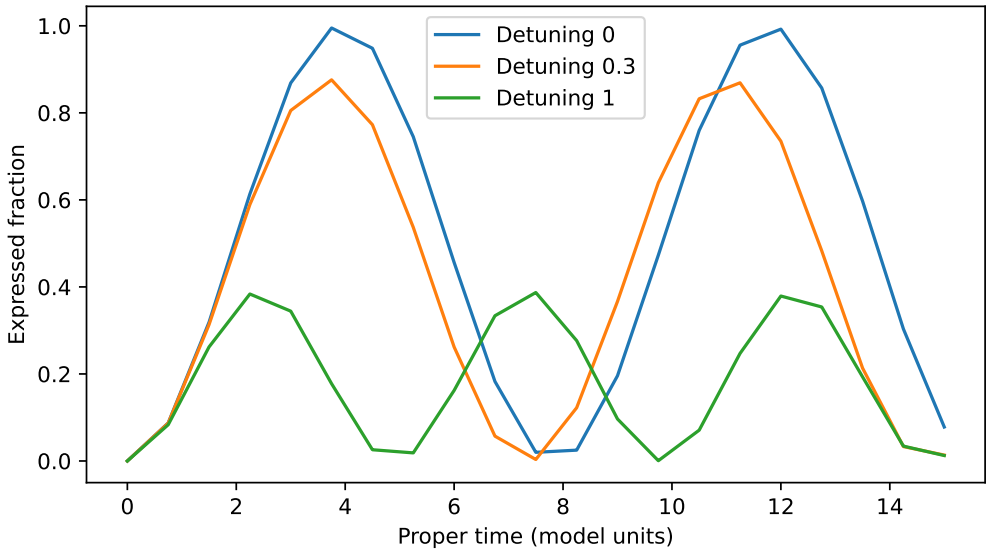

Figure 3: Coherent two-mode conversion for the declared model-unit coupling $g = 0.4$ and three detunings. These are calculated trajectories, not measured particle data. Return is a dynamical consequence of the same Hermitian coupling that creates actuation.

contribution compensates. Dropping that contribution can create an apparent missing-energy problem.

Explicitly, write $H_2 = H_P + H_A + H_{PA}$. Then

$$\frac{\mathrm{d}}{\mathrm{d}\tau}\langle H_P + H_A\rangle = \frac{\mathrm{i}}{\hbar}\langle[H_{PA}, H_P + H_A]\rangle = -\frac{\mathrm{d}}{\mathrm{d}\tau}\langle H_{PA}\rangle. \tag{16.7}$$

A conversion fraction of population is an energy fraction only when the energy carried by the labels and the interaction account justify that identification. Otherwise the two quantities must be reported separately. This is especially important when comparing a particle count with calorimetric energy.

16.4 The short-time law and the exponential approximation

Expanding (16.6) gives

$$P_A(\tau) = \frac{|g|^2\tau^2}{\hbar^2} + O(\tau^4). \tag{16.8}$$

By contrast a memoryless transition with constant rate Γ gives

$$1 - e^{-\Gamma\tau} = \Gamma\tau + O(\tau^2). \tag{16.9}$$

The two descriptions cannot be identical down to arbitrarily short time. An exponential rate is an effective approximation after a bath limit, dephasing, coarse graining or a specified renewal assumption. The microscopic phase-reserve construction need not, and generally does not, produce that form at every resolution. This observation resolves an otherwise artificial conflict between deterministic reversible dynamics and a convenient rate equation.

For a general normalized state of finite energy variance,

$$|\langle\psi|e^{-\mathrm{i}H\tau/\hbar}|\psi\rangle|^2 = 1 - \frac{(\Delta H)^2\tau^2}{\hbar^2} + o(\tau^2). \tag{16.10}$$

The quadratic term follows by multiplying the Taylor expansions of the amplitude and its conjugate. It motivates a direct short-time test only when the model specifies the accessible preparation, bandwidth and measurement procedure. It is not a prediction of an experimentally measurable time scale until ΔH is fixed.

16.5 A conservative dilation of apparent damping

An open expressed subsystem can lose amplitude while the total state remains pure and normalized. For a simple single-excitation example,

$$|A\rangle|0_R\rangle \longmapsto \sqrt{s}\,|A\rangle|0_R\rangle + \sqrt{1-s}\,|P\rangle|1_R\rangle. \tag{16.11}$$

The two reserve states are orthogonal. Tracing the reserve produces the amplitude-damping channel already defined in the effective field section. A full unitary extension exists after its action on the complementary subspace is specified. If A and P have unequal energies, $|1_R\rangle$ must carry the difference in an energy-conserving implementation. The map does not create that energy by assigning a probability.

This is the quantum counterpart of eliminating a classical oscillator reserve. The mathematical frameworks of completely positive maps and dynamical semigroups make the reduced description precise [49, 5]. Their use here is conditional on Hilbert-space quantum mechanics. Neither a reservoir nor an entangling unitary proves that classical threshold ensembles obey the Born rule.

16.6 Phase coherence is not entanglement

A classical collection of phases can produce interference and a nonzero coherence statistic. Entanglement refers instead to a composite quantum state that cannot be represented as a convex combination of product states. For example,

$$|\Psi\rangle = \frac{|P\rangle_A|A\rangle_B - |A\rangle_A|P\rangle_B}{\sqrt{2}} \tag{16.12}$$

is entangled under the supplied tensor-product composition. The correlation for spin-like measurements along directions $\mathbf{a}, \mathbf{b}$ is $-\mathbf{a}\cdot\mathbf{b}$ only after those measurement operators are defined. Deterministic trajectories and unknown initial conditions alone do not supply the tensor product or this measurement rule.

A full node derivation must identify the preparation measure, the local measurement interactions and the resulting joint probabilities, including Bell-type experiments [6, 7, 37]. It may choose a nonlocal, measurement-dependent or other carefully specified microscopic route, but that choice changes assumptions and testable consequences. The present reconstruction does not conceal such a choice inside the word chaos.

16.7 A useful negative result for a universal clock multiplier

If all two-mode energies are multiplied by the same positive factor q while reference time is used, then $U(t) = e^{-\mathrm{i}qH_2t/\hbar} = U_2(\tau)$ with $\tau = qt$. The amplitude of the conversion oscillation remains $|g|^2/(|g|^2 + \Delta^2/4)$ because g and Δ scale together. Only the parameterization of the trajectory changes.

Consequently, a clock multiplier by itself cannot fix an incorrect resonance contrast, a mass ratio, or an electromagnetic coupling inferred from a same-clock frequency ratio. It can fix an incorrect comparison of elapsed lifetimes or event rates. A physical EQEF effect on contrast requires an interaction that changes the relative Hamiltonian entries or the reserve coupling. That additional effect is a calculable hypothesis, not an automatic result of time dilation.

17. Gauge fields, matter and the Standard Model bridge

The conventional field-theory structures used in this section follow Yang–Mills gauge theory and electroweak symmetry breaking [55, 56]; their recovery is conditional on the declared field content.

17.1 Local phase covariance

Logical role: Conditional recovery; gauge group and field content declared.

Let a field transform as $\psi(x) \mapsto e^{\mathrm{i}q\chi(x)}\psi(x)$. Ordinary differentiation introduces an extra term proportional to $\partial_\mu\chi$. Define

$$D_\mu = \partial_\mu - \mathrm{i}qA_\mu, \qquad A_\mu \mapsto A_\mu + \partial_\mu\chi. \tag{17.1}$$

Direct substitution gives $D_\mu\psi \mapsto e^{\mathrm{i}q\chi}D_\mu\psi$. The connection is the mathematical structure needed to compare neighbouring phase conventions. Its curvature is

$$[D_\mu, D_\nu] = -\mathrm{i}qF_{\mu\nu}, \qquad F_{\mu\nu} = \partial_\mu A_\nu - \partial_\nu A_\mu. \tag{17.2}$$

If the effective action includes $-F_{\mu\nu}F^{\mu\nu}/4$ and a current coupling $-J^\mu A_\mu$, variation gives $\nabla_\mu F^{\mu\nu} = J^\nu$. Antisymmetry and the connection definition supply the homogeneous field equation. This is the Maxwell sector after a kinetic action and source have been specified.

For a matrix connection $D_\mu = \partial_\mu - \mathrm{i}gA_\mu$,

$$F_{\mu\nu} = \partial_\mu A_\nu - \partial_\nu A_\mu - \mathrm{i}g[A_\mu, A_\nu]. \tag{17.3}$$

The commutator generates non-Abelian self-interactions. Nothing in a single compact scalar phase alone selects which matrix group, representations or coupling g should be used.

17.2 From a link action to a gauge kinetic term

A lattice transporter from $x + a\hat{\mu}$ back to x can be written

$$P_\mu(x) = \exp\left[-\mathrm{i}g_0 \int_x^{x+a\hat{\mu}} A_\mu \mathrm{d}x^\mu\right] \tag{17.4}$$

in an Abelian branch. The product around a small plaquette is $P_{\mu\nu} = \exp[-\mathrm{i}g_0 a^2 F_{\mu\nu} + O(a^3)]$. For the Euclidean action

$$S_{\text{link}} = \beta \sum_{x,\mu<\nu} \big(1 - \operatorname{Re} P_{\mu\nu}(x)\big), \tag{17.5}$$

expanding the cosine and converting the site sum to an integral yields

$$S_{\text{link}} \longrightarrow \frac{\beta g_0^2}{4} \int \mathrm{d}^4x \, F_{\mu\nu} F_{\mu\nu}. \tag{17.6}$$

This illustrates the lattice-gauge route established by Wilson and its Hamiltonian development [2, 3]. It derives the leading continuum operator from a declared link action, but leaves its coefficient. Canonical normalization gives an effective matter coupling proportional to $1/\sqrt{\beta}$ in this convention. Selecting the topology of the links does not select β.

17.3 The matter representations used for recovery

The effective recovery target adopts

$$G_{\text{SM}} = SU(3)_C \times SU(2)_L \times U(1)_Y. \tag{17.7}$$

The following table gives one generation in left-handed Weyl notation, together with a Higgs doublet. These are declared Standard Model ingredients, not outputs already produced by R0. The Particle Data Group reviews provide the external particle-physics convention set [8].

Field	$SU(3)_C$	$SU(2)_L$	Hypercharge Y
Q	$\mathbf{3}$	$\mathbf{2}$	$1/6$
u^c	$\overline{\mathbf{3}}$	$\mathbf{1}$	$-2/3$
d^c	$\overline{\mathbf{3}}$	$\mathbf{1}$	$1/3$
L	$\mathbf{1}$	$\mathbf{2}$	$-1/2$
e^c	$\mathbf{1}$	$\mathbf{1}$	1
H	$\mathbf{1}$	$\mathbf{2}$	$1/2$

Electric charge is $Q_{\text{electric}} = T_3 + Y$ in this convention. The superscript c denotes the left-handed conjugate of a right-handed particle, and therefore reverses the corresponding Abelian charge.

17.4 What anomaly constraints can actually determine

A useful conditional derivation recovers the hypercharge ratios once the representations and Yukawa structure are specified. Let q, h, l be the hypercharges of Q, H, L. Gauge invariance of the operators QHu^c, $QH^\dagger d^c$ and $LH^\dagger e^c$ gives

$$u^c = -q - h, \qquad d^c = -q + h, \qquad e^c = -l + h, \tag{17.8}$$

where the symbols on the right of the field names now denote their hypercharges. The $SU(2)^2U(1)$ anomaly requires $3q + l = 0$. The mixed gravitational–$U(1)$ anomaly requires

$$6q + 3u^c + 3d^c + 2l + e^c = l + h = 0. \tag{17.9}$$

Hence $l = -3q$ and $h = 3q$. Choosing $h = 1/2$ as the normalization gives the table above. With those values,

$$2q + u^c + d^c = 0, \tag{17.10}$$

$$6q^3 + 3(u^c)^3 + 3(d^c)^3 + 2l^3 + (e^c)^3 = 0. \tag{17.11}$$

The pure colour anomaly cancels as $2 - 1 - 1 = 0$. There are four weak doublets counting colour, an even number, satisfying the parity condition associated with the global $SU(2)$ anomaly [9].

The supplied code checks these cancellations with exact rational arithmetic. This is a conditional structural result, not a derivation of the gauge group or the number of generations. Adding a right-handed-neutrino conjugate changes the constraint system: its charge can cancel the mixed gravitational condition, and an additional anomaly-free direction can remain. The field content must therefore be part of any uniqueness claim.

17.5 Electroweak symmetry breaking and masses

Choose the effective potential

$$V(H) = -\mu_H^2 H^\dagger H + \lambda (H^\dagger H)^2, \qquad \mu_H^2 > 0, \quad \lambda > 0. \tag{17.12}$$

At its minimum $H^\dagger H = v^2/2$ with $v^2 = \mu_H^2/\lambda$. In a convenient gauge, $H = (0, (v + h)/\sqrt{2})^T$. The quadratic fluctuation has

$$m_h^2 = 2\lambda v^2. \tag{17.13}$$

The covariant kinetic term produces a charged-vector mass and a neutral mass matrix proportional to $(gW^3 - g'B)^2$. Diagonalization gives

$$m_W = \frac{gv}{2}, \qquad m_Z = \frac{v}{2}\sqrt{g^2 + g'^2}, \qquad m_\gamma = 0, \tag{17.14}$$

with $\tan\theta_W = g'/g$ and $e = g \sin\theta_W = g' \cos\theta_W$. These are derived relations within the chosen Higgs and gauge action. The numerical values of g, g', v and λ remain inputs until a microscopic calculation fixes them.

For fermions, a Yukawa matrix Y_f gives $M_f = Y_f v/\sqrt{2}$. A singular-value decomposition produces the masses and the left- and right-handed rotations. The mismatch of the left-handed up- and down-quark rotations is

$$V_{\mathrm{CKM}} = L_u^\dagger L_d. \tag{17.15}$$

Thus the mixing matrix is calculable once the Yukawa matrices are known. Naming a persistent node as a fermion does not determine those matrices.

17.6 Neutrino mass and oscillation structure

One possible effective neutrino extension uses the dimension-five operator

$$\mathcal{L}_5 = -\frac{c_{\alpha\beta}}{2\Lambda}(\epsilon_{ab} L_\alpha^a H^b)(\epsilon_{cd} L_\beta^c H^d) + \mathrm{h.c.}, \tag{17.16}$$

with the Weyl-spinor contraction understood. In this convention it yields $M_\nu = c\,v^2/(2\Lambda)$. This is a Majorana-mass option, not an assumption that the experimental question of neutrino mass type is already settled. A Dirac extension introduces different fields and parameters.

After diagonalizing the charged-lepton and neutrino sectors, the mixing matrix U enters the propagation amplitude

$$\mathcal{A}_{\alpha\to\beta} = \sum_i U_{\beta i} \exp\left(-\frac{\mathrm{i} m_i^2 L}{2E}\right) U_{\alpha i}^* \tag{17.17}$$

in natural units and the relativistic vacuum limit. Squaring gives

$$P_{\alpha\to\beta} = \delta_{\alpha\beta} - 4\sum_{i>j} \mathrm{Re}\, K_{ij} \sin^2\Delta_{ij} + 2\sum_{i>j} \mathrm{Im}\, K_{ij} \sin(2\Delta_{ij}), \tag{17.18}$$

$$K_{ij} = U_{\beta i} U_{\alpha i}^* U_{\beta j}^* U_{\alpha j}, \qquad \Delta_{ij} = \frac{\Delta m_{ij}^2 L}{4E}. \tag{17.19}$$

Matter changes the Hamiltonian, as implemented in Volume II. Oscillation probabilities become event predictions only after flux, cross section, efficiencies, backgrounds and reconstructed-energy response are included.

17.7 Chirality and a lattice implementation

For a naive Euclidean lattice Dirac operator, replacing k_μ by $\sin(k_\mu a)/a$ introduces additional zeros at edges of the Brillouin zone. The conditions under which chirality and a simple local lattice spectrum conflict are formalized by the Nielsen–Ninomiya results [10]. They apply to specified assumptions, not to every conceivable discrete completion.

Constructive alternatives modify the regulator or the lattice chiral symmetry. The Ginsparg–Wilson relation and overlap constructions provide examples; Lüscher shows how a modified exact lattice chiral symmetry avoids the assumptions of the naive formulation [11, 12]. A node-based matter model must specify which mechanism it uses and verify the continuum representations. A scalar phase field alone does not supply a chiral fermion determinant.

17.8 Running couplings and composite matter

For an $SU(3)$ gauge theory with n_f active Dirac fundamental flavours, the one-loop running is

$$\mu\frac{\mathrm{d}g_s}{\mathrm{d}\mu} = -\frac{b_0 g_s^3}{16\pi^2}, \qquad b_0 = 11 - \frac{2n_f}{3}. \tag{17.20}$$

Integrating gives

$$\frac{1}{g_s^2(\mu)} = \frac{1}{g_s^2(\mu_0)} + \frac{b_0}{8\pi^2}\log\frac{\mu}{\mu_0}. \tag{17.21}$$

A dimensional scale can be introduced as

$$\Lambda = \mu \exp\left[-\frac{8\pi^2}{b_0 g_s^2(\mu)}\right] \tag{17.22}$$

at this order. The appearance of a scale through running is important, but the integration constant and matching conditions have not disappeared. This perturbative equation also does not itself calculate the nonperturbative hadron spectrum.

Stable or metastable node candidates must have calculable energies, decay channels and quantum numbers. In a Hamiltonian description, bound states satisfy $\hat{H}|n\rangle = E_n|n\rangle$ below the relevant continuum threshold. A resonance width Γ corresponds to lifetime $\hbar/\Gamma$ when Γ is in energy units. Scattering amplitudes and phase space then determine how such states appear in detectors.

17.9 A useful stability test for localized field matter

Consider a static real scalar configuration in d spatial dimensions with positive gradient energy T and nonnegative potential energy V. Under the rescaling $\phi_\lambda(x) = \phi(x/\lambda)$,

$$E(\lambda) = \lambda^{d-2}T + \lambda^d V. \tag{17.23}$$

Stationarity requires $(d-2)T + dV = 0$. For $d = 3$, this excludes a nontrivial stable finite-energy stationary configuration within that narrowly specified positive-energy scalar model. This calculation identifies what a viable matter construction must add: for example a conserved time-dependent charge, gauge structure, topological boundary conditions or additional derivative terms with a controlled stability analysis.

A persistent pattern is therefore a meaningful matter candidate only after its lifetime and stability have been demonstrated in the chosen dynamics. The same test is useful rather than discouraging: it distinguishes an actual binding mechanism from a relabelling of a spreading wave packet.

18. Particles as stable structures: spectrum, charge and decay

18.1 The energy of an excitation must be measured from a reference state

A localized pattern is a particle candidate only after its physical properties are identified. Its energy is a difference relative to a declared background, including gradient, interaction and reserve contributions. If a relativistic effective branch exists, the rest mass is the rest-frame excitation energy divided by c^2:

$$mc^2 = E_{\text{excitation}} - E_{\text{vacuum}}. \tag{18.1}$$

This is not generally the positive magnitude of a binding energy. For two already massive constituents with positive binding energy B, the bound-state rest energy is $(m_1 + m_2)c^2 - B$. Other field configurations may have most of their mass in positive field and interaction energies. The sign and background subtraction must come from the Hamiltonian.

An eigenproblem $H\psi_j = E_j\psi_j$ is meaningful after the operator, domain, boundary conditions and state space are specified. Naming an unknown eigenvalue electron mass does not determine its value or quantum numbers. The finite classical ring in this paper supplies normal-mode frequencies and nonlinear trajectories. It does not yet supply electron, quark and neutrino representations or their measured masses.

18.2 A localized minimum and its Hessian

For a conservative finite-dimensional system with equilibrium configuration q_*, expand

$$H = H_* + \frac{1}{2}\delta p^T M^{-1}\delta p + \frac{1}{2}\delta q^T K \delta q + O(\delta q^3). \tag{18.2}$$

The mode eigenproblem is $Kv = \omega^2 Mv$. With positive M, positive eigenvalues of the relevant constrained Hessian give real oscillation frequencies. Exact symmetry directions produce zero modes and should be factored out before declaring an instability. Negative eigenvalues give exponentially growing and decaying solutions; a positive mode does not have an imaginary frequency in the convention $e^{-\mathrm{i}\omega t}$.

This distinction corrects a common confusion between a growth exponent s and an oscillation frequency ω. Stability means $\mathrm{Re}\, s \le 0$ for a dissipative linear flow, or appropriate neutral oscillations in a conservative one. Since $s = -\mathrm{i}\omega$, those criteria should not be interchanged without the convention. The pole calculations in the test volume use both forms explicitly.

18.3 Why a scalar lump is not automatically stable

For a static real scalar field in three spatial dimensions with positive gradient energy T and nonnegative potential energy V, spatial rescaling gives

$$E(\lambda) = \lambda T + \lambda^3 V. \tag{18.3}$$

Stationarity at $\lambda = 1$ would require $T + 3V = 0$, which permits only the trivial configuration under these assumptions. This is the content of the elementary scaling obstruction associated with Derrick's analysis [54]. The result is conditional: it does not exclude lattice-pinned excitations, time-dependent charged configurations, gauge fields, topological boundary conditions or controlled higher-derivative terms.

It is therefore useful as a design test. A claimed stable particle must exhibit the feature that evades the restricted scaling argument. The feature then becomes part of the physical model and must be checked for positive energy and acceptable propagation. Simply asserting that a nonlinear term confines the field is not enough.

18.4 A worked topological example

In one spatial dimension consider a real field with energy

$$E = \int \mathrm{d}x \left[\frac{1}{2}(\partial_x \phi)^2 + \frac{\lambda_s}{4}(\phi^2 - v^2)^2\right], \qquad \lambda_s > 0. \tag{18.4}$$

For boundary values $\phi(-\infty) = -v$ and $\phi(\infty) = v$, complete the square:

$$E = \frac{1}{2}\int \mathrm{d}x \left[\phi' - \sqrt{\frac{\lambda_s}{2}}(v^2 - \phi^2)\right]^2 \tag{18.5}$$

$$+ \sqrt{\frac{\lambda_s}{2}} \int_{-v}^{v} (v^2 - \phi^2)\, \mathrm{d}\phi. \tag{18.6}$$

The lower bound is

$$E \geq \frac{2\sqrt{2\lambda_s}}{3} v^3. \tag{18.7}$$

It is attained by

$$\phi(x) = v \tanh\left[v\sqrt{\frac{\lambda_s}{2}}(x - x_0) \right]. \tag{18.8}$$

This is a stable minimum within the specified topological boundary sector. Its translation x_0 is a zero mode. The calculation demonstrates a genuine persistent field configuration and an energy fixed by its model parameters. It is not an electron: it has the wrong dimensional setting and no supplied electron charge, spin or statistics. Its value here is to show what an actual stability proof looks like.

A compact phase on a ring similarly has an integer winding when a continuous interpolation with admissible phase differences is defined. Whether that integer is exactly conserved depends on allowed defects, amplitude zeros and boundary processes. Topological labels are powerful, but cannot be treated as absolute conservation laws while simultaneously allowing arbitrary graph reconnection that changes them.

18.5 Mass hierarchies and the quantum numbers

Different stable structures may have different energies under one Hamiltonian. This is the legitimate meaning of a shared theory producing a particle spectrum. It does not require every particle to have the same energy or the same apparent conversion fraction. It requires that the Hamiltonian, representation content and fundamental couplings not be retuned to each observed mass.

A relativistic spinor satisfies a Clifford-algebra construction rather than an ordinary scalar phase equation. Requiring a first-order Hamiltonian $H = c\boldsymbol{\alpha} \cdot \mathbf{p} + \beta mc^2$ to square to $c^2p^2 + m^2c^4$ gives

$$\{\alpha_i, \alpha_j\} = 2\delta_{ij} I, \qquad \{\alpha_i, \beta\} = 0, \qquad \beta^2 = I. \tag{18.9}$$

This yields the Dirac structure once the required representation is introduced [52]. It is a conventional recovery target. The compact scalar rotor coordinates of the present finite model do not by themselves select this representation or a chiral Standard Model multiplet.

The distinction matters experimentally. A model could reproduce a rest-energy number while giving the wrong spin, magnetic moment, exchange statistics or scattering angular distribution. Those are failures of the particle identification even when the mass is numerically close. A convincing first alignment must therefore state which observable and which physical state it concerns.

18.6 Decay widths from the same interaction

If a state is unstable, its lifetime must follow from allowed couplings and accessible final states. In a weakly coupled quantum effective description, the decay width has the schematic form

$$\Gamma_{i\to f} = \frac{1}{2M_i} \int \mathrm{d}\Phi_f \, |\mathcal{M}_{i\to f}|^2 \tag{18.10}$$

in natural units, with symmetry factors and spin averages specified. The Lorentz-invariant phase space enforces four-momentum conservation. The proper lifetime is $\hbar/\Gamma$ when Γ is expressed as an energy. Branching fractions are ratios of partial widths to their sum [8].

A threshold determines whether a channel can open; it does not determine its amplitude. A lookup table of known masses can correctly forbid kinematically inaccessible channels while still predicting no cross section or lifetime. The microscopic completion must supply the interaction matrix elements or their deterministic ensemble analogue. This is where collider and decay tests become more informative than conservation identities.

A measured laboratory lifetime includes time dilation. Once a rest lifetime is used to normalize a rate, a moving lifetime tests the transformation law, not an independent derivation of that rest lifetime. Any additional conversion mechanism must be introduced in the rest-frame dynamics and then transformed consistently. The same rule applies to metastable atoms, mesons and precision clocks.

18.7 Neutrino phases and common energy offsets

With a specified mass matrix and mixing matrix, relativistic propagation has eigenphases $m_i^2 L/(2E)$ in natural units. A common offset to all m_i^2 contributes only an overall phase to oscillations. Measured oscillations therefore determine differences and mixing, not an absolute common mass without additional information. Matter adds flavor-dependent forward-scattering terms, whose standard formulation is due to Wolfenstein and subsequent work [59, 8].

The two-flavor result follows directly by diagonalizing a 2×2 Hermitian Hamiltonian:

$$P_{\alpha\to\beta} = \sin^2(2\theta)\,\sin^2\left(\frac{\Delta m^2 L}{4E}\right). \tag{18.11}$$

The similarity to (16.6) is mathematical, not proof that the new two-label reserve is a neutrino flavor system. That identification would require the observed weak-interaction preparation and detection states, the correct mixing matrix and a common physical mass spectrum.

18.8 Dark configurations and observational accountability

A weakly interacting stable mode could be a dark-sector candidate only after its abundance, gravitational stress and scattering interactions are specified. A configuration that is electromagnetically neutral is not automatically cosmologically abundant. A reservoir that stores energy is not automatically cold matter. A light scalar need not have the equation of state of a cosmological constant.

The same selected completion must connect its microscopic population to cosmological evolution, lensing and laboratory scattering. Different experimental domains constrain different combinations of those quantities. This is why the recoil and cosmology chapters retain abundance and interaction maps rather than absorbing their uncertainties into an unnamed universal constant. The model is falsifiable only when those maps are fixed before comparison.

19. Constants without numerical retrofitting

19.1 Dimensionless predictions come first

Logical role: Dimensional analysis and an identifiability result.

A numerical value depends on its units unless the quantity is dimensionless. Rescaling the units of length, time and mass changes the numerical values of dimensional quantities without changing the underlying physics. A dimensionless primitive model therefore needs an operational conversion before it can output metres, seconds or kilograms. This is not a restriction against emergent scales. It is a requirement to specify what a generated internal scale is being compared with.

Mass ratios, coupling strengths, mixing angles and normalized spectral ratios avoid that ambiguity. An internally generated length ℓ_*, time t_* and action scale σ_* can later be matched through relations such as

$$c_{\mathrm{eff}} = v_* \frac{\ell_*}{t_*}, \qquad \hbar_{\mathrm{eff}} = s_* \sigma_*, \qquad G_{\mathrm{eff}} = g_* \frac{c_{\mathrm{eff}}^3 \ell_*^2}{\hbar_{\mathrm{eff}}}, \tag{19.1}$$

where v_*, s_*, g_* are dimensionless outputs only if the microscopic model fixes them. These equations organize a possible scale map; assigning their right-hand sides to reproduce measurements is calibration.

The SI assigns exact numerical values to c, h, e and k_B. It does not make every dimensionless combination of electromagnetic quantities an exact definition. In the present SI, the electromagnetic coupling and the associated vacuum electromagnetic constants are linked through measurement rather than the older convention in which the vacuum permeability was fixed exactly. The NIST 2022 adjustment is the benchmark source used here [13].

19.2 Why a Planck identity is not a constant prediction

Given supplied $\hbar$, c and G, define

$$\ell_P = \sqrt{\frac{\hbar G}{c^3}}, \qquad t_P = \sqrt{\frac{\hbar G}{c^5}}, \qquad E_P = \sqrt{\frac{\hbar c^5}{G}}. \tag{19.2}$$

Algebra immediately gives $\ell_P / t_P = c$ and $E_P t_P = \hbar$. These identities are useful unit and implementation checks. They do not contain an independent equation from which the input constants can be determined. Replacing their names with node scales does not change the dependency.

A noncircular calculation must instead generate a relation that was not used to define the scales. For example, a microscopic spectrum could predict a ratio of two stable masses. Matching one mass to a reference unit would then leave a testable prediction for the other. The second mass cannot be used while choosing the microscopic rule.

19.3 The electromagnetic normalization calculation

Consider an effective Abelian sector in natural units,

$$\mathcal{L} = -\frac{Z_F}{4} F_{\mu\nu} F^{\mu\nu} + \overline{\psi} \left[\mathrm{i}\gamma^\mu (\partial_\mu - \mathrm{i} q g_0 A_\mu) - m \right] \psi, \qquad Z_F > 0. \tag{19.3}$$

The canonical field is $A_\mu^{\mathrm{can}} = \sqrt{Z_F} A_\mu$. Therefore

$$e_{\mathrm{phys}} = \frac{q g_0}{\sqrt{Z_F}}, \qquad \alpha_{\mathrm{EM}} = \frac{q^2 g_0^2}{4\pi Z_F}. \tag{19.4}$$

This is the essential normalization step. Compactness may quantize q relative to a basic charge. It does not fix the positive coefficient Z_F.

Proposition 19.1 (Coupling identifiability)**.** *If a set of primitive or effective assumptions permits both $Z_F = Z_1$ and $Z_F = Z_2 \neq Z_1$, while retaining the same specified q and g_0, it does not determine a unique electromagnetic coupling.*

Proof. Both choices satisfy those assumptions, but (19.4) gives $\alpha_2/\alpha_1 = Z_1/Z_2 \neq 1$. Therefore the assumptions do not imply a unique value. □

The proposition identifies a concrete calculation to perform; it does not preclude a microscopic rule from selecting Z_F. A complete derivation would obtain the effective action from the microscopic measure and update, extract the transverse gauge two-point function, canonically normalize the charged fields and match to the same physical observable used in the experimental determination.

Schematically,

$$\Gamma^{(2)}_{\mu\nu}(q) = Z_F(\mu)(q^2 g_{\mu\nu} - q_\mu q_\nu) + \text{gauge-fixing and higher-order terms.} \tag{19.5}$$

The required coefficient is a calculated response of the model, not an integer chosen to make an attractive decimal expansion. A useful computation must also state the renormalization prescription, the particles contributing to the running and the threshold matching to the low-energy electromagnetic coupling.

19.4 Running does not erase boundary conditions

A renormalization-group equation specifies how a coupling changes with scale. Integrating it requires a boundary condition or a uniquely selected fixed-point trajectory. Thus reproducing a beta function is substantial structural work, but it is not by itself a calculation of the coupling at a particular physical energy.

Dimensional transmutation can generate an exponentially separated scale, as the strong-coupling example in Section 12 illustrates. That mechanism offers a principled route to large hierarchies. Whether the required boundary condition follows from the node dynamics remains a separate calculation. Neither an exponential formula nor a topological label makes an otherwise adjustable parameter disappear.

19.5 The benchmark ledger

The measured target is kept distinct from the derivation. NIST gives the low-energy inverse fine-structure constant as 137.035999177(21) in the 2022 adjustment [13]. It is listed for comparison, not used anywhere in the threshold, seam, lattice or clock calculations. No expression in this book is fitted to that decimal value.

Quantity	Present role	What makes it a prediction
Capacity exponent and amplitude scale	Declared in R0; alternative all-time law derived from a declared error budget	A physical microscopic principle selects the law and parameters.
Mean resultant m	Declared coherence parameter in the renewal example	Derived distribution or dynamics fixes m independently of a clock measurement.
α_{EM}	Measured comparison target	The normalized gauge response and low-energy matching fix it.
Particle mass ratios and mixing	Effective spectrum and Yukawa targets	One microscopic spectrum and interaction algebra determine them.
G and the action scale	Physical matching quantities	Generated scale relations and a universal gravitational response fix the relevant dimensionless combinations.
H_0, densities and r_d	Supplied cosmology benchmark inputs	One expansion and thermal history derives them or predicts independent combinations.
Graviton mass coefficient	Parameter constrained by a published propagation analysis	A microscopic-to-waveform map fixes the coefficient before comparison.
Dark-sector scattering strength	Required input to a recoil prediction	A specified stable species and portal determine the interaction and abundance.

19.6 A practical non-retrofit rule

Every numerical result has a parameter record. Parameters may be defined, derived, calibrated on a declared training sample, or supplied for a comparator. A holdout prediction uses none of its target data to choose the functional form, discrete branch, tolerances or nuisance settings. A new model version can be developed after a comparison, but its next test needs a fresh holdout.

The present calculations are reproducible analyses of already visible public information. Hashing the code and input files records their identity; it does not retroactively make the calculations blind or prospectively registered. This distinction is especially important when the target is a famous constant whose value is already known to the analyst.

19.7 What the clock correction changes

A coordinate-time factor changes the representation of rates; it does not by itself select the invariant coefficient Z_F in the gauge kinetic term. For two frequencies measured by the same local clock, the common clock factor cancels from their ratio. An EQEF field

may alter a coupling only if its interaction with the charged and gauge fields changes the normalized response. Such an interaction must be calculated before comparing the coupling with experiment.

Accordingly, the earlier numerical coefficient denoted n_c is not replaced here by $1-\eta$, η, a proper-time rate or a clock factor. Those substitutions would be new physical hypotheses, not consequences of the chain rule. A time correction can repair a wrongly compared lifetime or counting rate while leaving a dimensionally inconsistent coupling formula unchanged. The test volume explicitly checks this separation.

20. Atomic structure and the meaning of a constant calculation

20.1 From a normalized gauge interaction to a Coulomb problem

A recovery calculation begins with the effective charged-particle and Maxwell sectors, not with a desired decimal value. In SI notation the static Maxwell equation is $\nabla\cdot\mathbf{E}=\rho_e/\epsilon_0$. For a point source q and spherical symmetry, integration over a sphere gives $4\pi r^2E_r=q/\epsilon_0$. Choosing the potential to vanish at infinity yields $V_e=q/(4\pi\epsilon_0 r)$. Two charges therefore have interaction energy $q_1q_2/(4\pi\epsilon_0 r)$. This fixes the familiar inverse-distance form after the field equation and normalization have been supplied.

For a hydrogenic nucleus of charge Ze and an electron, the nonrelativistic relative-coordinate Hamiltonian is

$$H_{\mathrm{C}}=-\frac{\hbar^2}{2\mu}\nabla^2-\frac{Z\alpha\hbar c}{r},\qquad \mu=\frac{m_em_N}{m_e+m_N},\qquad \alpha=\frac{e^2}{4\pi\epsilon_0\hbar c}. \tag{20.1}$$

The reduced mass follows by separating the center of mass of a two-body kinetic energy. It is not an optional correction chosen after the answer is known. The infinite-nuclear-mass limit is $\mu\to m_e$; measurements of a real hydrogen atom also require nuclear size, recoil, relativistic and radiative effects. Modern constant adjustments distinguish these ingredients and their correlations [39, 13].

20.2 A dimensionless radial equation

Define the length $a_\mu=\hbar/(\mu c\alpha)$ and the energy scale $E_\mu=\mu c^2\alpha^2$. With $r=a_\mu x$, the Schrödinger eigenproblem becomes

$$\left[-\frac{1}{2}\nabla_x^2-\frac{Z}{x}\right]\psi=\varepsilon\psi,\qquad E=E_\mu\varepsilon. \tag{20.2}$$

Separation into spherical harmonics gives the radial equation for $u(r)=rR(r)$,

$$-\frac{\hbar^2}{2\mu}u''+\left[\frac{\hbar^2l(l+1)}{2\mu r^2}-\frac{Z\alpha\hbar c}{r}\right]u=Eu. \tag{20.3}$$

For a bound state write $E=-\hbar^2k^2/(2\mu)$, $u=r^{l+1}e^{-kr}v(r)$. Regularity at the origin and square integrability at infinity require the remaining confluent-hypergeometric series to

terminate. Its termination condition is $\mu Z\alpha c/(\hbar k) = n$, where $n = n_r + l + 1$ is a positive integer. Thus

$$E_n = -\frac{\mu c^2 (Z\alpha)^2}{2n^2}. \tag{20.4}$$

The spectrum is a genuine consequence of the specified Coulomb Hamiltonian. Its dependence on α does not determine α: every positive value of that input defines a corresponding consistent spectrum.

This distinction is central to the reconstructed theory. A node model that yields this Hamiltonian has recovered an important law. To predict the coupling or mass ratio, it must also determine the normalization and spectrum from which α and μ are calculated. Replacing an experimental ionization energy into (20.4) and solving for m_e is an inverse measurement relation, not a parameter-free mass derivation.

20.3 What spectral ratios do predict

When the approximations of (20.4) apply, many ratios no longer depend on the supplied scale. For example,

$$\frac{E_3 - E_1}{E_2 - E_1} = \frac{1 - 1/9}{1 - 1/4} = \frac{32}{27}. \tag{20.5}$$

This dimensionless ratio is a prediction of the Coulomb problem. It is not new to MNT. It nevertheless illustrates the right logical pattern: a common Hamiltonian fixes several observables, and ratios can remain testable after an overall energy unit is calibrated. Relativistic and finite-size corrections change the ratio in calculable ways and must be included before a precision comparison.

For a small additional Hermitian interaction δH, the leading shift is

$$\delta E_n = \langle n|\delta H|n\rangle, \tag{20.6}$$

with degenerate perturbation theory used where appropriate. An EQEF interaction would have to specify this operator. An unspecified percentage added to each level has no predictive content. If $\delta H = bI$, all transition energies are unchanged; this is the phase-shift result of Section 16. A spatial or state-dependent coupling can instead alter the spectrum and is testable.

20.4 A concrete matrix-element example

For the normalized hydrogenic $1s$ state in the infinite-nuclear-mass approximation,

$$\psi_{1s}(r) = \frac{1}{\sqrt{\pi a_0^3}} e^{-r/a_0}, \qquad a_0 = \frac{\hbar}{m_e c\alpha}, \tag{20.7}$$

a proposed short-range interaction $\delta V(r) = g_X e^{-r/\ell}/r$ gives

$$\delta E_{1s} = \frac{4g_X}{a_0^3} \int_0^\infty r\, e^{-(2/a_0 + 1/\ell)r}\, \mathrm{d}r \tag{20.8}$$

$$= \frac{4g_X}{a_0^3 (2/a_0 + 1/\ell)^2}. \tag{20.9}$$

Here g_X has units of energy times length. The integral is elementary and demonstrates how an independently specified interaction produces a level shift. It does not identify g_X or ℓ with an EQEF value. That identification must follow from the microscopic response, not from a measured Lamb-shift residual.

The short-range limit $\ell \ll a_0$ gives $\delta E_{1s} \simeq 4 g_X \ell^2 / a_0^3$. The long-range limit gives $\delta E_{1s} \to g_X / a_0$. These checks expose dimensional or asymptotic mistakes before any data are fitted. Other levels must use the same g_X, ℓ and their own wavefunctions. A simultaneous spectroscopic test is then meaningful.

20.5 Radiative structure is not an arbitrary remainder

For a Dirac particle with minimal electromagnetic coupling the tree-level gyromagnetic factor is $g = 2$. Radiative corrections change the magnetic moment. The leading electron anomaly is

$$a_e = \frac{g_e - 2}{2} = \frac{\alpha}{2\pi} + O(\alpha^2), \tag{20.10}$$

as obtained in quantum electrodynamics [53]. The omitted terms are not free adjustments: they follow from a specified renormalized theory, with mass-dependent and other contributions at higher orders. A model cannot claim agreement at the measured precision merely by retaining the leading term. Conversely, recovering QED consistently provides a systematic route to those corrections once its physical inputs are fixed.

In a new interaction model, a change to a magnetic moment, a scattering amplitude and a level shift can be linked. Calculating only the observable that happens to agree is insufficient. The action, field content, regulator and matching prescription must be common. This is one reason the present paper emphasizes the effective-action coefficients rather than a catalog of isolated numerical coincidences.

20.6 Derived constants and their dependencies

Several useful scales follow algebraically from α, m_e, h, c:

$$R_\infty = \frac{\alpha^2 m_e c}{2h}, \qquad a_0 = \frac{\hbar}{m_e c \alpha}, \tag{20.11}$$

$$r_e = \frac{\alpha \hbar}{m_e c}, \qquad \lambda_C = \frac{h}{m_e c}, \tag{20.12}$$

$$\mu_B = \frac{e\hbar}{2m_e}, \qquad \sigma_T = \frac{8\pi}{3} r_e^2. \tag{20.13}$$

The classical radius r_e is a conventional electromagnetic scale, not a measurement that the electron is a rigid sphere of that radius. The Thomson cross section is the low-energy limit for a free electron. The Bohr radius and Rydberg constant are infinite-nuclear-mass reference scales. Assigning each formula its domain prevents a mathematically correct identity from becoming a misleading physical claim.

A small change in inputs gives

$$\frac{\delta R_\infty}{R_\infty} = 2\frac{\delta \alpha}{\alpha} + \frac{\delta m_e}{m_e} + \frac{\delta c}{c} - \frac{\delta h}{h} \tag{20.14}$$

at first order. Hence multiplying every named constant by the same correction does not preserve their algebraic relationships. If α, m_e, c, h were all multiplied by s, the Rydberg expression would scale as s^3, not s. A universal physical cause can have different derived effects, but those effects have to follow from the dependencies, not from applying the same percentage everywhere.

20.7 The proper-time spectral test

For a locally stationary system, an energy difference ΔE contributes relative phase $\Delta E\,\Delta\tau/\hbar$. Two transitions measured by the same local clock give

$$\frac{\nu_1}{\nu_2} = \frac{\Delta E_1}{\Delta E_2}. \tag{20.15}$$

The common clock factor cancels. Comparing the same transition at different gravitational potentials requires the metric frequency transfer as well. These two kinds of experiment are complementary: local ratios test relative couplings; transported comparisons test gravitational and kinematic response. Treating either as an absolute measurement of potential-to-actuation efficiency confuses distinct observables.

A meaningful EQEF test of atomic structure would derive δH from the same reserve or field interaction used elsewhere, calculate several independent transition shifts, retain clock and propagation effects, and compare the joint pattern. The present construction supplies a conservative mechanism and an inference framework. It does not insert a measured α into that mechanism and call the result an independent derivation of electromagnetism.

Part V

Gravity, cosmology and thermodynamics

21. From conversion resistance to a field model

21.1 What an effective realization must add

The author's field-like tension description fixes a conservation interpretation, not a unique action. To calculate a field value one must specify its degrees of freedom, kinetic normalization, interactions, initial or boundary data and observables. This section gives several familiar mathematical realizations so that the consequences can be worked out without inventing a new physical vocabulary. Each is an illustrative completion. They are not silently attributed to the earlier source or treated as equivalent alternatives after data are inspected.

A scalar is the simplest covariant example. In natural units $c = \hbar = 1$, let ϕ have action

$$S = \int \mathrm{d}^4x\sqrt{-g}\left[\frac{M^2}{2}R - \frac{1}{2}\nabla_\mu\phi\nabla^\mu\phi - V(\phi) + \mathcal{L}_A(\psi, g) - W(\phi, \psi)\right]. \tag{21.1}$$

The field equation is

$$\Box\phi - V_{,\phi} - W_{,\phi} = 0. \tag{21.2}$$

This equation follows by integrating the kinetic variation by parts, imposing the appropriate boundary conditions and varying ϕ. The stress tensor of the uncoupled scalar piece is

$$T^{\phi}_{\mu\nu} = \nabla_\mu\phi\nabla_\nu\phi - g_{\mu\nu}\left[\frac{1}{2}(\nabla\phi)^2 + V(\phi)\right]. \tag{21.3}$$

Its divergence is $(\Box\phi - V_{,\phi})\nabla_\nu\phi$. On the field equation this is $W_{,\phi}\nabla_\nu\phi$. The complementary matter-plus-interaction tensor carries the opposite divergence, and their sum is covariantly conserved. How interaction energy is assigned to the two tensors is a convention; the total is the physical conservation statement.

21.2 A reserve is not automatically a vacuum-energy fluid

A slowly varying scalar with potential-dominated energy can have pressure close to minus its density. A kinetic-dominated canonical scalar has positive pressure equal to its density. A massive oscillating field can have a different averaged equation of state. These regimes require an action and a solution, not only the phrase unused potential. The cosmology section works out the associated balances after declaring the effective branch.

For a canonical homogeneous scalar,

$$\rho_\phi = \tfrac{1}{2}\dot\phi^2 + V, \qquad p_\phi = \tfrac{1}{2}\dot\phi^2 - V. \tag{21.4}$$

Their ratio depends on the solution. It is therefore inappropriate to identify every unconverted contribution with a cosmological constant. The proposed interpretation leaves this role to be determined by the constitutive and gravitational dynamics.

21.3 Tension, gradients and propagation

A field can resist spatial variation through a positive gradient energy. For a static canonical field in a local flat region,

$$E[\phi] = \int \mathrm{d}^3x\left[\frac{1}{2}|\nabla\phi|^2 + V(\phi)\right]. \tag{21.5}$$

Variation gives $-\nabla^2\phi + V_{,\phi} = 0$. Expanding around a stationary background ϕ_0 gives a linear perturbation equation whose mass term is $V''(\phi_0)$. Positive kinetic energy and a nonnegative relevant Hessian are stability checks. A word such as tension does not guarantee them.

An explicitly kinetic generalization is $P(X,\phi)$ with $X = -\frac{1}{2}g^{\mu\nu}\partial_\mu\phi\partial_\nu\phi$. On a homogeneous timelike background, the decoupled perturbation has

$$c_s^2 = \frac{P_X}{P_X + 2XP_{XX}}, \tag{21.6}$$

under the specified effective description [14]. Positivity of numerator and denominator gives elementary gradient and kinetic requirements. In a coupled gravitational or multifield system the full matrices must be examined. This is how a qualitative resistance picture becomes a calculation of response, rather than an arbitrary damping number.

21.4 Damping requires somewhere for the transferred content to go

A damped expression such as $\ddot{x} + \gamma\dot{x} + \omega^2 x = 0$ decreases the oscillator energy at rate $-\gamma\dot{x}^2$. To represent the author's conservation premise, a reserve must gain the corresponding amount, or the oscillator must be understood as an open subsystem of a larger conservative system. An unexplained friction term alone is not the full model.

The two-oscillator construction of Section 8 demonstrates coherent exchange. Coupling to many modes can yield approximately irreversible damping over a declared time range. The resulting memory kernel, noise and dissipation then depend on the reservoir spectrum and its state. Assuming a memoryless constant damping rate is an approximation that must be stated. The same field parameter should determine the damping and any linked spectral shift if the microscopic dynamics require both.

21.5 A quantum transfer channel

For a two-label Hilbert-space example with expressed state $|A\rangle$ and reserve state $|P\rangle$, a survival factor $s = e^{-\Gamma\tau}$ defines

$$K_0 = \sqrt{s}|A\rangle\langle A| + |P\rangle\langle P|, \qquad K_1 = \sqrt{1-s}|P\rangle\langle A|. \tag{21.7}$$

The map $\rho \mapsto \sum_i K_i \rho K_i^\dagger$ is completely positive, and $\sum_i K_i^\dagger K_i = I$ proves trace preservation. For initial $|A\rangle$, the expressed population is s and the reserve population is $1 - s$. This demonstrates transfer without losing probability from the total description.

Energy conservation is a separate requirement. If the two labels have different energies, the difference must be included in an additional bath or interaction degree of freedom. For an equal-energy label model, conservation of occupancy is compatible with a constant assigned carrier energy. A trace identity must not be advertised as a derivation of all physical energy accounting.

A Markovian open-system formulation can be written using a Lindblad generator [5]. If the generator is $\mathcal{L}_\tau$, the reference-time equation is $\dot{\rho} = q(t)\mathcal{L}_\tau\rho$. Its complete positivity is preserved for a positive change of clock. Multiplying a state amplitude by an efficiency and then renormalizing can conceal the very missing events one intends to test; the nonselective map and the recorded outcomes must be retained.

21.6 No-signalling and conditioning

For a bipartite state, a trace-preserving local map on subsystem B leaves the reduced state of A unchanged:

$$\rho'_A = \mathrm{Tr}_B \sum_i (I \otimes K_i)\rho_{AB}(I \otimes K_i^\dagger) \tag{21.8}$$

$$= \mathrm{Tr}_B \left[\rho_{AB}(I \otimes \sum_i K_i^\dagger K_i) \right] = \rho_A. \tag{21.9}$$

This is an exact consequence of the supplied Hilbert-space and channel structure. It is not a derivation of those structures from classical phase thresholds. Conditioning on a selected outcome can change a conditional state, but the selection information must be communicated

to use that state. Ignoring that distinction can turn a detector-selection bias into an apparent physical signal.

21.7 Connection to the completed response calculation

The completed memory and response calculations in Sections 3 and 4 supply a concrete example of the object needed here, rather than an arbitrary number called the field loss. It is a response function calculated from the selected primitive dynamics. A possible program is to specify a stationary ensemble, perturb an external source, calculate a retarded response and extract low-frequency transport coefficients. The same generating functional should determine energy exchange, correlations and the normalization of effective fields.

For example, if an external source j couples to an observable O, its linear response is schematically

$$\delta\langle O(t)\rangle = \int \chi_R(t,t')j(t')\,\mathrm{d}t'. \tag{21.10}$$

The kernel is an output only after the evolution, state and coupling are fixed. Its imaginary and real parts govern dissipative and reactive response in the appropriate setting. No numerical kernel is inferred here from a collection of unrelated experimental residuals. The construction identifies precisely what must be computed to turn field-like conversion resistance into common cross-domain predictions.

22. A covariant phase–gravity completion

22.1 The action and its declared domain

Logical role: Conditional effective completion; not derived from R0.

A covariant action provides a common framework in which phase, amplitude, matter and geometry exchange energy consistently. In natural units with metric signature $(-,+,+,+)$, consider

$$S = \int \mathrm{d}^4x\sqrt{-g}\left[\frac{M_*^2}{2}F(\rho)\mathcal{R} - \frac{1}{2}Z(\rho)\nabla_\mu\rho\nabla^\mu\rho + P(X,\rho) - V(\rho) + \mathcal{L}_m\right], \tag{22.1}$$

where

$$Q_\mu = \partial_\mu\theta - qA_\mu, \qquad X = -\frac{1}{2}g^{\mu\nu}Q_\mu Q_\nu. \tag{22.2}$$

$\mathcal{R}$ is the Ricci scalar, not the primitive reinforcement functional R. M_* has mass dimension one, F is dimensionless, and P and V have mass dimension four. The normalization of ρ determines the dimensions assigned to Z. The matter Lagrangian includes the chosen Standard Model fields and any declared extra sector.

The functions F, Z, P and V specify an effective model family. A microscopic completion would calculate them, together with its domain of validity. Writing them down does not uniquely identify that completion. Their advantage is that equations of motion, stability and observational effects can now be derived consistently instead of attached separately to each phenomenon.

22.2 Metric variation and the stress tensor

Define $T^m_{\mu\nu} = -(2/\sqrt{-g})\delta S_m/\delta g^{\mu\nu}$. Up to the boundary term needed for a well-posed metric variation, varying (22.1) gives

$$M_*^2 F G_{\mu\nu} = T^m_{\mu\nu} + T^{\rho,\theta}_{\mu\nu} + M_*^2(\nabla_\mu\nabla_\nu F - g_{\mu\nu}\Box F), \tag{22.3}$$

where

$$T^{\rho,\theta}_{\mu\nu} = Z\partial_\mu\rho\partial_\nu\rho - \frac{Z}{2}g_{\mu\nu}(\nabla\rho)^2 + P_X Q_\mu Q_\nu + g_{\mu\nu}(P - V). \tag{22.4}$$

The potential appears once, in $g_{\mu\nu}(P - V)$. It must not be counted again as a separate term after being included in the phase-sector stress tensor.

The metric derivative of $F\mathcal{R}$ produces both $FG_{\mu\nu}$ and the two derivatives of F. These terms are essential whenever the effective gravitational strength varies with the amplitude field. Omitting them would spoil the consistency between metric and scalar equations.

22.3 Amplitude and phase equations

Varying ρ, with $P_{,\rho}$ taken at fixed X, gives

$$Z\Box\rho + \frac{1}{2}Z_{,\rho}(\nabla\rho)^2 + \frac{M_*^2}{2}F_{,\rho}\mathcal{R} + P_{,\rho} - V_{,\rho} = 0. \tag{22.5}$$

If there is no explicit θ dependence, the phase equation is

$$\nabla_\mu(P_X Q^\mu) = 0. \tag{22.6}$$

The overall sign assigned to the corresponding conserved current is a charge convention. Gauge-field variation includes the phase contribution to the gauge current as well as the matter contribution.

These equations follow from one action. They therefore permit a consistent exchange of energy between the sectors. Diffeomorphism invariance relates the divergence of the metric equation to the scalar, gauge and matter equations. For minimally coupled matter on its equations of motion, $\nabla_\mu T^{\mu\nu}_m = 0$; with explicit scalar–matter couplings, the exchange terms must instead be retained.

22.4 The Einstein limit

Take $F \to F_0 > 0$ constant, decouple any extra propagating scalar effects in the regime of interest, and let the vacuum part of $P - V$ supply a constant energy density. Equation (22.3) then has the Einstein form

$$G_{\mu\nu} + \Lambda g_{\mu\nu} = 8\pi G\, T_{\mu\nu}, \qquad 8\pi G = \frac{1}{M_*^2 F_0} \tag{22.7}$$

in natural units. The last relation identifies the gravitational coefficient in this decoupled limit. In a theory with a light nonminimally coupled scalar, a local gravitational-force measurement can include scalar exchange as well, so its effective Newton constant need not equal the bare tensor coefficient alone.

Restoring SI units gives

$$G_{\mu\nu} + \Lambda g_{\mu\nu} = \frac{8\pi G}{c^4} T_{\mu\nu}. \tag{22.8}$$

This is a conditional recovery from the covariant action. The remaining microscopic question is why the primitive realization produces the action and its coefficients.

22.5 Newtonian gravity, clocks and trajectories

In the weak-field, slow-motion regime with negligible extra scalar force, write

$$g_{00} = -(1 + 2\Phi/c^2), \qquad |\Phi|/c^2 \ll 1. \tag{22.9}$$

The leading 00 Einstein equation gives

$$\nabla^2\Phi = 4\pi G\rho_m. \tag{22.10}$$

The slowly moving geodesic equation then reduces to $\ddot{\mathbf{x}} = -\nabla\Phi$. A stationary clock measures

$$\mathrm{d}\tau = \sqrt{-g_{00}}\,\mathrm{d}t \simeq (1 + \Phi/c^2)\mathrm{d}t. \tag{22.11}$$

Thus the same metric determines gravitational force and clock rate. A phase-based clock interpretation becomes quantitatively useful only if its phase accumulation follows the same proper-time relation for all tested clock species.

For a free relativistic point particle, the action $S = -mc^2 \int \mathrm{d}\tau$ gives the geodesic equation. A quantum phase $e^{\mathrm{i}S/\hbar}$ then accumulates at rest-rate magnitude $mc^2/\hbar$. This is a bridge between phase, inertial mass and proper time after the action is supplied, not a separate derivation of a mass spectrum.

22.6 Stability and the number of degrees of freedom

The tensor kinetic term requires $F > 0$. Under an Einstein-frame rescaling, the radial kinetic coefficient includes

$$K_\rho = \frac{Z}{F} + \frac{3M_*^2}{2}\left(\frac{F_{,\rho}}{F}\right)^2. \tag{22.12}$$

Positivity of K_ρ is the radial-sector kinetic requirement in this field convention. For a homogeneous timelike phase background in a fixed-radial, decoupled phase analysis, the usual conditions are

$$P_X > 0, \qquad P_X + 2XP_{XX} > 0, \qquad c_s^2 = \frac{P_X}{P_X + 2XP_{XX}}. \tag{22.13}$$

They follow by expanding $P(X)$ to quadratic order in a phase perturbation: the denominator multiplies the time-derivative term and the numerator the spatial-gradient term. The corresponding general phase-fluid relations are standard in the k-inflation literature [14].

These conditions address specified subsectors. They are not a substitute for diagonalizing the full coupled scalar kinetic and gradient matrices on a time-dependent background. A potential minimum and a positive mass matrix must also be checked when assessing stability of a proposed vacuum.

A minimally coupled metric has two propagating tensor polarizations in its Einstein regime. A radial scalar and an ungauged phase generally add scalar modes. If a gauged phase is absorbed through a Higgs or Stueckelberg mechanism, the vector acquires a longitudinal degree of freedom instead. A physical completion must account for these modes and their couplings rather than count every phase structure as already part of the observed particle spectrum. In particular, the connection in this phase sector is not automatically the observed electromagnetic field: a charged condensate can give a gauge vector a mass, so a physical identification must preserve the required massless photon.

22.7 Gravitational-wave propagation in this action

For transverse-traceless tensor perturbations h_{ij} about a spatially flat homogeneous background, the quadratic tensor action in natural units is

$$S_T^{(2)} = \frac{M_*^2}{8} \int \mathrm{d}t\, \mathrm{d}^3x\, a^3 F \left[\dot{h}_{ij}\dot{h}_{ij} - \frac{\partial_k h_{ij}\partial_k h_{ij}}{a^2} \right]. \tag{22.14}$$

Varying gives, for each tensor polarization,

$$\ddot{h} + \left(3H + \frac{\dot{F}}{F}\right)\dot{h} + \frac{k^2}{a^2}h = 0. \tag{22.15}$$

The tensor speed equals one in these natural units for the specified action. A changing F affects amplitude damping. In the geometric-optics regime, with the source and detector assumptions treated consistently, this gives the propagation relation

$$\frac{d_L^{\mathrm{GW}}(z)}{d_L^{\mathrm{EM}}(z)} = \sqrt{\frac{F(0)}{F(z)}}. \tag{22.16}$$

This is a different observable from a graviton mass. The action (22.1) does not contain a tensor mass term merely because it includes a phase field. A mass-dispersion test is a separate phenomenological branch unless an explicit microscopic matching generates that operator.

22.8 A constraint check for genuine metric recovery

A covariant metric theory contains constraints as well as evolution equations. In an Einstein-limit canonical decomposition, the lapse and shift enforce the Hamiltonian and momentum constraints. With reduced Planck coefficient $M_{mPl}^2 = M_*^2 F_0$ and zero cosmological constant for this displayed form,

$$\mathcal{H}_\perp = \frac{2}{M_{mPl}^2\sqrt{h}}\left(\pi_{ij}\pi^{ij} - \frac{1}{2}\pi^2\right) - \frac{M_{mPl}^2\sqrt{h}}{2}\,{}^{(3)}\!\mathcal{R} + \mathcal{H}_\perp^m = 0, \tag{22.17}$$

$$\mathcal{H}_i = -2D_j\pi^j{}_i + \mathcal{H}_i^m = 0. \tag{22.18}$$

Recovering a gravitational wave equation alone is not enough to establish these constraints or the universal matter coupling. A microscopic geometry calculation should show how its gauge redundancy and constraint algebra produce the same physical degrees of freedom in the appropriate regime.

22.9 Black-hole limits and their normalization

In the decoupled Einstein vacuum, a spherical solution has

$$\mathrm{d}s^2 = -\left(1 - \frac{r_s}{r}\right) c^2 \mathrm{d}t^2 + \left(1 - \frac{r_s}{r}\right)^{-1} \mathrm{d}r^2 + r^2 \mathrm{d}\Omega^2, \qquad r_s = \frac{2GM}{c^2}. \tag{22.19}$$

The vanishing of the stationary coordinate clock rate at r_s is not itself a divergence of the freely falling local clock. Curvature is tested by invariants, such as

$$\mathcal{K} = R_{\mu\nu\rho\sigma} R^{\mu\nu\rho\sigma} = \frac{48 G^2 M^2}{c^4 r^6}. \tag{22.20}$$

For rotating solutions, horizon area also depends on angular momentum. With $\chi = cJ/(GM^2)$,

$$A = 8\pi \left(\frac{GM}{c^2}\right)^2 \left(1 + \sqrt{1 - \chi^2}\right). \tag{22.21}$$

A merger area test therefore needs spin information and a properly separated inspiral–ringdown inference, not just subtraction of catalog mass medians.

The semiclassical entropy and temperature are

$$S_{mBH} = \frac{k_B A}{4\ell_P^2}, \qquad T_{mH} = \frac{\hbar c^3}{8\pi G M k_B}. \tag{22.22}$$

Bekenstein's entropy argument and Hawking's particle-creation calculation provide the external physical basis for these relations [15, 16]. A microscopic capacity interpretation must reproduce the coefficient as well as the area scaling. If a proposed model simply assigns q independent states to each area patch a_0, then $S = k_B (A/a_0) \log q$. Matching the entropy fixes $a_0 = 4\ell_P^2 \log q$; without an independent derivation of the patch scale and state count, this is matching rather than a new prediction.

22.10 Finite phase gradients do not automatically resolve curvature

Consider the illustrative saturating kinetic form

$$P(X) = \Lambda_*^4 \left(1 - \sqrt{1 - 2X/\Lambda_*^4}\right). \tag{22.23}$$

Its real domain is $X \le \Lambda_*^4/2$, not $|X| \le \Lambda_*^4/2$. Negative spacelike values are not bounded below by this square root. Moreover,

$$P_X = (1 - 2X/\Lambda_*^4)^{-1/2}, \qquad c_s^2 = 1 - 2X/\Lambda_*^4 \tag{22.24}$$

in the homogeneous timelike phase sector. The energy density $2XP_X - P$ diverges as X approaches the upper endpoint from below. Thus an upper bound on one phase invariant does not by itself bound the stress tensor or every curvature invariant.

A constructive singularity analysis must solve the coupled field equations, exhibit regular invariants and geodesic behaviour, and match the exterior tested regime. The finite-gradient ansatz can be studied as a candidate ingredient, but it is not labelled a completed singularity-resolution proof here.

22.11 Exchange with the conversion field

The revised interpretation permits exchange between the expressed sector and the potential reservoir. In a covariant effective description the appropriate statement is

$$\nabla_\mu T_A^{\mu\nu} = Q^\nu, \qquad \nabla_\mu T_P^{\mu\nu} = -Q^\nu, \qquad \nabla_\mu T_{\rm tot}^{\mu\nu} = 0, \tag{22.25}$$

with interaction terms assigned consistently to the sector tensors. A positive local energy transfer is $Q = -u_\nu Q^\nu$ for a timelike unit observer u^μ. The spatial projection of Q^ν describes momentum transfer. An energy-only loss law is therefore insufficient for a relativistic drag mechanism: the momentum and stress response must be specified as well.

If the EQEF contribution is already included in $T_P^{\mu\nu}$ or in the scalar-sector stress tensor, it must not be added again as an independently fitted missing-energy density. Likewise, an effective metric that already describes the field's clock effect must not receive the same effect a second time through an additional lapse multiplier. The alternatives in Section 7 are distinct physical branches.

23. What it takes for a network to reproduce gravitational dynamics

The relativistic reference equations in this section use Einstein gravity [60].

23.1 Propagation geometry is not yet a gravitational field equation

A slowly varying quadratic network action can have the continuum form

$$S_\theta = \frac{1}{2}\int \mathrm{d}t\, \mathrm{d}^3x \left[A(x)(\partial_t\theta)^2 - B^{ij}(x)\partial_i\theta\partial_j\theta\right]. \tag{23.1}$$

Its principal differential operator determines characteristic propagation. Under appropriate positivity conditions one can represent that operator using an effective Lorentzian metric, up to the normalization and conformal information supplied by the measure and lower-order terms. This is a useful operational geometry. It does not by itself supply an equation determining A or B^{ij} from matter, nor does it guarantee that all species share the same characteristics.

The distinction is familiar in analogue gravity: a medium can produce an effective metric for selected excitations without reproducing the Einstein dynamics of that metric [61]. In the present reconstruction the finite graph, inertia and link stiffness are inputs. Their collective scalar wave equation is derived. A dynamical tensor gravitational sector is an additional physical construction, not a consequence of naming link stiffness curvature.

23.2 An explicit metric completion and its variation

Once a spacetime metric and a generally covariant matter action are supplied, the simplest two-derivative metric completion is

$$S = \frac{c^3}{16\pi G}\int \mathrm{d}^4x\sqrt{-g}(R - 2\Lambda) + S_m[g,\psi]. \tag{23.2}$$

Here $x^0 = ct$, so the gravitational prefactor is c^3. Define the stress tensor consistently by

$$\delta S_m = -\frac{1}{2c}\int \mathrm{d}^4x\sqrt{-g}\,T_{\mu\nu}\delta g^{\mu\nu}. \tag{23.3}$$

After including the appropriate boundary term or fixing admissible boundary variations, the metric variation gives

$$G_{\mu\nu} + \Lambda g_{\mu\nu} = \frac{8\pi G}{c^4}T_{\mu\nu}. \tag{23.4}$$

The result is a correct recovery from an Einstein–Hilbert action. To derive it microscopically, the network calculation must produce the curvature term, its sign and coefficient, the correct constraints, and universal matter coupling. A coefficient proportional to G is not determined merely by declaring a Planck length constructed from G.

The contracted Bianchi identity implies $\nabla_\mu T^{\mu\nu} = 0$ for the combined source. If expressed matter transfers energy to an EQEF field, its own stress tensor need not be separately conserved. The total, including the receiving sector and the interaction contribution, must satisfy the identity. This is the covariant extension of the finite-cell energy balance, not a demand that every expanding cosmology have a unique conserved global numerical energy.

23.3 The Newtonian limit checks both sign and normalization

Write a static weak metric as

$$\mathrm{d}s^2 = -(1 + 2\Phi/c^2)c^2\mathrm{d}t^2 + (1 - 2\Psi/c^2)\delta_{ij}\mathrm{d}x^i\mathrm{d}x^j. \tag{23.5}$$

For a slow test body the spatial geodesic equation gives $\ddot{\mathbf{x}} = -\nabla\Phi$ to leading order. In the Einstein limit with negligible anisotropic stress, $\Phi = \Psi$, and the field equation reduces to

$$\nabla^2\Phi = 4\pi G\rho_m. \tag{23.6}$$

For an isolated spherical mass this gives $\Phi = -GM/r$. A stationary clock satisfies

$$\frac{\mathrm{d}\tau}{\mathrm{d}t} \simeq 1 + \frac{\Phi}{c^2}, \tag{23.7}$$

while a slow moving one has the additional $-v^2/(2c^2)$ term. The same potential controls falling bodies and clock progression. An alternative EQEF account of gravity must reproduce their common relationship, not fit a clock factor independently of the force law.

A term $1 - E/c^2$ with E an energy is not such a clock factor: E/c^2 has units of mass. The correct weak gravitational ratio uses potential per unit mass, Φ/c^2. Reconstructing the intended idea therefore requires identifying which physical potential the node energy produces and through which stress-energy response.

23.4 Tensor modes and the universal propagation test

For the minimally coupled Einstein branch on a homogeneous background, the transverse traceless metric perturbation has two polarizations and a quadratic action proportional to

$$S_T \propto \sum_{s=+,\times}\int \mathrm{d}t\,\mathrm{d}^3x\,a^3\left[\dot{h}_s^2 - \frac{c^2}{a^2}(\nabla h_s)^2\right]. \tag{23.8}$$

The shared kinetic and gradient normalization gives tensor speed c. This is compatible with the selected multimessenger constraint [34]. It is a property of this metric completion, not evidence that an arbitrary scalar phase lattice already contains the tensor degrees of freedom.

A more general effective tensor action has coefficients G_T and F_T for the time and spatial terms, giving $c_T^2 = F_T/G_T$ in natural units. The microscopic matching must determine both. Stability requires positive kinetic energy and no negative gradient coefficient. Recovering a single propagation speed requires the matter light cone to agree as well. These conditions are equations to be checked, not terminology.

23.5 An alternative thermodynamic route and its explicit assumptions

Jacobson's equation-of-state derivation provides a second useful matching target [62]. In natural units $c = k_B = 1$, assume an entropy density s_A per horizon area, the local Unruh temperature $T = \hbar\kappa/(2\pi)$, and the Clausius relation $\delta Q = T\delta S$ for every local Rindler horizon. Let k^μ be a null generator with affine parameter λ, and use a local boost generator proportional to $-\kappa\lambda k^\mu$.

The matter heat flux and leading area change are proportional to

$$\delta Q = -\kappa \int \lambda T_{\mu\nu} k^\mu k^\nu \, \mathrm{d}\lambda \, \mathrm{d}A, \tag{23.9}$$

$$\delta S = -s_A \int \lambda R_{\mu\nu} k^\mu k^\nu \, \mathrm{d}\lambda \, \mathrm{d}A. \tag{23.10}$$

The second expression follows from the Raychaudhuri equation when expansion and shear vanish at the selected point to the order considered. Equality for all null directions yields

$$T_{\mu\nu} k^\mu k^\nu = \frac{\hbar s_A}{2\pi} R_{\mu\nu} k^\mu k^\nu. \tag{23.11}$$

Therefore $R_{\mu\nu} + f g_{\mu\nu} = (2\pi/\hbar s_A) T_{\mu\nu}$ for some scalar f. Conservation and the Bianchi identity give $f = -R/2 + \Lambda$, so

$$G_{\mu\nu} + \Lambda g_{\mu\nu} = \frac{2\pi}{\hbar s_A} T_{\mu\nu}, \qquad G = \frac{1}{4\hbar s_A}. \tag{23.12}$$

This is not a free derivation from the word entropy. Horizon entropy proportional to area, the local temperature, the Clausius law and universal local equilibrium are substantive assumptions. A node derivation could attempt to calculate s_A and justify these hypotheses, but it cannot obtain G by inserting the known area law and then count G as independently predicted.

23.6 Torsion as a distinct extension

The source ideas also allow local frame orientation and spin. An Einstein–Cartan completion uses a tetrad and an independent spin connection. Varying the connection relates torsion algebraically to the spin current for the simplest action. Eliminating that torsion produces a local spin-dependent interaction [63]. This supplies a conventional framework for a spin-sensitive lattice extension.

The presence of torsion does not automatically eliminate all singularities, nor does a pair of spin-$1/2$ constituents automatically form a spin-$1/2$ particle. Representation theory gives $1/2 \otimes 1/2 = 0 \oplus 1$. A viable fermion construction must specify an appropriate microscopic representation, odd composite, topological sector or other mechanism. No numerical calibration can repair the wrong representation.

The present scalar phase-reserve Hamiltonian deliberately does not pretend to be that full spinorial construction. It establishes conservative conversion and a controllable continuum scalar limit. The spin and metric chapters state the extra structures needed to extend it and the constraints those structures must meet.

23.7 The matching calculation in executable terms

A microscopic gravity calculation would choose background configurations and define coarse observables representing geometry. It would perturb the background, compute two-point and higher response functions, identify any tensor poles and constraints, and compare the resulting effective action to the covariant target. Gauge-dependent quantities must not be mistaken for observable modes. A scalar mode that shares a speed with light is not automatically a graviton.

At the same time, the matter effective action must be derived using the same background and normalization. The weak-field potential, clock rates, lensing and wave propagation then follow from one set of coefficients. If those coefficients require different fundamental values in different experiments, the selected microscopic completion fails. This gives the broad unification test a precise form without asserting that a sum of familiar terms has already accomplished it.

24. Cosmology and the age of the universe

24.1 One background for all cosmological observables

Logical role: Conditional cosmological recovery and a supplied-input benchmark.

A cosmological completion must use the same background solution for clock rates, expansion, redshift, distance and growth. Introducing one independent correction for each observable would obscure rather than explain their connection.

For a spatially flat homogeneous metric,

$$\mathrm{d}s^2 = -\mathrm{d}t^2 + a^2(t)\mathrm{d}\mathbf{x}^2, \qquad H = \dot{a}/a, \tag{24.1}$$

the action of Section 14 gives

$$3M_*^2 F H^2 = \rho_m + \frac{1}{2}Z\dot{\rho}^2 + 2XP_X - P + V - 3M_*^2 H\dot{F}, \tag{24.2}$$

$$-2M_*^2 F\dot{H} = \rho_m + p_m + Z\dot{\rho}^2 + 2XP_X + M_*^2(\ddot{F} - H\dot{F}). \tag{24.3}$$

Here ρ_m is the effective matter energy density in natural units, while ρ without a subscript is the radial field. The similar notation is conventional but should not be confused in numerical code. A homogeneous phase with vanishing spatial gauge-invariant gradient has $X = Q_0^2/2$.

The scalar equations, initial conditions and matter conservation equations complete this background system. A value of H_0 cannot be extracted until those functions and initial conditions have been fixed. In the constant-F, decoupled limit, these equations reduce to the standard Friedmann equations with the corresponding matter and vacuum components.

24.2 What a phase sector contributes to the energy budget

The homogeneous scalar-sector density and pressure are

$$\rho_{\rho,\theta} = \frac{1}{2}Z\dot{\rho}^2 + 2XP_X - P + V, \qquad p_{\rho,\theta} = \frac{1}{2}Z\dot{\rho}^2 + P - V. \tag{24.4}$$

For fixed radial amplitude and negligible potential, a pure kinetic choice $P = KX^n$ gives

$$\rho_\theta = (2n-1)P, \qquad w_\theta = \frac{1}{2n-1}. \tag{24.5}$$

A canonical phase kinetic term has $n = 1$ and $w = 1$, not automatically dark matter or dark energy. The choice $n = 2$ gives a radiation-like background equation of state. A positive constant potential with negligible kinetic energy gives $w \simeq -1$. These are conditional consequences of different actions, not equivalent interpretations of one unspecified latent capacity.

The revised EQEF interpretation concerns a field-like conversion resistance, not a mere name for unused capacity. Its cosmological influence is represented by the stress tensor and exchange currents of a specified effective realization. A dark-matter interpretation additionally requires suitable clustering and interactions; a dark-energy interpretation requires the corresponding pressure and perturbation response. Neither role is assigned simply from the existence of a conversion deficit.

24.3 Standard epochs from conservation

For a minimally coupled conserved perfect fluid in the Einstein limit,

$$\dot{\rho} + 3H(\rho + p) = 0. \tag{24.6}$$

If $p = w\rho$ with constant w, integration gives $\rho \propto a^{-3(1+w)}$. For a flat universe dominated by that fluid, $H^2 \propto \rho$, so

$$a(t) \propto t^{2/[3(1+w)]} \quad (w \neq -1). \tag{24.7}$$

Thus radiation gives $a \propto t^{1/2}$ and nonrelativistic matter gives $a \propto t^{2/3}$. A constant positive density gives exponential expansion. These elementary limits provide analytic tests for an implementation of the cosmological equations.

A microscopic onset of realized frames and the age of a later hot expanding branch need not be the same notion. The age integral below measures elapsed cosmic proper time in the specified expansion history. It is not an age assigned to an uncalibrated pre-geometric state space.

24.4 Redshift, distances and sound-horizon consistency

In a homogeneous metric with standard photon propagation,

$$1 + z = \frac{a_0}{a_e}, \qquad \nu_{\rm obs} = \frac{\nu_e}{1+z}, \qquad \Delta t_{\rm obs} = (1+z)\Delta t_e. \tag{24.8}$$

For the flat background, the radial Hubble distance and comoving transverse distance are

$$D_H(z) = \frac{c}{H(z)}, \qquad D_M(z) = c\int_0^z \frac{{\rm d}z'}{H(z')}. \tag{24.9}$$

With the usual photon-conservation and geometric propagation assumptions,

$$D_L = (1+z)D_M, \qquad D_A = \frac{D_M}{1+z}. \tag{24.10}$$

The isotropic baryon-acoustic-oscillation distance is

$$D_V(z) = \left[zD_H(z)D_M^2(z)\right]^{1/3}. \tag{24.11}$$

DESI measurements constrain combinations such as D_M/r_d, D_H/r_d and D_V/r_d, where

$$r_d = \int_{z_d}^{\infty} \frac{c_s(z)}{H(z)}{\rm d}z \tag{24.12}$$

is the sound horizon at baryon drag. The sound speed, drag epoch and high-redshift expansion depend on the thermal and particle content. A late-time distance fit with a supplied r_d is not an independent derivation of that early-universe scale [18, 17].

This matters for an age claim. Baryon-acoustic-oscillation distances alone do not generally fix an absolute time scale without assumptions or calibrators. A theory that changes early-time physics must recalculate r_d, rather than use a standard value while claiming an entirely new early expansion history.

24.5 The age integral and an analytic control

The cosmic age at scale factor one is

$$t_0 = \int_0^1 \frac{{\rm d}a}{aH(a)} = \int_0^\infty \frac{{\rm d}z}{(1+z)H(z)}. \tag{24.13}$$

For a flat matter-plus-cosmological-constant model,

$$H(a) = H_0\sqrt{\Omega_m a^{-3} + \Omega_\Lambda}, \qquad \Omega_m + \Omega_\Lambda = 1, \tag{24.14}$$

substitution of $u = a^{3/2}\sqrt{\Omega_\Lambda/\Omega_m}$ gives

$$H_0 t_0 = \frac{2}{3\sqrt{\Omega_\Lambda}}\,{\rm asinh}\sqrt{\frac{\Omega_\Lambda}{\Omega_m}}. \tag{24.15}$$

This is an exact analytic check for that two-component background.

With an added massless-radiation approximation,

$$H(a) = H_0\sqrt{\Omega_r a^{-4} + \Omega_m a^{-3} + \Omega_\Lambda}, \tag{24.16}$$

a numerically convenient finite integral is

$$H_0 t_0 = \int_0^1 \frac{a\,{\rm d}a}{\sqrt{\Omega_r + \Omega_m a + \Omega_\Lambda a^4}}. \tag{24.17}$$

This form avoids directly evaluating inverse powers of a at the lower endpoint.

24.6 Fresh numerical age calculation

The benchmark adopts $H_0 = 67.4\ \mathrm{km\,s^{-1}\,Mpc^{-1}}$, $\Omega_m = 0.315$, $\Omega_r = 9.2 \times 10^{-5}$ and $\Omega_\Lambda = 1 - \Omega_m - \Omega_r$. The first two are rounded Planck-like comparison values; the radiation treatment is an explicit approximation, not the full massive-neutrino background of a Planck parameter inference [17].

The computed results are

$$H_0 t_0 = 0.9506034672, \tag{24.18}$$

$$t_0 = 13.7906925\ \mathrm{Gyr} \quad \text{with the declared radiation term,} \tag{24.19}$$

$$t_0 = 13.7962346\ \mathrm{Gyr} \quad \text{without radiation, with flatness restored.} \tag{24.20}$$

The radiation-free quadrature agrees with (24.15) within the recorded numerical tolerance. The roughly 5.54 million-year difference between the two benchmarks is caused by the changed background assumptions, not a new measured discrepancy. Numerical quadrature precision is much smaller than the uncertainty associated with the supplied parameters and the simplified matter treatment.

These calculations meet a useful reproducibility requirement: the age, assumptions, units and integration formula are explicit. They are not a first-principles MNT age prediction. Such a prediction would obtain $H(a)$ and its absolute scale from the same microscopic completion used for the other sectors.

24.7 Perturbations, growth and early-time targets

The background is only part of cosmological recovery. In a suitable subhorizon linear regime, matter growth takes the form

$$\ddot{\delta}_m + 2H\dot{\delta}_m - 4\pi G_{\mathrm{eff}}(k, a)\rho_m \delta_m = 0. \tag{24.21}$$

The effective gravitational response and any difference between the two metric potentials must be derived from the same action that fixes the background and tensor propagation. A change in F that alters gravitational-wave damping cannot be adjusted independently in the growth calculation without introducing a different model.

A complete early-universe calculation additionally specifies the origin and evolution of primordial perturbations, the thermal history, light-element production, recombination and the relic populations. Under particular single-field slow-variation assumptions, relations such as $\mathcal{P}_\mathcal{R} \simeq H^2/(8\pi^2 M_{\mathrm{Pl}}^2 \epsilon c_s)$ can be derived; their assumptions and state choice cannot be imported as an unexplained primordial prediction of the threshold rule.

For a thermal dark-particle example, a number density obeys

$$\dot{n}_\chi + 3Hn_\chi = -\langle\sigma v\rangle(n_\chi^2 - n_{\chi,\mathrm{eq}}^2) \tag{24.22}$$

under the specified pair-annihilation and thermal-bath assumptions. The scattering interaction used in a detector and the interaction controlling the relic abundance must be connected consistently. This is an especially useful cross-domain test: a candidate cannot acquire a new density normalization in each experiment merely to improve agreement.

24.8 Thermal history as an independent requirement

The background expansion must also be compatible with the reaction network of primordial nucleosynthesis. In a reaction equation $\dot{n}_i + 3Hn_i = C_i$, the collision term C_i depends on nuclear and weak rates, temperature, chemical potentials and abundances. An exchange contribution from the reserve can alter both the expansion rate and the distribution functions entering these rates. Treating its energy as conserved in total does not ensure that either change is observationally acceptable. Precision nucleosynthesis methods illustrate the required separation of reaction inputs, weak corrections and cosmological evolution [68]. No primordial-abundance likelihood has been executed for the phase-reserve model in this edition.

25. Statistical mechanics, radiation and a conservative reserve

25.1 A deterministic state and an ensemble are different objects

Hamiltonian evolution assigns a unique trajectory to each specified initial state. Statistical mechanics assigns a measure to a set of such states. These are compatible descriptions, but the measure is additional information. In particular, a canonical distribution is not implied by the existence of a conserved Hamiltonian alone. It represents an equilibrium preparation with a temperature and a specified set of accessible degrees of freedom.

For the finite model, Liouville's equation is

$$\partial_\tau f + \{f, H_*\} = 0. \tag{25.1}$$

Integration over phase space preserves normalization. Under admissible boundary conditions, the fine-grained Gibbs entropy $S_G = -k_B \int f \log f \, \mathrm{d}\Gamma$ is constant, because Hamiltonian flow is incompressible. Apparent entropy increase in a reduced subsystem comes from coarse graining, correlations and ignored reserve variables. It is not destruction of the information in the full trajectory.

Tracing or integrating out the reserve generally introduces memory. Assuming that the reduced system is instantaneously memoryless is a further approximation. The exact derivation in Section 3 shows explicitly where that approximation enters. It also shows why the state of the reserve affects the result: two experiments with identical phase coordinates but different stored-mode preparation need not have identical subsequent conversion.

25.2 The canonical normalization and energy fluctuations

For a system in equilibrium at inverse temperature $\beta_T = 1/(k_B T)$,

$$Z = \mathrm{Tr}\, e^{-\beta_T H}, \qquad \langle E \rangle = -\partial_{\beta_T} \log Z, \qquad \mathrm{Var}(E) = \partial^2_{\beta_T} \log Z. \tag{25.2}$$

The classical integral replaces the trace where appropriate. Differentiating the mean energy with respect to temperature gives

$$C_V = \frac{\mathrm{Var}(E)}{k_B T^2} \geq 0 \tag{25.3}$$

for this canonical fixed-Hamiltonian system. These identities constrain thermal calculations and make useful numerical checks. They do not set the numerical SI value of k_B, which defines the relation between the kelvin and the energy unit in the present SI [38].

A harmonic quantum mode with energy levels $E_n = \hbar\omega(n + 1/2)$ has

$$Z_\omega = \frac{e^{-\beta_T\hbar\omega/2}}{1 - e^{-\beta_T\hbar\omega}}, \qquad \langle E\rangle = \frac{\hbar\omega}{2} + \frac{\hbar\omega}{e^{\beta_T\hbar\omega} - 1}. \tag{25.4}$$

The classical high-temperature limit of the thermal part is k_BT. This quantum mode formula assumes quantum energy levels; a continuous classical phase oscillator alone does not derive them. The reconstructed node mechanics and its conditional quantization must remain distinguished.

25.3 Deriving the blackbody law under its physical assumptions

For two transverse massless photon polarizations in three-dimensional continuum space, the mode density per unit volume and angular frequency is $\omega^2/(\pi^2c^3)$. The zero-chemical-potential Bose occupation is $1/(e^{\hbar\omega/k_BT} - 1)$. Multiplying by $\hbar\omega$ gives the thermal spectral energy density

$$u_\omega(T) = \frac{\hbar\omega^3}{\pi^2c^3}\frac{1}{e^{\hbar\omega/k_BT} - 1}. \tag{25.5}$$

This is the Planck radiation law [64]. Its derivation requires the photon dispersion, two physical polarizations, quantum statistics and thermal equilibrium. A node theory that recovers those structures recovers the law; simply inserting its final temperature does not explain a cosmological background.

With $x = \hbar\omega/(k_BT)$,

$$u(T) = \frac{(k_BT)^4}{\pi^2\hbar^3c^3}\int_0^\infty \frac{x^3}{e^x - 1}\,\mathrm{d}x. \tag{25.6}$$

Expand $1/(e^x - 1) = \sum_{n\geq 1} e^{-nx}$. Termwise integration gives $\int_0^\infty x^3e^{-nx}\mathrm{d}x = 6/n^4$, and the sum equals $\pi^4/15$. Therefore

$$u(T) = \frac{\pi^2k_B^4}{15\hbar^3c^3}T^4. \tag{25.7}$$

Isotropic radiation incident on a surface has flux $cu/4$. Consequently

$$j = \sigma T^4, \qquad \sigma = \frac{\pi^2k_B^4}{60\hbar^3c^2} = \frac{2\pi^5k_B^4}{15h^3c^2}. \tag{25.8}$$

The two forms are algebraically identical because $h = 2\pi\hbar$. Replacing one symbol by the other without its factors is an error, not a new physical correction. In the SI, h, k_B, c are fixed exactly, so the defining expression for σ is exact; a finite decimal display is rounded.

25.4 When the network would change a radiation spectrum

A lattice changes the mode density and dispersion outside its long-wavelength regime. A physical quantum network would have

$$u(T) = \sum_s \int_{\mathrm{BZ}} \frac{\mathrm{d}^3k}{(2\pi)^3}\frac{\hbar\omega_s(\mathbf{k})}{e^{\hbar\omega_s(\mathbf{k})/(k_BT)} - 1}, \tag{25.9}$$

with physical branches s, their degeneracies and the Brillouin zone specified. A finite graph uses a corresponding sum over modes. This is a concrete prediction route once the photon sector is identified. The scalar phase branch of the present model has one polarization, not the two electromagnetic polarizations. It therefore cannot be inserted into the photon formula without a gauge-field construction.

For $k_B T \ll \hbar c_*/a$, the thermally occupied low-frequency modes may approximate continuum radiation. Corrections then depend on the same lattice dispersion derived earlier, rather than an independently fitted thermal coefficient. A selected microscopic model must also reproduce the relevant spectral normalization. The cubic directional correction cannot be silently averaged away when the experiment resolves direction.

25.5 Fermi statistics and material-specific scales

For a spin-1/2 noninteracting gas at zero temperature, two states occupy each momentum cell. Counting states inside a Fermi sphere gives

$$n = \frac{k_F^3}{3\pi^2}, \qquad E_F = \frac{\hbar^2}{2m}(3\pi^2 n)^{2/3} \tag{25.10}$$

in the nonrelativistic limit. This is not one universal Fermi energy for all materials. Density, dispersion, band structure and interactions matter. Using $n = 10^{28}\,\mathrm{m}^{-3}$ and the supplied electron mass gives $E_F = 1.69253219\,\mathrm{eV}$ in the ideal-gas model. Changing the density to obtain a preferred number would be a different physical input.

The same distinction applies to sound speeds, atmospheric pressure, stellar radii and planetary orbital elements. A unifying fundamental theory must reproduce their governing equations and, given the relevant composition and initial conditions, their behavior. It need not assign a universal number to an environment-dependent quantity. Counting repeated material values as separately derived fundamental constants obscures rather than strengthens a test.

25.6 The reserve energy is not automatically dark energy

A homogeneous canonical scalar has $\rho = \dot\phi^2/2 + V$ and $p = \dot\phi^2/2 - V$ in natural units. A slowly changing potential-dominated state can have $w = p/\rho \simeq -1$. A kinetic-dominated state has $w \simeq 1$. For rapid bounded oscillations in $V(\phi) \propto |\phi|^n$, the averaged virial identity gives $\langle\dot\phi^2\rangle = n\langle V\rangle$, so

$$\overline{w} = \frac{n-2}{n+2}. \tag{25.11}$$

A quadratic potential gives matter-like average pressure, whereas a quartic one gives radiation-like pressure, under the stated rapid-oscillation and homogeneous approximations. The label unexpressed potential alone selects none of these equations of state.

The finite reserve in the master Hamiltonian is not an expanding cosmological fluid until a spacetime stress tensor and its volume dependence are defined. A proper cosmological completion must derive pressure as well as density and transfer current. Otherwise an arbitrarily assigned reserve can mimic whichever component is desired without a falsifiable prediction.

25.7 Vacuum effects and the work account

A static Casimir force concerns differences of field energy between boundary configurations. A dynamical Casimir experiment creates excitations under time-dependent boundary conditions, with energy supplied by the modulation. Superconducting-circuit experiments have observed such emission [65]. These effects provide useful analogies for conversion of a driven field configuration into observable quanta, not evidence for a limitless power source.

For an explicitly controlled Hamiltonian $H(z;\lambda(\tau))$,

$$\frac{\mathrm{d}H}{\mathrm{d}\tau} = \frac{\partial H}{\partial \lambda}\dot{\lambda} \tag{25.12}$$

along its Hamiltonian trajectory. The right-hand side is supplied work. Once the control source is included dynamically, its energy loss balances the gain elsewhere. Any proposed EQEF technology must provide this complete accounting, including preparation, resetting, heat and useful extracted work. A conservative interpretation is strengthened, not weakened, by imposing that requirement.

Part VI

Predictions, computations and physical implications

26. From a common physical model to experimental observables

26.1 The same theory, not the same numerical observable

A universal model does not predict that a clock frequency, a scattering cross section and a cosmic distance have the same numerical value. It predicts them through one set of dynamics and parameters. A useful common notation is

$$\vartheta \longrightarrow \{s_i, \phi_i, g_{\mu\nu,i}\} \longrightarrow f_i \longrightarrow \mu_{ib}, \tag{26.1}$$

where i denotes a physical experiment, s_i its independently specified preparation, f_i a physical distribution and μ_{ib} an expected detector bin. The same fundamental ϑ is used throughout. Beam conditions, source distance and apparatus response are not generally universal, but their provenance and uncertainty must be declared.

The observation operator is as important as the field equation. A physical effect can change an amplitude, a phase, a lifetime, an energy distribution or an event count. These changes are not interchangeable. For example, multiplying a waveform by a constant changes its amplitude but not its propagation phase; multiplying a Hamiltonian by a scalar clock factor reparameterizes its evolution; adding a multiple of the identity changes only a common phase. None of these operations automatically modifies a dimensionless coupling ratio.

The revised conversion idea therefore enters at the point where its physical mechanism acts. Negation at a source belongs in the source intensity or branching process. Return after

production belongs in propagation or the survival probability. An EQEF force belongs in trajectories and energy–momentum transfer. A change in clock progression belongs in the mapping between evolution time and measured time. The following examples make that placement explicit.

26.2 Event counts and finite exposures

For a source with local differential event rate $r_0(E, \tau)$, a conversion efficiency $\eta(E, \tau)$ and a detector response $\mathcal{R}_b(E, t)$, one possible counting model is

$$\mu_b = B_b + \int \mathrm{d}t \int \mathrm{d}E\, \mathcal{R}_b(E, t)\, q(t)\, \eta(E, t)\, r_0(E, t). \tag{26.2}$$

B_b is the expected background. The response includes detector efficiency and energy migration as appropriate. This form assumes that propagation and source-to-detector time mapping have already been incorporated consistently. A remote source generally needs a separate arrival-time transfer function, rather than identifying its coordinate clock with the detector's local proper clock.

The background should not be multiplied by a source-specific efficiency without a physical reason. If the same field affects the detector, the detector response must be recalibrated or jointly modeled. A freely adjustable detector normalization is degenerate with a constant conversion efficiency. A measurement with no independent normalization can constrain shape changes while remaining insensitive to a common amplitude loss.

A finite exposure measures a weighted efficiency,

$$\eta_{\mathrm{eff}} = \frac{\int \mathrm{d}t\, w(t)\eta(t)}{\int \mathrm{d}t\, w(t)}, \qquad w(t) = \epsilon_{\mathrm{det}}(t)q(t)r_0(t), \tag{26.3}$$

not usually the arithmetic time average of η. This is an immediate consequence of integrating the event intensity. Binning more finely is useful only when the experiment independently determines the time dependence and the data justify the additional resolution.

26.3 Clocks: relative changes versus absolute efficiency

Let two clock processes at the same location have intrinsic rates ω_{10} and ω_{20}, with conversion responses η_1 and η_2. Their reference-time rates are

$$\omega_1 = q\eta_1\omega_{10}, \qquad \omega_2 = q\eta_2\omega_{20}. \tag{26.4}$$

The measured ratio is

$$\frac{\omega_1}{\omega_2} = \frac{\eta_1}{\eta_2}\frac{\omega_{10}}{\omega_{20}}. \tag{26.5}$$

A common lapse cancels exactly. A universal, constant efficiency multiplying both clocks cancels as well. A differential experiment is sensitive to differences in response, drift or environmental dependence, not to an arbitrary unobservable common rescaling.

For a single clock compared between locations, the predicted gravitational and kinematic frequency transfer must be included before attributing a residual to conversion. The optical-clock and Galileo examples in Volume II test such relative responses. They do not measure the absolute available potential of an atomic transition. An independently calculated transition spectrum would be needed to turn them into an absolute microscopic normalization test.

26.4 Unstable particles and disappearance channels

For a constant decay hazard Γ_0 per particle proper time, the survival law is

$$S(\tau) = \exp(-\Gamma_0 \tau). \tag{26.6}$$

A moving particle with constant Lorentz factor γ has $\tau = t/\gamma$, giving a laboratory lifetime γ/Γ_0. If the conversion mechanism changes that hazard to $\eta\Gamma_0$, the corresponding lifetime is $\gamma/(\eta\Gamma_0)$. Thus a smaller event rate produces a *longer*, not a shorter, lifetime. The sign depends on which physical process is modeled.

A separate unobserved return channel can instead add a hazard Γ_P:

$$S(\tau) = \exp[-(\Gamma_{\text{visible}} + \Gamma_P)\tau], \qquad \frac{\mathrm{d}N_{\text{visible}}}{\mathrm{d}\tau} = \Gamma_{\text{visible}} N_0 S(\tau). \tag{26.7}$$

This shortens total survival while reducing the visible branching fraction. It is not equivalent to multiplying the visible rate by a constant. Time spectra, branching fractions and energy balance distinguish the hypotheses. The returned energy–momentum must be included in the reservoir or interaction field, even when it is not registered by the visible detector.

A comparison of moving and resting lifetimes often determines a *ratio* of effective rates. It cannot separately determine the potential decay rate and a universal constant efficiency if the measured rest lifetime is already used as the baseline. The positive-muon example is reported with that restriction in Volume II.

26.5 Collider distributions and invariant masses

For hadronic collisions, a predicted partonic interaction must be convolved with the parton distributions and detector response:

$$\sigma(pp \to X) = \sum_{ij} \int \mathrm{d}x_1 \mathrm{d}x_2 \, f_i(x_1, \mu_F) f_j(x_2, \mu_F) \widehat{\sigma}_{ij\to X}(x_1 x_2 s; \vartheta), \tag{26.8}$$

$$\mu_b = B_b + \mathcal{L} \int \mathrm{d}\Phi \, \mathcal{R}_b(\Phi) \frac{\mathrm{d}\sigma}{\mathrm{d}\Phi}. \tag{26.9}$$

The luminosity $\mathcal{L}$ is calibrated in the experiment's timing convention. Applying another arbitrary time factor to it after the fact can double count that calibration. A predicted modification of an unstable intermediate state belongs in its propagator, width and branching fractions before detector convolution.

The invariant mass

$$M^2 c^4 = E^2 - c^2 \mathbf{p}^2 \tag{26.10}$$

is unchanged by a Lorentz change of observer. A clock correction does not multiply the reconstructed invariant mass by q or $1/q$. The explicit boost tests in Volume II verify this elementary boundary. A changed physical mass requires a changed rest-frame spectrum, not a relabeling of the observer's clock. Standard kinematic definitions are taken from the Particle Data Group review [8].

26.6 Neutrinos and a common phase

In a laboratory time or propagation parameter, a Hermitian flavor Hamiltonian gives

$$\mathrm{i}\hbar\frac{\mathrm{d}\psi}{\mathrm{d}t} = H(t)\psi. \tag{26.11}$$

A mere reparameterization $\mathrm{d}\tau = q\mathrm{d}t$ produces $H_t = qH_\tau$. At the same physical endpoints the evolution operator is unchanged. If a field adds $\beta(t)I$, then

$$U'(t) = \exp\left[-\frac{\mathrm{i}}{\hbar}\int \beta(t')\mathrm{d}t'\right] U(t), \tag{26.12}$$

so all flavor probabilities $|U_{\beta\alpha}|^2$ are identical. An observable new oscillation effect needs a flavor-dependent Hamiltonian component, an altered matter profile, a changed production/detection process, or a physically specified open-system term.

A nonunitary effective propagation description must retain the probability in all channels. Renormalizing the surviving active flavors to one can erase the very disappearance signal being tested. The proper time of a massless photon is not used as the laboratory evolution parameter; for relativistic neutrinos the standard oscillation phase is derived with the appropriate spacetime propagation approximation. No universal clock correction alone selects mass differences or mixing angles.

26.7 Dark-matter recoil spectra

For a specified incident species, halo distribution and scattering law, the rate per target mass has the conventional structure

$$\frac{\mathrm{d}R}{\mathrm{d}E_R} = \frac{\rho_\chi}{m_\chi}\sum_T \frac{\xi_T}{m_T}\int_{v\geq v_{\min}} \mathrm{d}^3v\, f_{\mathrm{lab}}(\mathbf{v})\, v\frac{\mathrm{d}\sigma_T}{\mathrm{d}E_R}. \tag{26.13}$$

An EQEF hypothesis must specify whether it changes the population, the cross section, the energy transfer, or a detector response. A deficit in observed recoils could otherwise be explained by several different factors. The published XENONnT limit tables used in Volume II are conditional constraints on particular interactions and halo assumptions [22, 23]; they are not a direct measurement of E_P.

If a new process converts a recoil into an unobserved reservoir excitation, its kinematics and energy partition must be modeled before applying the detector threshold. A constant reduction in counting efficiency and a changed recoil-energy spectrum have different implications. A limit curve cannot be reused as a universal likelihood for any possible conversion model.

26.8 Gravitational waves: phase, damping and timing

A detector waveform is a response-weighted combination of the physical polarizations. For independent detectors with one-sided noise spectra $S_I(f)$, the usual Gaussian-noise likelihood is

$$\log\mathcal{L} = -\frac{1}{2}\sum_I (d_I - h_I \mid d_I - h_I)_I + \text{const}, \tag{26.14}$$

where

$$(a \mid b)_I = 4\,\mathrm{Re}\int \frac{\widetilde{a}^*(f)\widetilde{b}(f)}{S_I(f)}\mathrm{d}f. \tag{26.15}$$

A derived dispersion correction belongs in the phase of h_I. A modified effective Planck coefficient can change propagation damping. A source conversion process may change emission and source evolution. A clock-representation change alone changes the data and model coordinates consistently, leaving the statistical comparison invariant.

The published massive-mode bound and the conditional tensor-speed result address different branches. Neither follows from the existence of a scalar conversion field alone. A successful raw-strain analysis would need a waveform family, calibration model, source priors, noise treatment and a specified EQEF observable. The present numerical work tests wave-equation time reparameterization and published bound conversions, not that full likelihood.

26.9 Cosmological distance, counts and elapsed age

A cosmological clock change must preserve the relation between expansion, redshift and physical distance. If it is a coordinate change only, $H_t = qH_\tau$ and $\mathrm{d}\tau = q\mathrm{d}t$ preserve the physical distance and age integrals. If it is a new physical field interaction, the background and perturbations must be solved with that interaction.

This distinction prevents an apparent improvement obtained by changing only the theoretical distance while leaving the measurement convention fixed. For an invertible change of coordinates in a Gaussian data vector, transforming data, prediction and covariance together leaves χ^2 unchanged. The DESI reparameterization test in Volume II demonstrates this numerically. A genuine change to $H(z)$, the sound horizon or the relation between photons and clocks is a new cosmological model, not an algebraic correction to an already standardized table.

26.10 One observable specification per physical effect

The result of this section is a practical rule: locate the proposed conversion effect in a physical forward model before scoring a residual. The field response, rate convention, detector calibration and observable must not be inferred independently from the same discrepancy. The joint theory can then be tested by carrying one parameter set through its several forward models, with correlated uncertainties and overlapping datasets treated explicitly.

27. Predictions fixed by the reconstruction

27.1 A prediction must state its model and its observable

The finite conservative model is sufficiently specified to make predictions before a trajectory is computed. Some predictions contain dimensional model parameters; others are ratios in which those scales cancel. They are not claimed to be newly discovered laws of nature. They are consequences of this explicit construction, and a physical identification would make them experimentally falsifiable.

The distinction between a model prediction and a verified physical alignment is retained throughout. A theorem checked by numerical integration is a mathematical success. A synthetic experiment generated from that theorem is a check of an analysis method. An experiment in nature that was not used to select the equation would provide physical evidence. These three levels must not be combined into an overall percentage of correctness.

27.2 Prediction I: a fixed directional lattice correction

For the isotropic nearest-neighbor cubic phase model,

$$\frac{\omega}{c_* k} = 1 - \frac{a^2 k^2}{24} \sum_{j=1}^{3} \widehat{k}_j^4 + O(a^4 k^4). \tag{27.1}$$

At the same wave-number magnitude, the leading coefficient is $-1/24$ along an axis, $-1/48$ along a face diagonal, and $-1/72$ along a body diagonal. The axis-to-body-diagonal ratio is therefore exactly three. It does not depend on K, I or a clock-unit choice.

This statement is lost if the graph is made irregular, additional links are introduced, or direction is averaged. Those changes may define interesting models, but are not adjustments allowed after this test fails. A physical lattice interpretation would need to identify its orientation or derive why the observable averages over it. An analogue lattice with known geometry provides an immediate mathematical implementation test; an astronomical interpretation requires a justified mapping of its propagating degrees of freedom.

27.3 Prediction II: attenuation and frequency shift are linked

In the passive memoryless linear limit, the mode attenuation and oscillation frequency satisfy

$$\gamma_\lambda = \frac{\zeta \lambda}{2I}, \qquad \omega_{d,\lambda}^2 + \gamma_\lambda^2 = \frac{K\lambda}{I}. \tag{27.2}$$

Two modes therefore obey $\gamma_1/\gamma_2 = \lambda_1/\lambda_2$ under the same preparation. A decay rate fitted independently to every mode violates this prediction. At long wavelength $\lambda \simeq a^2 k^2$, so attenuation is proportional to k^2, not a common constant amplitude loss per arbitrary time step.

For a finite-memory reserve, the stronger statement is the shared susceptibility (4.3), not this limiting formula. The range in which the memoryless approximation applies must be declared using the measured or calculated reserve spectrum. An apparent failure outside that range tests the approximation, not necessarily the full conservative model. A claimed success must likewise not switch between the two descriptions without reporting it.

27.4 Prediction III: fluctuations are tied to drag

Under canonical reserve preparation, the same spectrum fixes

$$S_Q(\omega) = \frac{2k_B T}{\omega} \operatorname{Im} \chi_\lambda(\omega) \tag{27.3}$$

in the classical limit. This relates spontaneous fluctuations to a driven response. Temperature and preparation cannot be refitted to every frequency bin merely to force agreement. The

relation provides an independent channel after the response is characterized, although the general relation itself is established physics [43, 42].

This is a useful consequence of the conservation interpretation of EQEF. A reduced drag term should not be added without also considering the receiving degrees of freedom and, in a thermal state, their fluctuations. The framework thereby rules out a class of superficially attractive but physically incomplete damping-only corrections.

27.5 Prediction IV: a nonlinear recurrence ratio

The isolated equal-inertia two-node phase difference satisfies

$$\ddot{\delta} + \frac{2K}{I} \sin \delta = 0. \tag{27.4}$$

For turning amplitude $A < \pi$, its period is

$$T(A) = 4\sqrt{\frac{I}{2K}}\, \mathbb{K}\big(\sin^2(A/2)\big), \tag{27.5}$$

where $\mathbb{K}(m) = \int_0^{\pi/2} (1 - m \sin^2 u)^{-1/2} \mathrm{d}u$. Relative to the small-amplitude period,

$$\boxed{\frac{T(\pi/2)}{T(0)} = 1.180340599016096\ldots.} \tag{27.6}$$

This number is forced by the cosine interaction and the specified amplitude. It is not a mass ratio or a predicted value of α. Its role is a concrete demonstration of a dimensionless output that is calculated without using an experimental target. A change in measured amplitude or interaction law changes the prediction; it is not legitimate to scan them until an unrelated constant appears.

27.6 Prediction V: the readout threshold and reciprocal force

For the selected quartic readout, a slowly tilted metastable well disappears at

$$u_c = \frac{2}{3\sqrt{3}} = 0.3849001794597505\ldots. \tag{27.7}$$

The accompanying force on the phase system is fixed by the same coupling that tilts the readout. Omitting that reciprocal force generally violates conservation. The executed four-node readout simulation includes it and conserves total energy to an absolute error below 7.2×10^{-12} in its model units over the recorded interval.

This is a threshold of a particular nonlinear potential, not a universal energy density for all elementary particles. The geometry of a saddle-node transition is a well-defined mechanism for abrupt actuation. A physical particle-formation threshold would additionally require relativistic kinematics, quantum numbers, interactions and a detector model.

27.7 A common falsification protocol

For each physical application, the tested object is a tuple consisting of dynamics, state preparation, observable map, nuisance model and approximation domain. A failure cannot be repaired by altering an unreported member of that tuple. The appropriate protocol is to record the tuple, compute predictions with uncertainties, and compare measurements not used in its selection.

The proposed universal object is the microscopic law, not an identical value for every effective observable. For example, γ_λ changes across modes because λ changes while ζ remains fixed. Similarly, finite-time conversion changes with proper duration. The theory fails universality when the same declared physical configurations require incompatible fundamental couplings, not merely when two different systems have different rates.

Parameter-free here means independent of empirical target values, not free of mathematical assumptions. The exact number in the recurrence test still assumes a cosine interaction and an amplitude of $\pi/2$. Their physical selection is part of a unification claim. The present paper does not turn conditional predictions into established measurements by omitting those assumptions.

27.8 What would constitute the first distinctive physical alignment

A distinctive alignment would begin with a microscopic state and coupling normalization selected without the target measurement. The same construction would produce a detector-level observable different enough from a reference theory to discriminate between them. Its agreement with an unused measurement would then be evidence for that construction. A second independent domain would test whether the same microscopic choices remain valid.

The work reported here reaches explicit dynamics, exact identities, model-unit predictions and several conditional agreements with known measurements. It does not yet produce a unique low-energy electromagnetic coupling, a complete Standard Model spectrum or a cosmological history from the finite phase-reserve model. Therefore the count of newly established independent parameter-free physical alignments in this edition remains zero. This statement defines the scientific status of the completed manuscript; it does not erase the mathematical construction or the recorded results.

28. Executed calculations and comparison with measurements

28.1 A result ledger instead of an overall accuracy percentage

The computational companion records inputs, algorithms, tolerances, data sources and outcomes. The new Hamiltonian, memory, response and threshold calculations were executed for this reconstruction. The earlier baseline and proper-time analysis scripts were rerun from their supplied packages. Their assertions and outputs are retained with their original scopes. None is relabeled as a full raw-data likelihood when it is only a catalog, limit-table or educational calculation.

The combined executable suites record 946 successful assertions: 172 baseline checks, 23

retained numerical-audit checks, 325 proper-time and inference checks, 277 conservative-reconstruction checks 82 response/readout checks and 67 coupled-spectrum checks. These counts are implementation checks, not independent observations. Some verify that a proposed identity is false, that a control should be rejected, or that a numerical coordinate transformation cannot improve a likelihood. A large count is useful for reproducibility but has no direct interpretation as empirical accuracy.

28.2 The newly closed conservative model

The six-node ring uses the same phase inertia and nearest-neighbor stiffness on every link, with three specified reserve oscillators per link. Its couplings and initial state were chosen as explicit model-unit examples, not optimized against physical constants. The central recorded errors are

Check	Maximum recorded error
Relative drift of total Hamiltonian	3.04×10^{-13}
Time reversal, maximum state-coordinate difference	1.67×10^{-13}
Reference-time versus proper-time trajectory	6.64×10^{-13}
Direct reserve force versus exact memory expression	3.16×10^{-14}

The last three errors use the declared model-coordinate units, not SI measurement uncertainties. The exact memory comparison uses seven times and six links, with numerical quadrature independently evaluating the eliminated-reserve expression. The energy and momentum checks cover the recorded full trajectory rather than only its endpoint.

A separate conservative readout example includes reciprocal phase feedback. Its total-energy absolute error is 7.18×10^{-12} in model units. The readout crosses between the potential's regions and can oscillate; the absence of a dissipative bath in that example means the crossing is not falsely advertised as irreversible settling. The full trajectory is in the machine-readable dataset.

28.3 What the synthetic shared-efficiency test establishes

A generated four-channel experiment uses a common efficiency $\eta = 0.98$ and different known clock factors. Treating the channels as though those factors were identical gives a Poisson inconsistency statistic $D = 26943.62$. Applying the factors gives $D = 4.603$, with approximate three-degree-of-freedom tail probability 0.203. A separate calibration-and-holdout comparison gives $D \simeq 4.617$ under its stated covariance approximation.

The deliberately nonuniversal control remains incompatible after the same correction, with $D \simeq 1138.81$. Thus the method can correct a genuine clock mismatch without making every dataset pass. Because the data are synthetic, this is a validation of the inference method under a known generating model. It is not observed evidence that nature has $\eta = 0.98$, nor does it determine a physical EQEF field.

28.4 Real clock summaries

The optical height-step comparison uses the published measurement from Chou and colleagues [29], the declared height change and the weak-field reference shift. Its conditional residual is about 0.31 quoted standard deviations. The moving-muon comparison uses the published storage-ring lifetime [30], an independently published rest lifetime [31], and the rounded Lorentz factor in the source summary. Its residual is about −0.32 standard deviations under that simplified comparison.

The rounded Lorentz factor is not a reconstructed beam distribution. Consequently that number is not a new precision reanalysis of the historical experiment. It is a reproducible consistency calculation using stated summaries. The Galileo redshift result $(0.19\pm2.48)\times10^{-5}$ is likewise compatible with zero anomaly [32]. These comparisons support retaining the observed relativistic clock behavior. They do not isolate an absolute conversion efficiency from a separately known potential reservoir.

28.5 Gravity and gravitational waves

The universal metric branch has zero composition-dependent free-fall anomaly and coincident electromagnetic and tensor light cones. Those consequences are compatible with the selected MICROSCOPE and GW170817 constraints [33, 34]. Other effective branches need their own derived predictions; the compatible branch cannot be switched to after a different branch fails without recording a model change.

The computational material also converts a published massive-dispersion constraint and uses a versioned GW150914 catalog record [20, 21]. A massive-mode bound is not automatically a bound on cubic-lattice dispersion: their frequency dependence differs. No new raw strain likelihood, echo detection or waveform residual search is reported in this edition.

28.6 Collider, recoil and neutrino checks

Four displayed CERN educational dimuon records reproduce invariant masses within their input-rounding intervals; the maximum difference of central values is about 0.000289 GeV [24]. This checks four-vector arithmetic and precision handling. It does not predict a collider distribution or establish a new resonance.

Twenty published XENONnT limit rows, including the power-constrained interpretation used in the source release, are reconstructed [22, 23]. They are upper-limit diagnostics for specified interactions, not twenty observed EQEF signals. A microscopic recoil prediction still requires a stable dark species or another explicit interaction, abundance, target response and detector model.

Three-flavor neutrino and antineutrino propagation is evaluated for a DUNE-like baseline and stated matter density [25, 26]. Two numerical methods agree near machine precision and probabilities sum to one. This is a forecast benchmark with supplied oscillation parameters. It is not a fit to observed DUNE far-detector events and not a derivation of the mixing angles from the phase-reserve model.

28.7 The cosmology result is retained without retuning

The fixed background tested against the 13-entry DESI BAO vector and covariance gives

$$\chi^2 = 28.5062, \qquad p \simeq 0.007686 \tag{28.1}$$

under the stated fixed-prediction Gaussian comparison [18, 19]. The tail probability is not the probability that the theory is true or false. The residual indicates tension for that particular supplied background. It is not an exclusion of every cosmological model and is not counted as a successful MNT prediction.

The same radiation-inclusive benchmark gives an elapsed cosmic proper age of 13.7906925 Gyr. This uses supplied expansion parameters and is not generated by the finite microscopic Hamiltonian. A separate analytic audit using $H_0 = 70\,\mathrm{km\,s^{-1}\,Mpc^{-1}}$, $\Omega_m = 0.3$ and no radiation gives 13.46698395 Gyr. The input choices are not interchanged to claim a better age result.

A consistent change of time coordinates leaves the physical distance prediction and properly transformed likelihood unchanged. It therefore cannot repair the fixed DESI residual by itself. An EQEF cosmology must change physical stress-energy, expansion, propagation or source physics through declared equations, then confront the same measurements.

28.8 Constants and the final evidentiary boundary

The new reference dataset recomputes 28 derived quantities from declared SI definitions and CODATA inputs [38, 13, 39]. Their mathematical dependencies are recorded. They are not counted as 28 independent predictions. The dimensionless coupling normalization and particle spectrum remain physical matching quantities rather than numbers extracted from a universal time multiplier.

The positive result of this reconstruction is thus specific: an explicit conservative microscopic example, a derived nonlocal-in-time conversion response, a consistent proper-time comparison, a set of conditional quantitative predictions, and rerunnable comparisons with selected known measurements. A final empirical claim of unification would require the additional matching chain stated in the conclusion. The manuscript does not replace that chain with a percentage.

29. Physical implications and the completed reconstruction

29.1 What has become an equation rather than a metaphor

The physical idea retained throughout this paper is that expression can change without destroying the conserved content of a closed system. The reconstructed Hamiltonian assigns degrees of freedom to both the phase system and the receiving reserve. It specifies their mutual force, so the reserve is not an unexplained sink. Eliminating it yields memory, return and preparation dependence. Adding a conservative nonlinear readout gives a concrete threshold mechanism with reciprocal backreaction.

These are actual mathematical consequences of an explicit model. Total energy is conserved, the finite flow is well posed, the phase convention has the stated symmetry, and

clock reparameterization leaves a trajectory invariant. The associated numerical calculations independently verify those properties and several exact solutions. This is mathematical closure of the selected finite reference construction.

The construction also clarifies the meaning of a measured deficit. An incomplete conversion fraction can depend on the proper observation interval, the state of the reserve and the measured channel while the underlying couplings remain fixed. A changing fraction is not by itself evidence against universality. A different coupling required for identical defined physical conditions is.

29.2 What follows for time

A sequence of updates provides order. A physical clock requires a stable relation between its observable progression and the events being compared. The parametrized Hamiltonian construction separates those ideas. Once proper time is used for local dynamics, reference-time rates carry the chain-rule factor $\mathrm{d}\tau/\mathrm{d}t$. A common factor can cancel from local clock ratios, so an absolute universal slowing is not identifiable from those ratios alone.

This places the time-dilation clarification on a firm footing. It can correct rate and lifetime comparisons that mixed clock conventions. It does not change dimensionless couplings or invariant masses merely by relabeling time. If EQEF is meant to cause the metric clock effect, its metric coupling must be derived and applied once; it must not then be multiplied into the result a second time.

29.3 What follows for matter and interactions

Persistent configurations require stability, a physical spectrum and a representation of their observable charges and spin. The cosine graph predicts coherent modes and nonlinear recurrences. The quartic readout predicts a sharp response threshold. The quantum examples predict reversible population transfer. None of these facts alone identifies the electron or selects its measured mass.

The conditional field-theory chapters show how conventional quantum, gauge and gravitational equations follow after their additional structures are stated. Those recovery calculations are important: they provide a common language and explicit requirements for a more complete microscopic selection. They must not be read backward as proof that every assumption used in the recovery has already been derived from nodes.

A unifying microscopic theory would remove the freedom in those matching structures. It would predict the gauge normalization, matter representations, chirality, dimensionless mass ratios and gravitational response together. That is more restrictive than adding one term for each known force. The present paper identifies the relevant coefficients and constraints rather than choosing their values to match a list of constants.

29.4 What follows for gravity and cosmology

A conservative local reserve must contribute to the combined stress tensor in a covariant extension. Its pressure and equation of state depend on its action and state. It can behave neither as cold matter nor as a cosmological constant merely by being unseen. The cosmological

equations must evolve the receiving sector as well as the expressed one and must include expansion work.

The age of the universe is an integral of a physical expansion history. A microscopic update index without a derived clock and expansion map does not by itself determine an age in years. The supplied-background age and DESI comparison therefore remain reference calculations. Their value is that the assumptions and residuals are now visible and reproducible, not that they independently prove the proposed origin of spacetime.

A finite-energy phase configuration also does not automatically remove every gravitational singularity. Curvature, causal completeness and the stress-energy equations must be analyzed in the selected geometric completion. The black-hole thermodynamic formulas included here are correctly normalized conditional recoveries from their established assumptions, not direct astronomical detections of the microscopic reserve.

29.5 Ten requirements that the physical completion cannot evade

	Requirement	Status in this reconstruction
1	A complete conservative dynamics	Closed for the declared finite phase-reserve model, with reciprocal readout extension.
2	Positive energy and controlled stability	Proven for the stated Hamiltonian; effective spectra checked in their declared regimes.
3	Correct clock comparisons	Exact reparameterization and proper-time rate rules established; physical clock-to-node identification remains additional.
4	A measurable conversion observable	Energy and population definitions are distinct; inference degeneracies and required independent calibration are specified.
5	Quantum composition and outcome probabilities	Quantum recovery is conditional; a microscopic Born-rule and Bell-correlation derivation is not established.
6	One matter spectrum and gauge normalization	Matching equations and representation constraints are explicit; observed particle values are not generated by the finite scalar model.
7	Universal gravity and tensor waves	A conditional covariant branch reproduces tested metric consequences; its emergence is a separate matching problem.
8	Detector-level experimental predictions	Existing limited comparisons are rerun; no unperformed raw-data search is claimed.
9	A common cosmological history	Consistent evolution and age formulas are given; the fixed benchmark residual is retained.

	Requirement	Status in this reconstruction
10	Predictions that survive independent domains	Target-free model relations are derived; no new independent parameter-free physical alignment is claimed.

29.6 The remaining physical closure is four well-defined selections

The first selection is the physical microscopic state space and dynamics: why the chosen graph, reserve spectrum and couplings describe nature rather than one consistent example. The second is the quantum and matter map: how that construction generates the observed probability structure, gauge normalization and spectrum. The third is the geometric map: how the same degrees of freedom yield a universally coupled metric and its cosmological evolution. The fourth is the measurement map: how the frozen construction generates joint detector-level predictions without a separate fit in each domain.

These selections are not missing explanatory prose. They are mathematical and empirical conditions. The equations and tests in this edition give them precise targets. A successful closure could replace the illustrative reference construction while retaining the conservation and inference framework; an unsuccessful choice must be rejected rather than protected by additional unexplained coefficients.

29.7 Final statement

This edition is a finished mathematical reconstruction and testable candidate framework, not a claim that a demonstrated theory of all observed physics has been completed. It establishes a conservative mechanism for the intended actuation–potential exchange, derives its memory and response, and supplies complete reproducible calculations for the comparisons actually performed. It also makes explicit which familiar laws are recovered conditionally and which physical quantities remain to be derived.

The resulting scientific claim is narrower than universal empirical confirmation, but substantially more definite than a symbolic sum of unexplained terms: a specified Hamiltonian, exact implications, reproducible predictions and clear tests that can reject its physical identification. No final numerical agreement is inserted in place of an unperformed derivation.

Technical appendices

A. A precise primitive framework

A.1 State spaces, equivalence and observables

Logical role: Definitions and mathematical consequences.

Let $(\mathcal{S}, \Sigma)$ be a measurable space of microscopic descriptions. An equivalence relation $\sim$ identifies descriptions that are intended to represent the same physical possibility. Write $\pi : \mathcal{S} \to \overline{\mathcal{S}} = \mathcal{S}/\!\sim$ for the quotient map. An observable O that is insensitive to the descriptive redundancy must satisfy

$$s \sim s' \quad \Longrightarrow \quad O(s) = O(s'). \tag{A.1}$$

Consequently $O = \overline{O} \circ \pi$ for a function $\overline{O}$ on the quotient, provided the corresponding measurability conditions are met. The quotient removes multiple descriptions of the same outcome. It does not establish that every infinite set of possibilities is finite. The strings 1, 1.0 and 1.00 represent one number; the infinitely many distinct integers remain distinct.

A future physical equivalence is stronger than equality of one currently chosen observable. Two hidden states can have the same current readout and different future dynamics. Therefore equivalence must also respect the update.

Proposition A.1 (Dynamics on equivalence classes)**.** *Let $K(s, A)$ be a Markov transition kernel on $\mathcal{S}$. A transition law on equivalence classes is well defined if, for every measurable quotient set $\overline{A}$,*

$$K(s, \pi^{-1}\overline{A}) = K(s', \pi^{-1}\overline{A}) \qquad \text{whenever } s \sim s'. \tag{A.2}$$

Under this condition, $\overline{K}(\pi(s), \overline{A}) = K(s, \pi^{-1}\overline{A})$ is independent of the representative chosen.

Proof. The right-hand side has the same value for every representative of $\pi(s)$ by (A.2). It is a probability measure in $\overline{A}$ because inverse images preserve complements and countable disjoint unions. Thus it defines a quotient transition law. Without the equality, two representatives of the same alleged physical state would predict different next-state probabilities. □

This condition supplies a direct test for any proposed quotient. For a finite state model, one adds the transition probabilities into each target equivalence class and checks equality for source states in the same class. For a deterministic update, a sufficient condition is $s \sim s' \Rightarrow U(s) \sim U(s')$.

A.2 The minimum complete specification

The measurable state-space potential in this section is not yet an energy reserve. The latter requires an observable map, as specified in Section 1. A mathematically executable realization is specified by

$$\mathfrak{M} = (\mathcal{S}, \Sigma, \sim, \mu, U, R, B, J_0, J_1, O, \Pi_0). \tag{A.3}$$

Its entries have different jobs. Π_0 is an initial distribution; it cannot be omitted when predictions depend on initial conditions. R and B are real-valued functions with a common

scale. The inequality is strictly $R > B$ in this edition; choosing $R \geq B$ defines a different model at boundary states. J_1 must specify the post-event state, not only announce that an event occurred.

The state space must include every variable needed by the next update. A rule depending on the last two frames is Markovian on the enlarged state (s_n, s_{n-1}), even if it is not Markovian on s_n alone. No separate physical archive is necessary; the relevant memory can reside in the current enlarged state.

For measurable F and a fresh input independent of the current state, the transition kernel is

$$K(s, A) = \int \mathbf{1}_A\big(F(s, \xi)\big)\, \mu(\mathrm{d}\xi). \tag{A.4}$$

The probability of a finite trajectory of measurable events is then obtained by successive integration against Π_0 and K. In a finite or countable state model this reduces to products and sums. Existence of such a stochastic process is therefore a separate, tractable question from whether its observables describe the physical world.

A.3 Probability, amplitude and intensity are distinct

A probability law Π assigns nonnegative weights with total one. A complex amplitude $ae^{\mathrm{i}\theta}$ can interfere with another amplitude and need not itself be a probability. A phasor sum

$$Z_N = \sum_{j=1}^{N} a_j e^{\mathrm{i}\theta_j} \tag{A.5}$$

has amplitude $A_N = |Z_N|$ and intensity $I_N = |Z_N|^2$. Neither is automatically a normalized Born probability. Normalization and the measurement rule belong to the quantum extension.

This distinction also fixes threshold powers. If the amplitude threshold is $B_N = \kappa N^p$, then the exactly equivalent intensity threshold is

$$A_N > \kappa N^p \quad \Longleftrightarrow \quad I_N > \kappa^2 N^{2p}. \tag{A.6}$$

Using I_N on the left and retaining the amplitude exponent on the right changes the model. In particular, the amplitude window $1/2 < p < 1$ corresponds to an intensity exponent between one and two.

If reinforcement combines several channels,

$$I(s) = \sum_{A} w_A \left| \sum_{j \in A} a_j e^{\mathrm{i}\theta_j} \right|^2, \qquad w_A \geq 0, \tag{A.7}$$

then the channel partition, the weights and the corresponding intensity capacity are all part of the specification. A single-channel theorem cannot be applied to a changing multichannel rule without checking its assumptions.

A.4 Updates and physical time

The integer n orders updates. Ordering is not yet an SI time coordinate. A clock observable can be a recurrence, a phase accumulated by a stable mode, or a count of designated events. If a clock has a reproducible period of k updates and a physical period τ_0, then

$$N_{\mathrm{tick}}(n) = \lfloor n/k \rfloor, \qquad \tau(n) = \tau_0 N_{\mathrm{tick}}(n). \tag{A.8}$$

The first equation is dimensionless. The second introduces the clock's conversion scale. A derivation of clock-rate ratios can already be meaningful before one chooses seconds as a unit.

A deterministic map on a finite state space eventually repeats a state. Once a state repeats, its future repeats, so the trajectory is eventually periodic. The conclusion changes for stochastic systems, infinite state spaces and maps with growing counters. A finite irreducible Markov chain is recurrent in the probabilistic sense, but it does not generally execute a deterministic cycle. An unbounded event counter does not become periodic merely because the rule updates indefinitely.

A usable clock also needs a distribution of tick intervals. If τ is a first-crossing time, the survival function $S_n = \mathbb{P}(\tau > n)$ and the hazard

$$h_n = \mathbb{P}(\tau = n \mid \tau \geq n) \tag{A.9}$$

characterize that distribution. Reporting the average of the trajectories that happened to cross discards censored trajectories and can conceal a substantial probability of no tick within the observation window.

A.5 What is retained when a frame is replaced

Consider a deterministic map $F : \mathcal{S} \to \mathcal{S}$. If it is one-to-one, the previous state is mathematically recoverable from the current state on the image of F. If it is many-to-one, distinct predecessors can produce the same successor. These are different forms of state replacement.

A unitary quantum update is invertible. An observed subsystem may nevertheless appear irreversible because information is transferred to other degrees of freedom. A classical reset can instead be genuinely many-to-one within the specified state space. The phrase "the previous frame is not separately stored" does not decide which case applies. The map does.

This distinction makes the framework compatible with careful information accounting. One can describe a current state that contains all causal information relevant to the next update without postulating an extra archive of past universes. Whether that information is microscopically reversible is then a property to prove, not a conclusion drawn from the word replacement.

A.6 The first-principles input rule

At the primitive stage, no measured electromagnetic coupling, particle mass, gravitational constant, cosmological density or observed expansion rate is used to choose U, R, B or J.

Conversely, an effective benchmark is allowed to use such values, provided they remain labelled as inputs.

The correct dependency structure is

$$\begin{aligned} &\text{declared microscopic model} \\ &\quad \longrightarrow \text{derived structures and dimensionless ratios} \\ &\quad \longrightarrow \text{physical scale identification} \\ &\quad \longrightarrow \text{observable prediction.} \end{aligned} \tag{A.10}$$

Initial conditions, discrete model choices, normalizations and boundary conditions are included in that dependency record. Calling a parameter an integer or a topological quantity does not exempt it from the rule: selecting an integer after looking at a target number can still constitute fitting.

B. An auxiliary threshold model and a persistent statistical clock

This appendix studies a separately declared stochastic threshold model. It is not the deterministic node–reserve Hamiltonian of the main text, nor a derivation of stochastic noise from it. Its purpose is to retain the exact first-passage and clock results at their stated assumptions.

B.1 R0: a complete classical benchmark

Logical role: Constructive example introduced in this edition.

This retained mathematical example is not an EQEF field realization and does not determine a conversion efficiency. Its threshold and input choices remain declared examples. An explicit model is valuable even before it is identified with physical reality. It determines whether the proposed ingredients are sufficient to run an update, assign an event and obtain a reproducible distribution. The following model closes those mathematical choices without using experimental values.

The state is $s = (N, x, y, r, k)$. Here $N \in \mathbb{N}_0$ is the number of accumulated increments since the last event; $(x, y) \in \mathbb{Z}^2$ is the phasor sum; r is the most recent realized orientation label, initially undefined; and k counts realized events. Initially $N = x = y = k = 0$. At each update choose

$$\xi \in \{1, -1, \mathrm{i}, -\mathrm{i}\}, \qquad \mathbb{P}(\xi) = 1/4, \tag{B.1}$$

independently of the current state. Add its Cartesian components to (x, y) and increment N. Use $R = \sqrt{x^2 + y^2}$ and $B = N^{3/4}$. If $R > B$, set

$$r \leftarrow \frac{x + \mathrm{i}y}{\sqrt{x^2 + y^2}}, \qquad k \leftarrow k + 1, \qquad (N, x, y) \leftarrow (0, 0, 0). \tag{B.2}$$

Otherwise retain the accumulated state and emit no event. The output consists of the event flag and, at an event, the orientation label. The label is a classical orientation, not a one-component quantum ray; all nonzero one-component Hilbert vectors would represent the same ray under arbitrary overall-phase equivalence.

The threshold decision can be made using integers alone:

$$(x^2 + y^2)^2 > N^3. \tag{B.3}$$

This eliminates floating-point ambiguity at the threshold. The choices $p = 3/4$ and $\kappa = 1$ are mathematical benchmark choices. They are not asserted to be selected uniquely by the ontology. The increment law has quarter-turn and reflection symmetry; it is not an assumption of exact continuous rotational symmetry at the primitive level.

B.2 Exact first-passage distribution

Let $a_n(x, y)$ count length-n increment sequences that end at (x, y) and have not crossed earlier. Set $a_0(0, 0) = 1$. From each surviving state at step $n - 1$, add its count to each of the four successors. A successor satisfying (B.3) contributes to the first-crossing count h_n; otherwise it contributes to a_n.

There are 4^n equally likely unconstrained paths of length n, so

$$\mathbb{P}(\tau = n) = \frac{h_n}{4^n}, \qquad \mathbb{P}(\tau > n) = \frac{\sum_{x,y} a_n(x, y)}{4^n}. \tag{B.4}$$

The exact conservation check is

$$\sum_{j=1}^{n} \frac{h_j}{4^j} + \frac{\sum_{x,y} a_n(x, y)}{4^n} = 1. \tag{B.5}$$

All quantities can be represented as integer counts and rational probabilities. Two increments in the same direction cause the first possible event at step two, with probability $1/4$. No surviving trajectory can cross at step three: its largest possible squared radius is five, and $5^2 < 3^3$.

The 64-step calculation gives

$$\mathbb{P}(\tau \le 64) = 0.3887047543593976. \tag{B.6}$$

The independent Monte Carlo implementation gives 0.38816 from 50,000 paths, with binomial standard error 0.002180. Both implementations use the same specified model, but different methods: exhaustive state-count propagation versus sampled paths. The difference is about one quarter of a Monte Carlo standard error.

B.3 An infinite-horizon certificate

A finite calculation does not by itself decide whether surviving trajectories eventually cross. For R0, the remaining tail can nevertheless be bounded rigorously.

For the real component X of one R0 increment,

$$\mathbb{E}e^{\lambda X} = \frac{1 + \cosh \lambda}{2} = \cosh^2(\lambda/2) \le e^{\lambda^2/4}. \tag{B.7}$$

The inequality follows, for example, by integrating $\tanh t \le t$ for $t \ge 0$ and using evenness. Chernoff optimization gives $\mathbb{P}(\sum X_j \ge a) \le e^{-a^2/N}$. Applying this to the four coordinate tails yields

$$\mathbb{P}(|Z_N| > N^{3/4}) \le 4e^{-\sqrt{N}/2}. \tag{B.8}$$

An event after step T implies an unconstrained phasor overflow at some $N > T$. The union bound and monotonicity therefore give

$$\mathbb{P}(T < \tau < \infty) \le \sum_{N>T} 4e^{-\sqrt{N}/2} \tag{B.9}$$

$$\le 4 \int_T^\infty e^{-\sqrt{x}/2} \mathrm{d}x \tag{B.10}$$

$$= 16(\sqrt{T} + 2)e^{-\sqrt{T}/2}. \tag{B.11}$$

The exact dynamic program through $T = 512$ gives $\mathbb{P}(\tau \le 512) = 0.38879800489245525$. Combining it with the bound yields the outward-rounded certificate

$$0.3887980 < \mathbb{P}(\tau < \infty) < 0.3936071, \qquad \mathbb{P}(\tau = \infty) > 0.6063929. \tag{B.12}$$

The upper and lower endpoints are not confidence limits. They combine an exact finite-prefix calculation with an analytic tail inequality.

This is a concrete distinction between a threshold event and a durable clock. Pure independent zero-mean increments do not guarantee a continuing sequence of events under R0. This motivates adding persistent reinforcement when using this particular threshold/reset design as a reliable clock. A sufficient construction can itself be closed mathematically.

B.4 A coherent extension with finite mean tick time

Define Rm by retaining the same update, threshold and reset, but taking an increment from the positive real direction with an added mixture weight $m \in (0, 1]$. Equivalently,

$$\mathbb{P}(\xi = 1) = \frac{1 + 3m}{4}, \qquad \mathbb{P}(\xi = -1) = \mathbb{P}(\xi = \mathrm{i}) = \mathbb{P}(\xi = -\mathrm{i}) = \frac{1 - m}{4}. \tag{B.13}$$

Then $\mathbb{E}\xi = m$. The direction of the mean is a chosen reference direction for this example; no preferred direction in physical spacetime is inferred from it.

Theorem B.1 (Finite-mean renewal clock)**.** *For independent, identically distributed bounded unit increments with mean resultant $m \neq 0$, amplitude capacity κN^p with $p < 1$, and independent resets to the same initial accumulation state, the first-crossing time is almost surely finite and has finite expectation. Repeated resets generate a renewal clock with asymptotic event rate $1/\mathbb{E}\tau$ per primitive update.*

Proof. Rotate the complex coordinates so that $m = |m| > 0$ is real. For

$$N \ge N_0 = \left\lceil (2\kappa/m)^{1/(1-p)} \right\rceil, \tag{B.14}$$

the capacity is at most $mN/2$. Survival through N implies $|Z_N| \le \kappa N^p$, and therefore $\mathrm{Re}\, Z_N \le mN/2$. Hoeffding's lower-tail bound gives

$$\mathbb{P}(\tau > N) \le e^{-m^2 N/8}, \qquad N \ge N_0. \tag{B.15}$$

Thus $\mathbb{P}(\tau = \infty) = 0$ and $\mathbb{E}\tau = \sum_{N \ge 0} \mathbb{P}(\tau > N) < \infty$. Independent resets make the successive waiting times independent and identically distributed. Their sample mean converges to $\mathbb{E}\tau$, so the number of completed intervals divided by the accumulated update count converges to its reciprocal. □

The theorem supplies a dimensionless persistent-clock mechanism within this explicitly chosen model class. It does not identify a second, a Planck interval or the measured speed of light.

For $m = 0.2$, $\kappa = 1$ and $p = 3/4$, 10,000 simulated waiting times give a mean of 262.7814 updates, with Monte Carlo standard error 3.5983 updates. The largest observed waiting time is 2257. No path is censored at the declared horizon 16,384, where (B.15) bounds the remaining tail probability by 2.6461×10^{-36}. This is a mathematical clock benchmark with a declared coherence input, not a physical frequency fit.

B.5 What has and has not been selected

R0 and Rm are fully executable: their state, distribution, threshold, reset, output and initial conditions are explicit. Their probabilities and clock statistics are therefore reproducible. The construction demonstrates that the conceptual ingredients can be assembled into a complete stochastic model and that persistent coherence can yield a finite-mean clock.

They do not select the parameter m, the physical spatial dimension, a quantum Hilbert space, a gravitational action or the observed matter spectrum. Those structures are not hidden inside the word node. The following sections construct their mathematical interfaces separately so that a future microscopic selection can replace the benchmark choices without changing the meaning of a derived result.

C. Dimensional normalization and complete differentiation

C.1 What a correction is allowed to change

A mathematical repair and a physical completion are different operations. Repairing a missing chain-rule factor is unambiguous once the independent variables are specified. Choosing a new potential, a cutoff, a field normalization or a probability rule is an additional physical assumption. This appendix separates the two. It supplies the elementary calculus needed to implement a proposed node interaction without using agreement with a target as a substitute for that calculus.

A dimensionless kernel $\mathcal{K}$ can be converted to an energy by $E = E_*\mathcal{K}$. A density u contributes an energy $\int u \, \mathrm{d}^3x$, or uV in a uniform cell. A frequency ω contributes $\hbar\omega$ only in a branch with the quantum energy-frequency relation. A normalized state amplitude is not itself an energy. These rules follow from the physical quantity definitions; calling the sum a unified equation does not remove their dimensional requirements [38, 13].

For example, $(\hbar c)^2/G$ has SI dimensions $\mathrm{kg}^3\,\mathrm{m}^3\,\mathrm{s}^{-2}$, not those of energy and not those of a dimensionless wave amplitude. It cannot be added directly to $\exp(-iEt/\hbar)$. Multiplying by an arbitrarily selected power of a mass or length would change the hypothesis. The constructive replacement is to define a Hamiltonian with consistent energy units, not to force an incompatible prefactor into the state.

C.2 Independent variables and scale factors

Let

$$u = \frac{r}{\ell_*} + \frac{\tau}{t_*}, \qquad \mathcal{K}(r,\tau,\varphi) = 1 + a\tanh u + b\sinh\varphi + C(r,\tau) + e(r,\tau,\varphi). \tag{C.1}$$

Here ℓ_* and t_* are positive length and time scales; u, a, b, C, e are dimensionless. The symbol e in this appendix is a correction function, not the elementary charge. It can instead be set identically to zero in a fully specified model. Keeping it unspecified does not close the dynamics.

If r, τ, φ are independent coordinates and the derivative holds the others fixed,

$$\partial_r\mathcal{K} = \frac{a}{\ell_*}\operatorname{sech}^2 u + C_r + e_r, \tag{C.2}$$

$$\partial_\tau\mathcal{K} = \frac{a}{t_*}\operatorname{sech}^2 u + C_\tau + e_\tau, \tag{C.3}$$

$$\partial_\varphi\mathcal{K} = b\cosh\varphi + e_\varphi. \tag{C.4}$$

No phase derivative appears in $\partial_r\mathcal{K}$ unless a dependence of φ on r is specified. If $\varphi = \varphi(r,\tau)$, the derivative of the composed function includes $b\cosh\varphi\,\varphi_r$ and corresponding chain terms from e. Both conventions are legitimate, but they cannot be mixed within one line.

For $e = 0$ and a composed phase, the second spatial derivative is

$$\frac{\mathrm{d}^2\mathcal{K}}{\mathrm{d}r^2} = -\frac{2a}{\ell_*^2}\operatorname{sech}^2 u\tanh u + b\left[\sinh\varphi\,(\varphi_r)^2 + \cosh\varphi\,\varphi_{rr}\right] + C_{rr}. \tag{C.5}$$

At independent fixed phase, the term in square brackets vanishes. The corresponding time derivative is

$$\frac{\mathrm{d}^2\mathcal{K}}{\mathrm{d}\tau^2} = -\frac{2a}{t_*^2}\operatorname{sech}^2 u\tanh u + b\left[\sinh\varphi\,(\varphi_\tau)^2 + \cosh\varphi\,\varphi_{\tau\tau}\right] + C_{\tau\tau}. \tag{C.6}$$

For the same composed phase, the mixed derivative is

$$\frac{\mathrm{d}^2\mathcal{K}}{\mathrm{d}r\mathrm{d}\tau} = -\frac{2a}{\ell_* t_*}\operatorname{sech}^2 u\tanh u + b\left[\sinh\varphi\,\varphi_r\varphi_\tau + \cosh\varphi\,\varphi_{r\tau}\right] + C_{r\tau}. \tag{C.7}$$

These relations retain the factor of two from differentiating $\operatorname{sech}^2 u$ and the second derivative of a composed phase. They are also direct unit checks: every term in a second spatial derivative has inverse-length-squared units.

Along a trajectory, the total derivative is

$$\frac{\mathrm{d}\mathcal{K}}{\mathrm{d}t} = \partial_r\mathcal{K}\,\dot r + \partial_\tau\mathcal{K}\,q(t) + \partial_\varphi\mathcal{K}\,\dot\varphi, \qquad q = \mathrm{d}\tau/\mathrm{d}t. \tag{C.8}$$

An extra clock factor belongs here because a proper-time dependence has been composed with reference time. It does not justify applying the factor a second time to quantities that have already been transformed.

C.3 Compact phase versus noncompact strain

A phase is defined modulo 2π. A physical energy built only from that compact coordinate must assign the same value to φ and $\varphi + 2\pi$. The function $\sinh\varphi$ is not periodic and therefore cannot be the globally defined energy of an otherwise unconstrained compact phase. It can instead describe a noncompact variable, or a local approximation with an explicitly restricted domain and an eventual periodic completion.

The construction in the main text chooses $\sin\delta$ and $1 - \cos\delta$ precisely so that its energy is well defined on the phase torus. This is a model selection with an identifiable symmetry reason. It does not prove that every admissible periodic potential has the same spectrum: additional harmonics such as $1 - \cos 2\delta$ change the nonlinear dynamics even though they preserve the global symmetry.

Likewise, a complex expression such as

$$F = \omega e^{i\varphi} + \sum_p g_p \sin(h_p r + i\varphi) \tag{C.9}$$

can be an amplitude or an intermediate complex kernel, but it is not generically a real scalar energy. A real energy might be formed from a specified real part, a Hermitian quadratic form, or paired conjugate terms. Each choice produces a different observable map. A complex amplitude cannot be inserted into a Hamiltonian as a scalar potential without checking Hermiticity and the intended physical role.

C.4 Energy-density differentiation

For a constant density scale ρ_0 and a dimensionless correction $\varepsilon(r)$,

$$\rho_q(r) = \rho_0 \left[1 + \sum_m d_m \tanh(f_m r) + \varepsilon(r) \right], \tag{C.10}$$

where f_m has inverse-length units. Its derivative is

$$\rho_q'(r) = \rho_0 \left[\sum_m d_m f_m \operatorname{sech}^2(f_m r) + \varepsilon'(r) \right]. \tag{C.11}$$

The factor ρ_0 multiplies the correction derivative as well as the harmonic derivatives. If ρ_0 varies, its product-rule contribution must also be retained. Integrating the density to obtain energy introduces the cell geometry and boundary conditions. A force is then derived from that energy with its physical coordinate held consistently, rather than by treating a density derivative as a force without a volume factor.

C.5 The bounded pairing kernel

Consider the dimensionless geometric weight

$$P(r) = \frac{1}{1 + (r/d_0)^2}, \qquad d_0 > 0. \tag{C.12}$$

It lies in $(0, 1]$ and falls as r^{-2}. A bounded weight is not automatically a normalized probability density. In three dimensions,

$$\int_{|x|<R} P(|x|)\, \mathrm{d}^3x = 4\pi d_0^3 \left[\frac{R}{d_0} - \arctan(R/d_0)\right], \tag{C.13}$$

which diverges as $R \to \infty$. A probability distribution over neighbors therefore requires a finite graph, a cutoff, or a sufficiently fast additional envelope, followed by normalization. Calling P an interaction weight avoids that problem until a probability model is explicitly introduced.

On a finite graph, a normalized neighbor-selection rule could be $P_{ij}/\sum_{k\in\mathcal{N}_i} P_{ik}$. That is a valid additional stochastic rule, not a consequence of Hamiltonian determinism. Alternatively, the same weights can enter a deterministic potential or graph Laplacian. The two uses should not be interchanged when claiming an emergent Born rule.

C.6 Energy terms, phases and physical conversion

A spatially uniform, state-independent term $b(\tau)$ added to a quantum Hamiltonian produces a common phase

$$U_b(\tau) = \exp\left[-\frac{i}{\hbar}\int_0^\tau b(s)\mathrm{d}s\right] U_0(\tau). \tag{C.14}$$

The density matrix and all expectation values remain the same. A relative energy shift between coupled states changes their dynamics, and an off-diagonal coupling transfers amplitude. The two-state construction in the main text makes this distinction explicit. An EQEF contribution confined to a common phase cannot by itself determine an actuation efficiency.

For a time-dependent noncommuting Hamiltonian the correct propagator is

$$U(\tau) = \mathcal{T}\exp\left[-\frac{i}{\hbar}\int_0^\tau H(s)\mathrm{d}s\right]. \tag{C.15}$$

Using $e^{-iH(\tau)\tau/\hbar}$ instead generally introduces extra derivative terms and omits time ordering. For a constant Hamiltonian, the ordinary exponential is correct. A scalar formula for one stationary eigenstate is not a full many-body evolution law until the Hamiltonian, domain and state space have been selected.

C.7 A concrete recurrence check

The Bohr ground-state energy and classical orbital period are

$$E_1 = -\frac{1}{2}m_e c^2\alpha^2, \qquad T_{\mathrm{orb}} = \frac{2\pi\hbar}{m_e c^2\alpha^2}. \tag{C.16}$$

Their product is $E_1 T_{\mathrm{orb}}/\hbar = -\pi$, not -2π. Thus the stationary-state phase after that orbital time is -1, not $+1$. Doubling the period restores a 2π phase recurrence, but gives no equation selecting α: the same factor occurs in both energy and period and cancels. The distinction between an orbital period and an energy-eigenstate phase period is part of the ordinary atomic model [50, 51].

More fundamentally, a global sign of a state is not an observable difference. Imposing a return of an unobservable global phase does not quantize an otherwise free coupling. Physical recurrence conditions must concern relative phases, boundary conditions or observables. This is why the selected lattice dispersion and nonlinear period ratio are meaningful model consequences, while an identity obtained by substituting an α-dependent orbital period cannot determine α.

C.8 A precise limit on what conservation alone selects

There is a simple constructive nonuniqueness argument. Both H_* and

$$H_*^{(\lambda)} = H_* + \lambda K \sum_e (1 - \cos 2\delta_e), \qquad \lambda \geq 0, \tag{C.17}$$

preserve the compact phase, global phase symmetry, finite-state-variable evolution, positive energy bound and exact total conservation. Yet their small-angle stiffnesses differ by $4\lambda K$, and their nonlinear periods differ as well. Neither conservation nor the phrase potential-to-actuation chooses λ.

This does not disprove the physical idea. It proves that a unique numerical spectrum requires an additional physical selection principle. The present paper freezes $\lambda = 0$ as its explicit demonstration rather than quietly varying it until a number matches a measurement. An additional term can be investigated, but doing so defines a new declared model whose independent predictions must be tested anew.

D. Reference identities and observable definitions

D.1 The role of this appendix

This appendix gathers conventional relations needed to compare a microscopic proposal with established physics. They are not additional independent predictions of the phase-reserve Hamiltonian. Each relation identifies which physical inputs are required. Numerical substitution using measured inputs is a useful unit and implementation test, but the dependent quantities must not be counted again as if they supplied new microscopic information. Metrological conventions follow the SI Brochure and CODATA, while particle conventions follow the fixed reference edition of the Review of Particle Physics [38, 39, 8].

The distinction is particularly important for long lists of constants. An electron mass, its rest energy in joules, its rest energy in electron volts, its Compton wavelength and its charge-to-mass ratio share inputs. Agreement among their correctly converted values is not five independent predictions of the electron sector. The same applies to the several Planck scales and to the several ways of expressing a cosmological energy density.

D.2 Electromagnetic normalization in SI and natural units

Let $e > 0$ denote the magnitude of the elementary charge, so the electron has charge $-e$. In SI,

$$\alpha = \frac{e^2}{4\pi\epsilon_0\hbar c}, \qquad \mu_0\epsilon_0 c^2 = 1. \tag{D.1}$$

Using $h = 2\pi\hbar$ gives

$$\mu_0 = \frac{2\alpha h}{e^2 c}, \qquad \epsilon_0 = \frac{e^2}{2\alpha h c}, \qquad k_e = \frac{1}{4\pi\epsilon_0} = \frac{\alpha\hbar c}{e^2}. \tag{D.2}$$

After the 2019 SI revision, h, e, c have exact defining values, whereas α, μ_0 and ϵ_0 retain experimental uncertainty. The former exact convention $\mu_0 = 4\pi \times 10^{-7}$ H/m is not an exact current physical constraint [38, 13]. An electromagnetic-normalization derivation cannot use the measured ϵ_0 to obtain α and then count the result as independent of measured α.

In rationalized natural units, the dimensionless electromagnetic coupling is $e_{\text{nat}} = \sqrt{4\pi\alpha}$. Its numerical value is not the number of coulombs in the SI elementary charge. A weak-interaction formula such as $G_F = g^2/(4\sqrt{2}m_W^2)$ requires natural-unit g and a mass expressed consistently in energy units. Substituting $1.602176634 \times 10^{-19}$ coulombs directly for e_{nat} is not a unit conversion.

D.3 Atomic lengths and their dependencies

For an electron with mass m_e,

$$\lambda_C = \frac{h}{m_e c}, \qquad \overline{\lambda}_C = \frac{\hbar}{m_e c}, \qquad r_e = \frac{\alpha\hbar}{m_e c}, \qquad a_0 = \frac{\hbar}{m_e c\alpha}. \tag{D.3}$$

Consequently $r_e = \alpha\overline{\lambda}_C$ and $a_0 = \overline{\lambda}_C/\alpha$. The classical electron radius r_e is an electromagnetic length scale, not a measurement of a rigid electron surface. The Bohr radius is an atomic scale, not a proton radius. A microscopic model must produce the relevant charge distribution or scattering amplitude before a physical size can be assigned to one of its configurations.

The conventional Rydberg and Hartree energy scales are

$$R_\infty = \frac{\alpha^2 m_e c}{2h}, \qquad E_R = hcR_\infty = \frac{1}{2}\alpha^2 m_e c^2, \qquad E_h = 2E_R. \tag{D.4}$$

The two-body Coulomb problem uses the reduced mass $\mu = m_e M/(m_e + M)$ in place of m_e. This is why a real hydrogen ionization energy is not exactly the infinite-nuclear-mass Rydberg energy. Relativistic, finite-size and radiative corrections add further terms. The elementary Coulomb derivation in the main text gives the leading spectrum and wavefunctions; precision spectroscopy requires the entire specified comparison model [50, 51, 8].

D.4 Magnetic moments and spin factors

The Bohr and nuclear magnetons are

$$\mu_B = \frac{e\hbar}{2m_e}, \qquad \mu_N = \frac{e\hbar}{2m_p}. \tag{D.5}$$

Using positive g_e for the electron's magnitude convention,

$$\boldsymbol{\mu}_e = -g_e\mu_B\frac{\mathbf{S}}{\hbar}. \tag{D.6}$$

For a spin-up projection $S_z = \hbar/2$, $\mu_{e,z} = -g_e\mu_B/2$. A quoted magnetic moment for a fully polarized spin-one-half particle therefore contains the factor of one half. The proton

convention gives $\mu_{p,z} = g_p \mu_N/2$, and the conventional neutron g factor is defined using the nuclear magneton, which contains the proton mass, despite the neutron being neutral.

The eigenvalue of $\mathbf{S}^2$ is $s(s+1)\hbar^2$, whereas that of S_z is $m_s\hbar$. For $s = 1/2$, the magnitude associated with $\mathbf{S}^2$ is $\sqrt{3}\hbar/2$, not $\hbar/2$. The latter is a maximal component. A proposal deriving spin must produce the representation and its algebra, not just insert $s = 1/2$ into a dimensional formula [52, 8].

D.5 Scattering lengths, cross sections and form factors

For an unpolarized electromagnetic wave scattering from a free nonrelativistic electron in the low-photon-energy limit,

$$\frac{\mathrm{d}\sigma}{\mathrm{d}\Omega} = \frac{r_e^2}{2}(1 + \cos^2\theta). \tag{D.7}$$

Integration over solid angle gives $\sigma_T = 8\pi r_e^2/3$. The formula fixes a cross section after m_e and α are specified; it is not a separate derivation of either input. At higher energies, recoil changes the angular distribution and total cross section.

For a normalized electric form factor in natural units,

$$G_E(Q^2) = 1 - \frac{1}{6} r_E^2 Q^2 + O(Q^4), \qquad r_E^2 = -6 \left.\frac{\mathrm{d}G_E}{\mathrm{d}Q^2}\right|_0 . \tag{D.8}$$

If Q is quoted in energy units and r_E in metres, the appropriate factor of $(\hbar c)^2$ must be restored. For a chosen shape $G_E = 1/(1 + Q^2/\Lambda_F^2)$ the result is $r_E = \sqrt{6}/\Lambda_F$ in natural units. The scale Λ_F must be obtained independently; choosing it from the observed radius is a calibration.

At leading order for an S state, a small nuclear charge radius contributes

$$\Delta E_{\mathrm{fs}} = \frac{2\pi Z\alpha\hbar c}{3} r_N^2 |\psi_{nS}(0)|^2, \qquad |\psi_{nS}(0)|^2 = \frac{1}{\pi n^3 a_Z^3}, \tag{D.9}$$

where $a_Z = \hbar/(\mu c Z\alpha)$. The factor of π cancels upon substitution. A radius inferred by inverting a measured finite-size shift is not a parameter-free radius prediction. These conventions and the separation of hadronic, atomic and radiative contributions are essential for comparing unlike precision measurements [8].

D.6 Planck units and dimensional information

The usual Planck scales are constructed from supplied $G, \hbar, c$:

$$\ell_P = \sqrt{\hbar G/c^3}, \qquad t_P = \sqrt{\hbar G/c^5}, \qquad m_P = \sqrt{\hbar c/G}, \tag{D.10}$$

$$E_P = m_P c^2, \qquad T_P = E_P/k_B, \qquad \rho_P = m_P/\ell_P^3 = \frac{c^5}{\hbar G^2}, \tag{D.11}$$

$$p_P = \rho_P c^2 = \frac{c^7}{\hbar G^2}, \qquad q_P = \sqrt{4\pi\epsilon_0 \hbar c}. \tag{D.12}$$

The reduced Planck mass used in many field actions is $\overline{M}_P = m_P/\sqrt{8\pi}$ when units are restored appropriately. Confusing reduced and unreduced masses introduces an 8π factor in

the gravitational action. The equations above are valuable checks, but solving their definition for G after supplying ℓ_P or m_P derived from measured G is circular as a prediction of G.

Choosing model units so that one of these quantities equals one is a coordinate convention on dimensional quantities. A first-principles relation between gravity and particle physics should instead specify a dimensionless quantity, such as $Gm_e^2/(\hbar c)$ or a predicted ratio of the microscopic length to an independently generated particle Compton wavelength.

D.7 Rest masses, binding energies and reaction thresholds

For a particle in a Lorentz-invariant branch,

$$E^2 = p^2c^2 + m^2c^4, \tag{D.13}$$

so mc^2 is the rest energy. A bound composite mass is the total energy of the bound configuration divided by c^2, measured relative to a consistently specified vacuum. If $B > 0$ denotes the energy required to dissociate the bound object, then

$$M_{\text{bound}} = \sum_i m_i - \frac{B}{c^2}. \tag{D.14}$$

The binding contribution is negative relative to separated constituents. Setting a negative potential-well depth equal to a positive particle rest mass without specifying the constituent and vacuum energies omits this distinction.

For a nucleus,

$$B(Z,N) = \left[Zm_p + Nm_n - M_{\text{nucleus}}\right]c^2. \tag{D.15}$$

Atomic masses must first be adjusted for electron masses and electronic binding. A nuclear mass inserted into this equation carries the measured binding information; the equation alone is not a nuclear-force calculation. Predicting B requires a Hamiltonian and many-body solution, including the strong-interaction inputs at the stated approximation level.

Relativistic production thresholds depend on the invariant $s = (p_1 + p_2)^2$ in natural units. At threshold, $\sqrt{s} \geq \sum_f m_f$ for the specified final state. The beam energy of one incoming particle in a fixed-target setup is not equal to the center-of-mass energy. A single local threshold functional must be mapped to these invariants and to allowed quantum numbers before it can predict collider rates [8].

D.8 Weak processes and neutrino observables

At tree level in the Standard Model,

$$m_W = gv/2, \quad m_Z = v\sqrt{g^2 + g'^2}/2, \quad G_F = 1/(\sqrt{2}v^2), \quad m_h^2 = 2\lambda_H v^2. \tag{D.16}$$

These are relationships among Lagrangian parameters. They are not exact loop-level relations between every experimentally extracted mass and every coupling scheme. The on-shell definition $\sin^2\theta_W = 1 - m_W^2/m_Z^2$ and a running renormalized weak mixing angle are different quantities. Comparing their central values as though they were the same observable creates an artificial discrepancy [56, 8].

For example, in natural units the leading muon decay width is

$$\Gamma_\mu = \frac{G_F^2 m_\mu^5}{192\pi^3}\left[1 - 8x + 8x^3 - x^4 - 12x^2 \ln x\right](1 + \delta_{\rm rad}), \quad x = m_e^2/m_\mu^2. \tag{D.17}$$

The lifetime in seconds is $\hbar/\Gamma_\mu$ when the width is in energy units. Radiative and other prescribed corrections are necessary at precision level. Inferring G_F from a measured lifetime is a calibration with conventional electroweak theory, not a derivation of G_F from a node threshold [31, 8].

For three light neutrinos, define $\Delta m_{ij}^2 = m_i^2 - m_j^2$ and a unitary mixing matrix U. In vacuum,

$$P_{\alpha\to\beta} = \left|\sum_i U_{\beta i} U_{\alpha i}^* \exp\left[-\frac{i m_i^2 c^3 L}{2\hbar E}\right]\right|^2 . \tag{D.18}$$

Adding the same mass-squared offset to every m_i^2 produces only a common phase and leaves these probabilities unchanged. Thus oscillations cannot determine the absolute mass scale by themselves. The quantities relevant to beta decay, cosmology and neutrinoless double-beta decay are respectively

$$m_\beta^2 = \sum_i |U_{ei}|^2 m_i^2, \qquad \Sigma m_i, \qquad m_{\beta\beta} = \left|\sum_i U_{ei}^2 m_i\right| . \tag{D.19}$$

The last can involve phase cancellations and presumes the light-Majorana exchange mechanism. It is not obtained by dividing one effective mass bound by a single mixing probability. Matter effects add a flavor-dependent forward-scattering potential, as developed by Wolfenstein [59]; the DUNE-style calculation in Volume II uses that specified effective framework rather than claiming observed detector counts.

D.9 Strong-interaction scales and light pseudoscalars

The renormalization scale is an essential part of a quark mass or a strong coupling. To one loop in a specified massless-flavor regime,

$$\mu\frac{\mathrm{d}\alpha_s}{\mathrm{d}\mu} = -\frac{\beta_0}{2\pi}\alpha_s^2, \quad \beta_0 = 11 - \frac{2}{3}n_f, \quad \alpha_s(\mu) = \frac{4\pi}{\beta_0 \ln(\mu^2/\Lambda_{\rm QCD}^2)}. \tag{D.20}$$

Threshold matching and higher-order terms change the practical relation. Asymptotic freedom follows from the non-Abelian gauge theory under its field-content assumptions [57, 58]. The integration constant $\Lambda_{\rm QCD}$ is not fixed by solving this differential equation without a boundary condition.

At leading chiral order, the light pseudoscalar relations take the schematic form $m_\pi^2 = B_0(m_u + m_d)$ and $m_{K^+}^2 = B_0(m_u + m_s)$, where B_0 is an independently defined low-energy parameter with mass units. A convention in which a condensate appears instead can contain F_π^2 in the denominator; the condensate then has mass-cubed units. Mixing the two definitions produces a dimensional error. A proposed node spectrum must recover the chiral Ward identities and calculate or match these low-energy parameters rather than change a numerical scale after comparing a pion mass [8].

D.10 Thermal peaks and material-dependent quantities

The blackbody law written as a function of frequency has its maximum at the positive solution of $3(1 - e^{-x}) = x$, whereas the law per unit wavelength has its maximum at the positive solution of $5(1 - e^{-x}) = x$. The roots are approximately 2.821439 and 4.965114, respectively. Consequently the wavelength displacement constant is

$$b = \frac{hc}{k_B x_5}, \qquad \lambda_{\max} T = b, \tag{D.21}$$

not the expression obtained by substituting the frequency root into a wavelength formula. The two maxima do not transform into one another by $\lambda = c/\nu$ because spectral densities carry different Jacobians [64].

For a nonrelativistic spin-one-half free Fermi gas at zero temperature,

$$k_F = (3\pi^2 n)^{1/3}, \quad E_F = \hbar^2 k_F^2/(2m), \quad P = \frac{2}{5} n E_F. \tag{D.22}$$

The value depends on density, particle mass and the free-gas approximation. A number described as the Fermi energy of a metal is not a universal constant. The reference calculation with $n = 10^{28}\ \mathrm{m}^{-3}$ and electron mass gives 1.69253 eV before interactions and band structure. It is not adjusted to a separate material's Fermi energy.

For a dilute ideal gas, $p = nk_BT$ and $c_s^2 = (\partial p/\partial \rho)_s = \gamma k_B T/m$. This speed depends on temperature, composition and the thermodynamic process. Atmospheric pressure, terrestrial gravity and the speed of sound in air are environmental observables; fundamental laws predict them only with appropriate planetary, material and boundary data. They are not dimensionless microscopic constants selected by a bare phase-update equation.

D.11 Orbital and stellar observables

For two Newtonian point masses, the relative coordinate obeys $\ddot{\mathbf{r}} = -G(M+m)\mathbf{r}/r^3$. Circular motion yields $v^2 = G(M+m)/r$, and an ellipse with semimajor axis a has

$$T^2 = \frac{4\pi^2 a^3}{G(M+m)}. \tag{D.23}$$

The specific orbital energy is $-G(M+m)/(2a)$ and the specific angular momentum obeys $h_{\mathrm{orb}}^2 = G(M+m)a(1-e_{\mathrm{orb}}^2)$. Eccentricity and orbital orientation are initial-condition information, not universal constants. A dynamical theory does not predict Earth's axial tilt or a particular planetary radius without a model of their history and material constitution.

A spherical object's surface gravity is GM/R^2 in the nonrotating Newtonian approximation, escape speed is $\sqrt{2GM/R}$, and the gravitational binding energy of a uniform sphere is $-3GM^2/(5R)$. The last coefficient changes with the density profile. A luminosity described as thermal obeys $L = 4\pi R^2 \sigma T_{\mathrm{eff}}^4$ by the definition of effective temperature; this relation does not independently calculate the nuclear energy-generation rate or stellar radius.

Relativistic hydrostatic equilibrium in the perfect-fluid, spherical and stationary Einstein branch satisfies

$$\frac{\mathrm{d}m}{\mathrm{d}r} = 4\pi r^2 \rho, \qquad \frac{\mathrm{d}p}{\mathrm{d}r} = -\frac{G(\rho + p/c^2)(m + 4\pi r^3 p/c^2)}{r^2[1 - 2Gm/(rc^2)]}. \tag{D.24}$$

Here ρ is mass-equivalent density. The equation of state $p(\rho)$ and central density are required. A proposed EQEF stress component must be included consistently in that equation of state and in the gravitational field equations, not appended as a force selected to obtain a desired maximum mass. Compact-object equations and their observational interpretation are used here at the effective-physics level [8].

D.12 Black holes and finite-energy implications

In the Schwarzschild exterior, the horizon radius is $r_s = 2GM/c^2$. The area is $A = 4\pi r_s^2$. In the semiclassical Einstein branch,

$$S_{\mathrm{BH}} = \frac{k_B c^3 A}{4G\hbar}, \qquad T_H = \frac{\hbar c^3}{8\pi G M k_B}. \tag{D.25}$$

These statements combine gravity, quantum field theory on the background and thermodynamics. They are not consequences of total energy conservation alone [15, 16]. An elementary blackbody-area estimate of the power gives $\hbar c^6/(15360\pi G^2 M^2)$, but actual emission involves species-dependent transmission factors and available particle degrees of freedom. The estimate is not a direct observation of stellar black-hole Hawking radiation.

A positive microscopic Hamiltonian does not by itself prove that every emergent curvature invariant is bounded. The map to geometry and the allowed energy-density concentration must be established. Similarly, preserving a microscopic state does not alone establish a unitary observable evaporation process after inaccessible degrees of freedom are traced out. Those are separate dynamical questions; their requirements are stated rather than replaced by a general claim that a finite lattice resolves every singularity.

D.13 Cosmological density, age and structure

Use ρ for mass-equivalent density and $u = \rho c^2$ for energy density. Then

$$\rho_c = \frac{3H^2}{8\pi G}, \quad \rho_\Lambda = \frac{\Lambda c^2}{8\pi G}, \quad u_\Lambda = \frac{\Lambda c^4}{8\pi G}. \tag{D.26}$$

The symbol u_Λ denotes energy density; the notation is not a new field. A uniform vacuum-energy term in a volume is $E_\Lambda = u_\Lambda V$. Using $\Lambda c^2 V/(8\pi G)$ as an energy instead produces mass units. The factors of c^2 distinguish a density convention, not a small correction that can be fitted away.

For standard photon propagation, $1 + z = a_0/a_e$ and an emitted time interval obeys $\Delta t_{\mathrm{obs}} = (1 + z)\Delta t_e$. The age since the chosen initial expanding branch is

$$t_0 = \int_0^1 \frac{\mathrm{d}a}{aH(a)}. \tag{D.27}$$

A specified H_0 and composition determine this integral, but the age is not generally $1/H_0$. For the flat matter-plus-vacuum approximation,

$$H_0 t_0 = \frac{2}{3\sqrt{1 - \Omega_m}} \operatorname{asinh} \sqrt{\frac{1 - \Omega_m}{\Omega_m}}. \tag{D.28}$$

The numerical test in Volume II compares this analytic expression with quadrature. The Planck and DESI comparisons retain the cosmological assumptions and covariance of their respective published products [17, 18, 19].

A successful expansion history does not supply a successful CMB spectrum. For scalar perturbations, an effective calculation requires an initial curvature spectrum and transfer functions,

$$C_\ell^{XY} = 4\pi \int \frac{\mathrm{d}k}{k} \mathcal{P}_\mathcal{R}(k) \Delta_\ell^X(k) \Delta_\ell^Y(k). \tag{D.29}$$

The transfer functions depend on the coupled gravitational, photon, baryon and neutrino equations and recombination. The standard perturbative construction is laid out by Ma and Bertschinger [66]. A homogeneous EQEF balance is not a replacement for those perturbation equations, sound speeds and anisotropic stresses.

For comparison with a conventional halo model, the Navarro–Frenk–White profile is

$$\rho(r) = \frac{\rho_s}{x(1+x)^2}, \quad x = r/r_s, \qquad M(<r) = 4\pi\rho_s r_s^3 \left[\ln(1+x) - \frac{x}{1+x}\right]. \tag{D.30}$$

The mass follows by integrating $4\pi r^2 \rho$. The corresponding circular speed follows from $v_c^2 = GM(<r)/r$. Its two scale parameters are supplied or fitted halo parameters, not predictions of the phase-reserve construction. Matching a galaxy requires the baryonic distribution and observational uncertainties as well [67]. Dark matter, modified gravity and conversion effects must be compared through actual force and lensing equations, not through a common descriptive label.

D.14 What a complete comparison records

For every numerical output, the record should state the physical quantity, units, frame, approximation, independent inputs, source of those inputs and the model prediction before a measurement is compared. A count of computations must be accompanied by a count of independent constraints and fitted parameters. Derived quantities inherit correlations from their inputs.

The reconstruction therefore retains the relationships in this appendix as conventional reference physics. Their role is to make the physical matching problem explicit and to prevent a units error, a duplicate entry, an environmental input or a model assumption from masquerading as a new parameter-free alignment. The conditional model predictions developed earlier have a different role: their coefficients are calculated from the frozen Hamiltonian, and their eventual comparison requires an independently specified physical realization.

E. A detailed two-reservoir solution and inverse problem

E.1 Eigenvectors and the exact propagator

With the state $x = (E_A, E_P)^T$ and generator

$$M = \begin{pmatrix} -b & a \\ b & -a \end{pmatrix}, \tag{E.1}$$

the left null vector is $(1, 1)$ and the right null vector is $(a, b)^T$. The second eigenvalue is $-(a + b)$ with right eigenvector $(1, -1)^T$. For $s = a + b > 0$ the exponential is

$$e^{M\tau} = \frac{1}{s}\begin{pmatrix} a + be^{-s\tau} & a(1 - e^{-s\tau}) \\ b(1 - e^{-s\tau}) & b + ae^{-s\tau} \end{pmatrix}. \tag{E.2}$$

Every entry is nonnegative for $a, b, \tau \geq 0$, and each column sums to one. These two elementary properties prove preservation of the nonnegative simplex and of total content. They also provide an independent way to validate a numerical differential-equation solver.

At $a = b = 0$ the exponential is the identity, obtained separately rather than dividing by $s = 0$. At $a = 0, b > 0$, expression relaxes entirely into the reserve. At $b = 0, a > 0$, the reserve eventually becomes expressed. These limiting cases show which physical interpretation is implied by each boundary of the parameter space.

E.2 Which measurements would identify the rates?

For independently known total content E, equilibrium fraction $f = E_A^*/E$ and relaxation rate s, the inverse equations are

$$a = fs, \qquad b = (1 - f)s. \tag{E.3}$$

This is an identifiable two-observable inverse problem provided the clock measuring s is independently defined. If the forward rate is factored as $a = \eta k$, equilibrium and relaxation determine a, not η and k separately. A third independent piece of information about the attempted rate k is required. This is the precise counterpart of the potential-rate degeneracy in the event-count model.

For small uncertainties, the Jacobian from (f, s) to (a, b) is

$$J = \begin{pmatrix} s & f \\ -s & 1 - f \end{pmatrix}, \qquad C_{ab} = JC_{fs}J^T. \tag{E.4}$$

The correlation between f and s matters. Treating their fitted errors as independent can overstate or understate the precision of a shared-rate claim. Near $f = 0$ or 1, a constrained likelihood is preferable to an unconstrained Gaussian approximation.

E.3 A time-dependent generator

For varying $a(\tau), b(\tau)$, total content remains constant and

$$\dot{E}_A + s(\tau)E_A = a(\tau)E. \tag{E.5}$$

An integrating factor gives

$$E_A(\tau) = e^{-S(\tau)}\left[E_A(0) + E\int_0^\tau a(u)e^{S(u)}\mathrm{d}u\right], \quad S(\tau) = \int_0^\tau s(u)\mathrm{d}u. \tag{E.6}$$

This expression remains valid without commuting matrix generators because the conserved total reduces the problem to one scalar equation. A general multichannel system instead requires a time-ordered propagator. The distinction prevents applying an ordinary matrix exponential to a genuinely time-dependent noncommuting quantum or classical evolution without justification.

F. An explicit correlated-error calculation

F.1 Efficiency ratios

Let y be a measured rate with expectation ηw and independently determined exposure w. To first order,

$$\operatorname{Var}(\widehat{\eta}) \simeq \frac{\operatorname{Var}(y)}{w^2} + \frac{y^2 \operatorname{Var}(w)}{w^4} - \frac{2y \operatorname{Cov}(y, w)}{w^3}. \tag{F.1}$$

The covariance term is essential when the same calibration affects the count and exposure. A residual efficiency compatible with one is not evidence that the reservoir is absent; it is a constraint on the particular observable combination under the specified calibration.

For two rates, $\log \eta = \log y - \log q - \log r_0 - \log \epsilon_{\mathrm{det}}$ has gradient $(1, -1, -1, -1)$ with respect to the four log variables. Its covariance follows from the quadratic form with their full covariance matrix. A highly precise count cannot overcome an unknown absolute normalization. The usual square-root count improvement applies only when systematic uncertainties are already controlled.

F.2 Training uncertainty enters every holdout prediction

If a training estimate $\widehat{\eta}$ has variance V_η and holdout expectations are $\mu_i = w_i \widehat{\eta}$, the calibration contribution to their covariance is

$$C_{ij}^{\mathrm{cal}} = w_i w_j V_\eta. \tag{F.2}$$

It is a rank-one shared uncertainty, not one independent calibration error per holdout channel. Adding it only to the diagonal would count the same calibration differently in every experiment. The test volume uses this shared term in the synthetic holdout residual and separately evaluates a common-efficiency likelihood.

F.3 An observationally equivalent family

For any positive c consistent with the allowed parameter range,

$$(q, \eta, r_0) \mapsto (cq, \eta/c, r_0) \tag{F.3}$$

preserves a one-channel expectation $q\eta r_0$. Independent information is what breaks this family, not higher numerical precision in the same product. The same reasoning applies to source abundance times cross section, luminosity times production rate, and clock normalization times transition frequency when their components are not otherwise known.

G. Notation and dimensional conventions

The microscopic update index n is dimensionless. A physical proper-time interval $\Delta\tau$ is introduced only through an operational clock mapping. $q = \mathrm{d}\tau/\mathrm{d}t$ is a positive comparison factor; it is not a universal energy-loss fraction. In the quotient-state discussion the map is written π to avoid confusing it with that clock factor.

E_A, E_P, E_{int} are energy assignments in an effective model. J_+, J_- have energy per proper-time units. The attempted event rate r_0 has count per proper-time units and is not automatically J_{pot}; conversion between them requires a specified energy per event or differential event distribution. The efficiency η and detector efficiency ϵ_{det} are dimensionless but describe different mechanisms.

The symbol Γ denotes a proper-time hazard. A per-frame probability $p = 1 - e^{-\Gamma\Delta\tau}$ depends on the interval even when Γ does not. The capacity exponent is p only inside the phase-threshold sections, where its meaning is stated; no relation to the conversion probability is intended. The electromagnetic coupling is α_{EM}, while a gravitational-redshift violation parameter is explicitly labeled by its experiment.

Natural units $c = \hbar = 1$ are used in field-theory sections unless SI factors are written. The metric signature is $(-, +, +, +)$. The speed of light and Planck constant used in numerical unit conversions are supplied SI definitions, not new predictions. A scalar field ϕ represents an illustrative EQEF completion; the field and its inferred residual efficiency are never identified without a constitutive relation.

External references

[1] W. Hoeffding, “Probability Inequalities for Sums of Bounded Random Variables,” *Journal of the American Statistical Association* **58**, 13–30 (1963). doi:10.1080/01621459.1963.10500830.

[2] K. G. Wilson, “Confinement of quarks,” *Physical Review D* **10**, 2445 (1974). doi:10.1103/PhysRevD.10.2445.

[3] J. Kogut and L. Susskind, “Hamiltonian formulation of Wilson’s lattice gauge theories,” *Physical Review D* **11**, 395 (1975). doi:10.1103/PhysRevD.11.395.

[4] A. M. Gleason, “Measures on the Closed Subspaces of a Hilbert Space,” *Journal of Mathematics and Mechanics* **6**, 885–893 (1957). doi:10.1512/iumj.1957.6.56050; original-paper record and abstract.

[5] G. Lindblad, “On the generators of quantum dynamical semigroups,” *Communications in Mathematical Physics* **48**, 119–130 (1976). doi:10.1007/BF01608499.

[6] J. S. Bell, “On the Einstein Podolsky Rosen paradox,” *Physics Physique Fizika* **1**, 195–200 (1964). doi:10.1103/PhysicsPhysiqueFizika.1.195.

[7] J. F. Clauser, M. A. Horne, A. Shimony and R. A. Holt, “Proposed Experiment to Test Local Hidden-Variable Theories,” *Physical Review Letters* **23**, 880 (1969); erratum **24**, 549 (1970). doi:10.1103/PhysRevLett.23.880.

[8] S. Navas et al. (Particle Data Group), “Review of Particle Physics,” *Physical Review D* **110**, 030001 (2024), with the 2025 update. doi:10.1103/PhysRevD.110.030001; official review index. Particle conventions, kinematics, cosmology and statistical methods are used as external effective-physics references.

[9] E. Witten, “An SU(2) anomaly,” *Physics Letters B* **117**, 324–328 (1982). doi:10.1016/0370-2693(82)90728-6.

[10] H. B. Nielsen and M. Ninomiya, “A no-go theorem for regularizing chiral fermions,” *Physics Letters B* **105**, 219–223 (1981). doi:10.1016/0370-2693(81)91026-1.

[11] M. Lüscher, “Exact chiral symmetry on the lattice and the Ginsparg–Wilson relation,” *Physics Letters B* **428**, 342–345 (1998). arXiv:hep-lat/9802011; doi:10.1016/S0370-2693(98)00423-7.

[12] H. Neuberger, “More about exactly massless quarks on the lattice” (1998). arXiv:hep-lat/9801031.

[13] National Institute of Standards and Technology, *2022 CODATA Recommended Values of the Fundamental Physical Constants*, released 2024. Official all-constants text table. Accessed 6 September 2026. Exact SI definitions and measured reference constants retain their respective roles.

[14] J. Garriga and V. F. Mukhanov, "Perturbations in k-inflation" (1999). arXiv:hep-th/9904176.

[15] J. D. Bekenstein, "Black Holes and Entropy," *Physical Review D* **7**, 2333 (1973). doi:10.1103/PhysRevD.7.2333.

[16] S. W. Hawking, "Particle creation by black holes," *Communications in Mathematical Physics* **43**, 199–220 (1975). doi:10.1007/BF02345020.

[17] N. Aghanim et al. (Planck Collaboration), "Planck 2018 results. VI. Cosmological parameters," *Astronomy & Astrophysics* **641**, A6 (2020). arXiv:1807.06209; doi:10.1051/0004-6361/201833910.

[18] M. Abdul-Karim et al. (DESI Collaboration), "DESI DR2 Results II: Measurements of Baryon Acoustic Oscillations and Cosmological Constraints" (2025). arXiv:2503.14738v2. Compressed distance-vector interpretation and sample definitions.

[19] DESI DR2 BAO likelihood data distributed in *CobayaSampler/bao_data*, directory `desi_bao_dr2`. Repository directory; GC-combined mean vector; GC-combined covariance. Accessed 6 September 2026; local input bytes recorded separately.

[20] Gravitational Wave Open Science Center, *GW150914*, catalog GWTC-1-confident, version 3. Versioned event record. Accessed 6 September 2026. The numerical calculation uses catalog source-parameter summaries, not raw strain.

[21] T. Baka et al., "Testing general relativity with gravitational waves: Improving and extending modified dispersion relation tests," *Physical Review D* **113**, 064064 (31 March 2026). doi:10.1103/bgvh-c1wj; arXiv:2511.00497.

[22] E. Aprile et al. (XENON Collaboration), "First Search for Light Dark Matter in the Neutrino Fog with XENONnT," *Physical Review Letters* **134**, 111802 (2025). arXiv:2409.17868; public release doi:10.5281/zenodo.14522707.

[23] XENONnT Collaboration, *light_wimp_data_release*. Official public repository; SI limit CSV; Light-mediator limit CSV. Accessed 6 September 2026.

[24] CERN Open Data Portal, *Histogram visualization: educational dimuon example*. Displayed CSV example; associated educational sample record 700. Accessed 6 September 2026. Only the four displayed example rows are used in this edition.

[25] T. Alion et al., "Experiment Simulation Configurations Used in DUNE CDR" (2016). arXiv:1606.09550.

[26] B. Abi et al. (DUNE Collaboration), "Deep Underground Neutrino Experiment (DUNE), Far Detector Technical Design Report, Volume II: DUNE Physics" (2020). arXiv:2002.03005.

[27] Fermi National Accelerator Laboratory, "DUNE will use liquid-argon time projection chamber technology both near and far" (May 2026). Official experiment-status report. Accessed 6 September 2026.

[28] A. Einstein, “Zur Elektrodynamik bewegter Körper,” *Annalen der Physik* **17**, 891–921 (1905). doi:10.1002/andp.19053221004. Relativistic clock comparisons are used as an established reference, not as a claimed derivation from EQEF.

[29] C. W. Chou, D. B. Hume, T. Rosenband and D. J. Wineland, “Optical Clocks and Relativity,” *Science* **329**, 1630–1633 (2010). doi:10.1126/science.1192720; NIST-hosted primary paper. Figure 3 supplies the height-step comparison used here.

[30] J. Bailey et al., “Measurements of relativistic time dilatation for positive and negative muons in a circular orbit,” *Nature* **268**, 301–305 (1977). doi:10.1038/268301a0. Published positive-muon lifetime and rounded abstract Lorentz factor; no full beam-distribution reanalysis.

[31] D. M. Webber et al. (MuLan Collaboration), “Measurement of the Positive Muon Lifetime and Determination of the Fermi Constant to Part-per-Million Precision,” *Physical Review Letters* **106**, 041803 (2011). arXiv:1010.0991; doi:10.1103/PhysRevLett.106.041803. Independent rest-lifetime input.

[32] P. Delva et al., “Gravitational Redshift Test Using Eccentric Galileo Satellites,” *Physical Review Letters* **121**, 231101 (2018). arXiv:1812.03711; doi:10.1103/PhysRevLett.121.231101.

[33] P. Touboul et al., “MICROSCOPE Mission: Final Results of the Test of the Equivalence Principle,” *Physical Review Letters* **129**, 121102 (2022). arXiv:2209.15487.

[34] B. P. Abbott et al., “Gravitational Waves and Gamma-rays from a Binary Neutron Star Merger: GW170817 and GRB 170817A,” *Astrophysical Journal Letters* **848**, L13 (2017). arXiv:1710.05834.

[35] R. Aliberti et al., “The anomalous magnetic moment of the muon in the Standard Model: an update” (2025). arXiv:2505.21476. Reference prediction and hadronic-input qualifications.

[36] D. P. Aguillard et al. (Muon $g-2$ Collaboration), “Measurement of the Positive Muon Anomalous Magnetic Moment to 127 ppb” (2025). arXiv:2506.03069. Experimental world-average comparison as reported in the cited release.

[37] L. K. Shalm et al., “Strong Loophole-Free Test of Local Realism,” *Physical Review Letters* **115**, 250402 (2015). arXiv:1511.03189.

[38] Bureau International des Poids et Mesures, *The International System of Units (SI)*, ninth edition (2019), version 4.01, June 2026. doi:10.59161/AUEZ1291. Exact defining constants and current unit conventions.

[39] P. J. Mohr, D. B. Newell, B. N. Taylor and E. Tiesinga, “CODATA recommended values of the fundamental physical constants: 2022,” *Reviews of Modern Physics* **97**, 025002 (2025). doi:10.1103/RevModPhys.97.025002; arXiv:2409.03787.

[40] E. Noether, "Invariante Variationsprobleme," *Nachrichten von der Gesellschaft der Wissenschaften zu Göttingen, Mathematisch-Physikalische Klasse*, 235–257 (1918). English translation by M. A. Tavel, "Invariant Variation Problems," arXiv:physics/0503066.

[41] R. Zwanzig, "Nonlinear generalized Langevin equations," *Journal of Statistical Physics* **9**, 215–220 (1973). doi:10.1007/BF01008729.

[42] H. Mori, "Transport, Collective Motion, and Brownian Motion," *Progress of Theoretical Physics* **33**, 423–455 (1965). doi:10.1143/PTP.33.423.

[43] R. Kubo, "The fluctuation-dissipation theorem," *Reports on Progress in Physics* **29**, 255–284 (1966). doi:10.1088/0034-4885/29/1/306.

[44] R. P. Feynman and F. L. Vernon, Jr., "The theory of a general quantum system interacting with a linear dissipative system," *Annals of Physics* **24**, 118–173 (1963). doi:10.1016/0003-4916(63)90068-X.

[45] A. O. Caldeira and A. J. Leggett, "Path integral approach to quantum Brownian motion," *Physica A* **121**, 587–616 (1983). doi:10.1016/0378-4371(83)90013-4.

[46] E. H. Lieb and D. W. Robinson, "The finite group velocity of quantum spin systems," *Communications in Mathematical Physics* **28**, 251–257 (1972). doi:10.1007/BF01645779.

[47] D. N. Page and W. K. Wootters, "Evolution without evolution: Dynamics described by stationary observables," *Physical Review D* **27**, 2885–2892 (1983). doi:10.1103/PhysRevD.27.2885.

[48] C. Rovelli, "Time in quantum gravity: An hypothesis," *Physical Review D* **43**, 442–456 (1991). doi:10.1103/PhysRevD.43.442.

[49] V. Gorini, A. Kossakowski and E. C. G. Sudarshan, "Completely positive dynamical semigroups of N-level systems," *Journal of Mathematical Physics* **17**, 821–825 (1976). doi:10.1063/1.522979.

[50] N. Bohr, "On the constitution of atoms and molecules," *Philosophical Magazine*, series 6, **26**, 1–25 (1913). doi:10.1080/14786441308634955.

[51] E. Schrödinger, "Quantisierung als Eigenwertproblem," *Annalen der Physik* **384**, 361–376 (1926). doi:10.1002/andp.19263840404.

[52] P. A. M. Dirac, "The quantum theory of the electron," *Proceedings of the Royal Society A* **117**, 610–624 (1928). doi:10.1098/rspa.1928.0023.

[53] J. Schwinger, "On Quantum-Electrodynamics and the Magnetic Moment of the Electron," *Physical Review* **73**, 416–417 (1948). doi:10.1103/PhysRev.73.416.

[54] G. H. Derrick, "Comments on Nonlinear Wave Equations as Models for Elementary Particles," *Journal of Mathematical Physics* **5**, 1252–1254 (1964). doi:10.1063/1.1704233.

[55] C. N. Yang and R. L. Mills, "Conservation of Isotopic Spin and Isotopic Gauge Invariance," *Physical Review* **96**, 191–195 (1954). doi:10.1103/PhysRev.96.191.

[56] S. Weinberg, “A Model of Leptons,” *Physical Review Letters* **19**, 1264–1266 (1967). doi:10.1103/PhysRevLett.19.1264.

[57] D. J. Gross and F. Wilczek, “Ultraviolet Behavior of Non-Abelian Gauge Theories,” *Physical Review Letters* **30**, 1343–1346 (1973). doi:10.1103/PhysRevLett.30.1343.

[58] H. D. Politzer, “Reliable Perturbative Results for Strong Interactions?” *Physical Review Letters* **30**, 1346–1349 (1973). doi:10.1103/PhysRevLett.30.1346.

[59] L. Wolfenstein, “Neutrino oscillations in matter,” *Physical Review D* **17**, 2369–2374 (1978). doi:10.1103/PhysRevD.17.2369.

[60] A. Einstein, “Die Grundlage der allgemeinen Relativitätstheorie,” *Annalen der Physik* **354**, 769–822 (1916). doi:10.1002/andp.19163540702.

[61] C. Barceló, S. Liberati and M. Visser, “Analogue Gravity,” *Living Reviews in Relativity* **8**, 12 (2005); updated review, arXiv:gr-qc/0505065, version 4 (2024). Analogue propagation geometry is distinguished from autonomous Einstein dynamics.

[62] T. Jacobson, “Thermodynamics of Spacetime: The Einstein Equation of State,” *Physical Review Letters* **75**, 1260–1263 (1995). doi:10.1103/PhysRevLett.75.1260; arXiv:gr-qc/9504004.

[63] F. W. Hehl, P. von der Heyde and G. D. Kerlick, “General relativity with spin and torsion and its deviations from Einstein’s theory,” *Physical Review D* **10**, 1066–1069 (1974). doi:10.1103/PhysRevD.10.1066.

[64] M. Planck, “Ueber das Gesetz der Energieverteilung im Normalspectrum,” *Annalen der Physik* **309**, 553–563 (1901). doi:10.1002/andp.19013090310.

[65] C. M. Wilson, G. Johansson, A. Pourkabirian, M. Simoen, J. R. Johansson, T. Duty, F. Nori and P. Delsing, “Observation of the dynamical Casimir effect in a superconducting circuit,” *Nature* **479**, 376–379 (2011). doi:10.1038/nature10561; arXiv:1105.4714.

[66] C.-P. Ma and E. Bertschinger, “Cosmological Perturbation Theory in the Synchronous and Conformal Newtonian Gauges,” *Astrophysical Journal* **455**, 7–25 (1995). arXiv:astro-ph/9506072.

[67] J. F. Navarro, C. S. Frenk and S. D. M. White, “A Universal Density Profile from Hierarchical Clustering,” *Astrophysical Journal* **490**, 493–508 (1997). doi:10.1086/304888; arXiv:astro-ph/9611107.

[68] C. Pitrou, A. Coc, J.-P. Uzan and E. Vangioni, “Precision big bang nucleosynthesis with improved Helium-4 predictions,” *Physics Reports* **754**, 1–66 (2018). doi:10.1016/j.physrep.2018.04.005; arXiv:1801.08023.